

Graphical Model Inference with Erosely Measured Data

Lili Zheng

Department of Electrical and Computer Engineering, Rice University
and

Genevera I. Allen

Department of Electrical and Computer Engineering, Rice University,
Department of Computer Science, Rice University,
Department of Statistics, Rice University,

Department of Pediatrics-Neurology, Baylor College of Medicine,
Jan and Dan Duncan Neurological Research Institute, Texas Children’s Hospital

Abstract

In this paper, we investigate the Gaussian graphical model inference problem in a novel setting that we call *erose* measurements, referring to irregularly measured or observed data. For graphs, this results in different node pairs having vastly different sample sizes which frequently arises in data integration, genomics, neuroscience, and sensor networks. Existing works characterize the graph selection performance using the minimum pairwise sample size, which provides little insights for erosely measured data, and no existing inference method is applicable. We aim to fill in this gap by proposing the first inference method that characterizes the different uncertainty levels over the graph caused by the erose measurements, named GI-JOE (**G**raph **I**nference when **J**oint **O**bservations are **E**rose). Specifically, we develop an edge-wise inference method and an affiliated FDR control procedure, where the variance of each edge depends on the sample sizes associated with corresponding neighbors. We prove statistical validity under erose measurements, thanks to careful localized edge-wise analysis and disentangling the dependencies across the graph. Finally, through simulation studies and a real neuroscience data example, we demonstrate the advantages of our inference methods for graph selection from erosely measured data.

Keywords: Uneven measurements, missing data, graph structure inference, FDR control, graph selection

1 Introduction

Graphical models have been powerful and ubiquitous tools for understanding connection and interaction patterns hidden in large-scale data [29], by exploiting the conditional dependence relationships among a large number of variables. For instance, graphical models have been applied to learn the connectivity among tens of thousands of neurons [57, 9, 48], gene expression networks [2, 16], sensor networks [14, 13], among many others. The last decade has witnessed a plethora of new statistical methods and theory proposed for various types of models in this area, including the Gaussian graphical models [59, 39, 18, 35, 7], graphical models for exponential families and mixed variables [56, 55, 10], Gaussian copula models [31, 32, 17], etc.

Despite the abundant literature in this area, most existing methods and theory for graphical models assume even measurements over the graph, where either all variables are measured simultaneously, or they are missing with similar probabilities. However, many real large-scale data sets usually take the form of *erose measurements*, which are irregular over the graph and different pairs of variables may have *drastically different sample sizes*. Such data sets frequently arise from genetics, neuroscience, sensor networks, among many others, due to various technological limits.

1.1 Problem Setting and Motivating Applications

To fix ideas, consider the following sparse Gaussian graphical model: $x \sim \mathcal{N}(0, \Sigma^*)$, $\Theta^* = (\Sigma^*)^{-1}$, where $\Theta^* \in \mathbb{R}^{p \times p}$ is the sparse precision matrix. The graph structure is dictated by the nonzero patterns in Θ^* : $\mathcal{G} = (V, E)$, $V = \{1, \dots, p\}$, $E = \{(i, j) : \Theta_{ij}^* \neq 0\}$. Suppose that we only have access to the following observations: $\{x_{i, V_i} : V_i \subseteq [p]\}_{i=1}^n$, where V_i is the observed index set of data point i . Then the joint observation set for node pair (j, k) is $O_{jk} = \{i : j, k \in V_i\}$ of size $n_{jk} = |O_{jk}|$. There are a number of applications where n_{jk} can be drastically different over different node pairs (j, k) .

Heterogeneous missingness: In a variety of biological experiments, some variables could be missing or have erroneous zero reads (dropouts) much more than others, e.g., the expression levels of certain genes [19, 23, 20, 27], or the abundance of some microbes [53]. Figure 1 shows the observational patterns and pairwise sample sizes of two real single-cell RNA sequencing (scRNA-seq) data sets, which is far from uniform.

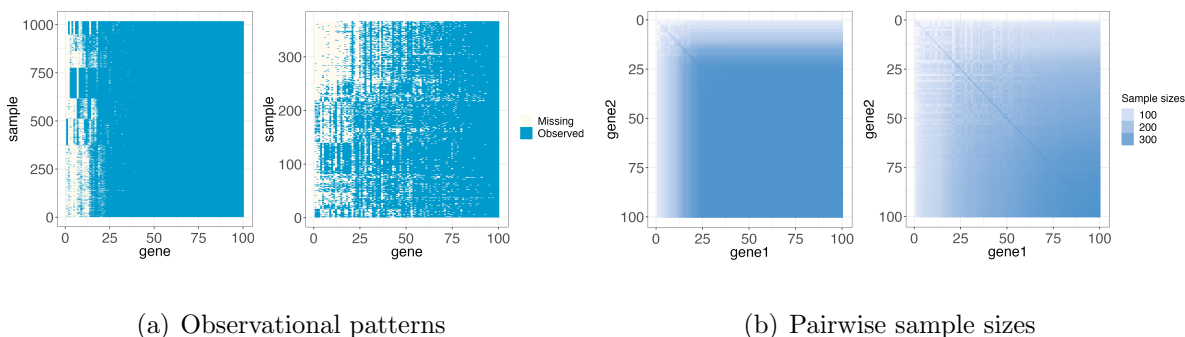


Figure 1: Observational patterns and pairwise sample sizes of two real scRNA-seq data sets [11, 12], including top 100 genes with the highest variances. The pairwise sample sizes range from 0 to 1018 (*chu* data, left) and from 12 to 366 (*darmanis*, right).

Data integration / size-constrained measurements: Non-simultaneous and uneven measurements also frequently arise from data integration and size-constrained measurements. For instance, to better understand the neuronal circuits from neuronal functional activities, one promising strategy is to estimate a large neuronal network [57, 48, 8] from in vivo calcium imaging data sets [38, 36, 44]. However, to ensure a sufficient temporal resolution of the recording, the spatial resolution is limited, putting a constraint on the number of neurons simultaneously measured [3, 63], and neuron pairs that are further from each other are less likely to be measured together. In genome-wide association studies (GWAS), it is also desirable to integrate genomic data across multiple sources due to the limited sample sizes of each data set, while these different sources might have different genomic coverage [6]. Similar measurement constraints also arise from sensor networks where it is extremely expensive to synchronize a large number of sensors [14, 13].

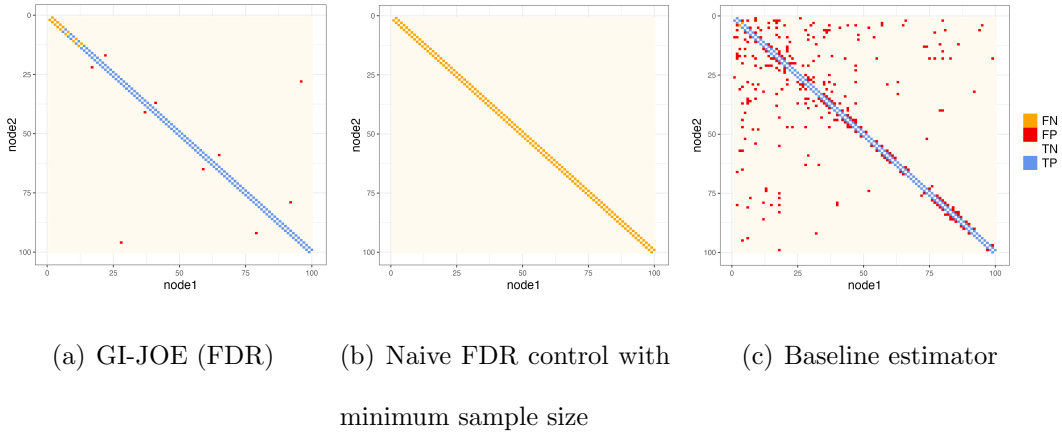


Figure 2: Graph selection and inference for a chain graph with 100 nodes, when the data has the *darmanis* measurement pattern (see Figure 1). The graph selected by our GI-JOE (FDR) approach is presented in (a); (b) is obtained by an ad hoc implementation of the debiased graphical lasso [24] that plugs in the minimum pairwise sample size, which is too conservative and identifies no edge at all; (c) is the estimated graph by a baseline approach [28], which plugs in a covariance estimate into the graphical lasso, and the many false positives suggest that the graph selection problem with such data set is non-trivial.

1.2 Limitations of Existing Works for Erode Measurements

To learn graphical models from erosely measured data, one might want to leverage the current literature on graphical models with missing data [42, 28, 51, 37]. However, most of these works assume the variables are missing independently with the same missing probability. While [37] allows for arbitrary missing probabilities and dependency in their problem formulation, their theoretical guarantees still hinge on the minimum observational probability. Using the minimum pairwise sample size over the whole graph to characterize the performance of the graph learning result can be too coarse and provides little insights to erosely measured data sets. Interestingly, one recent work [62] provides a localized theoretical guarantee for neighborhood selection consistency, requiring only sample size conditions imposed upon the corresponding neighbors instead of all node pairs. Such theoretical results suggest that the estimation accuracy should vary over the graph when measurements are erose, and a coarse characterization based on the minimum sample size would only provide

insights for the worst part of the graph estimate.

Inspired by this intuition, here arises one natural question: can we provide an inference method that quantifies the different uncertainty levels over the graph? Prior works on graphical model inference mostly consider simultaneous measurements of all variables which leads to the same sample size over the graph [24, 40, 21, 58, 34, 25]; or they consider the missing data setting where all variables are missing independently with the same missing probability [4], still leading to approximately the same sample sizes. To the best of our knowledge, there is no applicable graph inference method for the general observational patterns and erose measurements that we are considering. If practitioners want to apply these existing inference methods with erosely measured data, they have to come up with one single sample size quantity n to determine the uncertainty levels for each edge. To ensure the validity of the test, one ad hoc way might be to plug in the minimum pairwise sample size, which can be extremely conservative and has no power (see Figure 2(b)).

The rest of the paper is organized as follows. We first review the set-ups and neighborhood selection results from [62] in Section 2, which serves as an inspiration and basis of our graph inference method under erose measurements; We then introduce our GI-JOE approach, the key contribution of this paper, in Section 3 and 4. In particular, Section 3 is devoted to the edge-wise inference method, and for any node pair, we characterize its type I error and power based on the sample sizes involving the node pair’s neighbors. Section 4 focuses on the FDR control procedure, also shown to be theoretically valid under appropriate conditions. The numerical experiments including simulations and real data examples are included in Sections 5. We conclude with discussion of some open questions in Section 6.

Notations: For any matrix $A \in \mathbb{R}^{p_1 \times p_2}$, let $\|A\|_\infty = \max_{j,k} |A_{j,k}|$, $\|A\| = \sup_{\|u\|_2=1} \|Au\|_2$ be its spectral norm, and $\|A\|_\infty = \max_{j=1,\dots,p_1} \sum_{k=1}^{p_2} |A_{j,k}|$ be the matrix-operator ℓ_∞ to ℓ_∞ norm. For any tensor $\mathcal{T} \in \mathbb{R}^{p_1 \times p_2 \times p_3 \times p_4}$ and matrix $A \in \mathbb{R}^{p_1, q_1}$ define the tensor-matrix/vector product $\mathcal{T} \times_1 A \in \mathbb{R}^{q_1 \times p_2 \times p_3 \times p_4}$ as follows: $(\mathcal{T} \times_1 A)_{i_1, i_2, i_3, i_4} = \sum_{j_1=1}^{p_1} A_{j_1, i_1} \mathcal{T}_{j_1, i_2, i_3, i_4}$.

Similarly we extend this definition of tensor-matrix product to other modes.

2 Graph Selection with Erode Measurements

In this section, we review the set-up and neighborhood selection theory in [62], as it forms the basis of our inference procedure and theory presented in Section 3. In particular, [62] studied a variant of the neighborhood lasso method. We follow their approach and focus on the neighborhood lasso instead of other graph estimation methods such as graphical lasso [59] or CLIME [7], since its form makes it easier to disentangle the effects of different parts of the graphs on each other.

The neighborhood lasso algorithm proposed in [62] consists of two steps: estimating the true covariance Σ^* and plug in the estimate into a neighborhood lasso estimator. An unbiased estimate $\widehat{\Sigma}$ is defined as follows: given observations $\{x_{i,V_i}\}_{i=1}^n$, for each entry (j, k) , $\widehat{\Sigma}_{j,k} = \frac{1}{n_{j,k}} \sum_{i:j,k \in V_i} x_{i,j}x_{i,k}$. However, one drawback of $\widehat{\Sigma}$ is its possibly negative eigenvalues, which could lead to both optimization and statistical issues in neighborhood lasso. To ensure convexity and preserve the entry-wise error bounds for $\widehat{\Sigma}_{j,k} - \Sigma_{j,k}^*$, an additional projection step upon the positive semi-definite cone is considered:

$$\widetilde{\Sigma} = \arg \min_{\Sigma \succ 0} \max_{j,k} \sqrt{n_{j,k}} |\Sigma_{j,k} - \widehat{\Sigma}_{j,k}|, \quad (1)$$

where $n_{j,k}$ is the pairwise sample size associated with node pair (j, k) , defined as in Section 1.1. The projection problem (11) can be solved by the ADMM, and we include the detailed optimization steps in Section A of the Appendix.

Given the covariance estimate $\widetilde{\Sigma}$, for any target node a of which we want to estimate the neighborhood, consider the following neighborhood regression problem:

$$\widehat{\theta}^{(a)} = \arg \min_{\theta \in \mathbb{R}^p, \theta_a = 0} \frac{1}{2} \theta^\top \widetilde{\Sigma} \theta - \widetilde{\Sigma}_{a,\cdot} \theta + \sum_{j=1}^p \lambda_j^{(a)} |\theta_j|, \quad (2)$$

where $\lambda^{(a)} = (\lambda_1^{(a)}, \dots, \lambda_p^{(a)})^\top \in \mathbb{R}^p$ is a vector of tuning parameters, with each entry $\lambda_j^{(a)}$ corresponding to a potential edge connecting node j and a . The solution $\widehat{\theta}^{(a)}$ serves as an

estimate for $\theta^{(a)*} = \arg \min_{\theta \in \mathbb{R}^p, \theta_a=0} \frac{1}{2} \theta^\top \Sigma^* \theta - \Sigma_{a,\cdot}^* \theta$, which satisfies $\theta_{\setminus a}^{(a)*} = (\Sigma_{\setminus a, \setminus a}^*)^{-1} \Sigma_{\setminus a, a}^* = \frac{1}{\Theta_{a,a}^*} \Theta_{\setminus a, a}^*$, and hence the support set of $\theta^{(a)*}$ equals the true neighborhood of node a : $\mathcal{N}_a = \{j \neq a : \Theta_{a,j}^* \neq 0\}$. Then one can estimate \mathcal{N}_a by the support of $\widehat{\theta}^{(a)}$: $\widehat{\mathcal{N}}_a = \{j \neq a : \widehat{\theta}^{(a)} \neq 0\}$. It was shown in [62] that the neighborhood selection consistency is guaranteed with sample size conditions involving the neighbors of node a . Here, we present a similar theoretical result, with only a slight modification on the tuning parameter choice, while the proofs are very similar. In particular, the following assumption and quantities are useful: $\kappa_1^{(a)} = \|\theta^{(a)*}\|_1$, $\kappa_2^{(a)} = \left\| (\Sigma_{\mathcal{N}_a, \mathcal{N}_a}^*)^{-1} \right\|_\infty$, $\kappa_3^{(a)} = \left\| \Sigma_{(\overline{\mathcal{N}}_a)^c, \mathcal{N}_a}^* \right\|_\infty$, $\theta_{\min}^{(a)} = \min_{\theta_j^{(a)*} \neq 0} |\theta_j^*|$. Also let $\gamma_a = \frac{\max_{j \in \overline{\mathcal{N}}_a^c} \min_k n_{j,k}}{\min_{j \in \mathcal{N}_a} \min_k n_{j,k}}$ denote the sample size ratio between non-neighbors of a and neighbors of a .

Assumption 1 (Mutual incoherence condition). *The population covariance Σ^* satisfies*

$$\left\| \Sigma_{(\overline{\mathcal{N}}_a)^c, \mathcal{N}_a}^* (\Sigma_{\mathcal{N}_a, \mathcal{N}_a}^*)^{-1} \right\|_\infty \leq 1 - \gamma \text{ for some } 0 < \gamma \leq 1.$$

Theorem 1 (Neighborhood Selection Consistency, Similar to [62]). *Consider the model setting described in Section 1.1 and the estimator $\widehat{\theta}^{(a)}$ defined in (2). Suppose Assumption 1 holds, and the tuning parameters $\lambda_j^{(a)}$'s in (2) satisfy*

$$\lambda_j^{(a)} \asymp \|\Sigma^*\|_\infty \frac{\|\Theta_{:,a}^*\|_1}{\Theta_{a,a}^*} \sqrt{\frac{\log p}{\min_k n_{j,k}}}. \text{ If } \gamma_a \leq \left(\frac{2-c\gamma}{2-\gamma}\right)^2 \text{ for some constant } c > 0, \text{ and}$$

$$\min_{j \in \mathcal{N}_a} \min_k n_{j,k} \geq \frac{C_2 \|\Sigma^*\|_\infty^2 \kappa_2^2}{\gamma^2} \left[(\kappa_3^2 + 1) d_a^2 + \frac{(\gamma + 4)^2 (\kappa_1 + 1)^2}{(\theta_{\min}^{(a)})^2} \right] \log p, \quad (3)$$

then $\widehat{\mathcal{N}}_a = \{j : \widehat{\theta}_j^{(a)} \neq 0\} = \mathcal{N}_a$ with probability at least $1 - p^{-c}$ for some absolute constants $c, C_1, C_2 > 0$.

For completeness, we still include the proof of Theorem 1 in Section G of the Appendix. We also extend the analysis for estimation errors and show ℓ_2 and ℓ_1 error bounds for $\widehat{\theta}^{(a)} - \theta^{(a)*}$, which are useful for our inference theory. These new error bounds, some discussion of Theorem 1 and a pictorial illustration of the sample size condition for recovering node a ' neighborhood can be found in Section B of the Appendix. Theorem 1 suggests it is possible to provide a localized characterization of the graph estimation performance under erose

measurements, and this inspires us to develop an inference method that quantifies the uneven uncertainty levels over the graph.

3 Edge-wise Inference: Quantifying Uncertainties from Erode Measurements

In this section, we propose our GI-JOE method for edge-wise inference with erode data. The key idea follows the debiased lasso [45], while the main challenge and innovation is characterizing the uncertainty level associated with each edge-wise statistic. We first introduce our edge-wise debiased statistic $\tilde{\theta}_b^{(a)}$, and characterize its asymptotic distribution in Section 3.1; We further propose a consistent estimator of its variance and establish statistical validity of edge-wise inference in Section 3.2.

Throughout this section, suppose that we are interested in testing whether there is an edge between node $a \neq b$. To debias $\hat{\theta}_b^{(a)}$ defined in (2), we consider a debiasing matrix $\Theta^{(a)*} \in \mathbb{R}^{p \times p}$, which satisfies $\Theta_{a,:}^{(a)*} = 0$, $\Theta_{:,a}^{(a)*} = 0$, and $\Theta_{\setminus a, \setminus a}^{(a)*} = (\Sigma_{\setminus a, \setminus a}^*)^{-1}$. Denote by $\mathcal{N}_j^{(a)}$ the support set of $\Theta_{j,:}^{(a)*}$ and $\bar{\mathcal{N}}_j^{(a)} = \mathcal{N}_j^{(a)} \cup j$. By block matrix inverse formula, $\Theta_{j,:}^{(a)*} = \Theta_{j,:}^* - \frac{\Theta_{j,a}^*}{\Theta_{a,a}^*} \Theta_{a,:}^*$ and hence is also sparse with $d_j^{(a)} = |\mathcal{N}_j^{(a)}| \leq d_a + d_j$. We estimate its b th row $\Theta_{b,:}^{(a)*}$ by performing another neighborhood regression for node b :

$$\hat{\Theta}_{b, \setminus b}^{(a)} = -\hat{\tau}^{(a,b)} \hat{\theta}_{\setminus b}^{(a,b)}, \quad \hat{\Theta}_{b,b}^{(a)} = \hat{\tau}^{(a,b)}, \quad (4)$$

$$\hat{\theta}^{(a,b)} = \arg \min_{\theta \in \mathbb{R}^p, \theta_a = \theta_b = 0} \frac{1}{2} \theta^\top \tilde{\Sigma} \theta - \tilde{\Sigma}_{b,:} \theta + \sum_{k=1}^p \lambda_k^{(a,b)} |\theta_k|, \quad (5)$$

$$\hat{\tau}^{(a,b)} = (\tilde{\Sigma}_{b,b} - \tilde{\Sigma}_{b,:} \hat{\theta}^{(a,b)})^{-1},$$

and $\lambda_k^{(a,b)}$'s are tuning parameters depending on the pairwise sample sizes $\min_{i \in [p]} n_{i,b}$. Then the

debiased neighborhood lasso estimator for node pair (a, b) is

$$\tilde{\theta}_b^{(a)} = \hat{\theta}_b^{(a)} - \hat{\Theta}_{b,:}^{(a)} (\hat{\Sigma} \hat{\theta}^{(a)} - \hat{\Sigma}_{:,a}). \quad (6)$$

Here we use $\widehat{\Sigma}$ in the second debiasing term instead of $\widetilde{\Sigma}$, since $\widehat{\Sigma}$ has a closed form for each entry, making it possible to derive normal approximation result.

3.1 Normal Approximation of Debaised Edge-wise Statistic

Although the edge-wise statistic $\widetilde{\theta}_b^{(a)}$ defined in (6) is similar to the debaised lasso in the literature, its asymptotical normality is not readily present due to the erose measurement setting we are concerned with. In the following, we present a novel characterization of $\widetilde{\theta}_b^{(a)}$ that consists of a bias term and an asymptotically normal error term, each term depending on one pairwise sample size quantity, respectively. Before presenting the main theorem, we first define and discuss these two key sample size quantities.

Given the target node pair (a, b) , define two sets of node pairs involving a, b 's neighbors: $S_1(a, b) = \{(j, k) : j \text{ or } k \in \mathcal{N}_a \cup \overline{\mathcal{N}}_b^{(a)}\}$, $S_2(a, b) = \{(j, k) : \Theta_{j,b}^{(a)*} \Theta_{k,a}^* + \Theta_{k,b}^{(a)*} \Theta_{j,a}^* \neq 0\}$, where $\overline{\mathcal{N}}_b^{(a)}$ and matrix $\Theta^{(a)*}$ are defined in the beginning of Section 3. Here the order of a and b matters since we first apply neighborhood lasso for node a and then debias its entry $\widehat{\theta}_b^{(a)}$. The following proposition characterizes the index set $S_2(a, b)$ and $\overline{\mathcal{N}}_b^{(a)}$ through their relationships with $\overline{\mathcal{N}}_a$ and $\overline{\mathcal{N}}_b$. Figure 3 also gives a pictorial illustration of $S_1(a, b)$ and $S_2(a, b)$ for a chain graph.

Proposition 1. *For any given support set $\overline{E} \subseteq [p] \times [p]$, the following holds except when $\Theta_{\overline{E}}^* \in \mathbb{R}^{|\overline{E}|}$ falls in a measure zero set: (i) $S_2(a, b) = (\overline{\mathcal{N}}_a \times \overline{\mathcal{N}}_b^{(a)}) \cup (\overline{\mathcal{N}}_b^{(a)} \times \overline{\mathcal{N}}_a)$. (ii) If $b \in \mathcal{N}_a$, $\overline{\mathcal{N}}_b^{(a)} = \overline{\mathcal{N}}_a \cup \overline{\mathcal{N}}_b$; otherwise, $\overline{\mathcal{N}}_b^{(a)} = \overline{\mathcal{N}}_b$.*

The two key sample size quantities are then defined as the minimum pairwise sample sizes within these two sets: $n_1^{(a,b)} = \min_{(j,k) \in S_1(a,b)} n_{j,k}$, $n_2^{(a,b)} = \min_{(j,k) \in S_2(a,b)} n_{j,k}$, which will be shown to determine the bias and variance of the edge-wise statistic. Similar to the the support recovery guarantee in Theorem 1, here we also define the sample size ratio for node b here by $\gamma_b^{(a)} = \frac{\max_{j \in \overline{\mathcal{N}}_b^{(a)c}} \min_k n_{j,k}}{\min_{j \in \mathcal{N}_b^{(a)}} \min_k n_{j,k}}$. The following covariance parameters are also useful: let

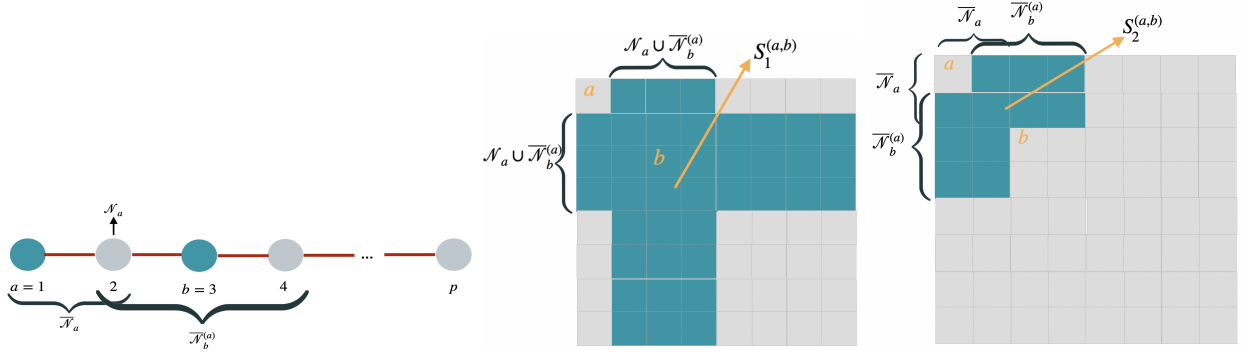


Figure 3: An illustration of the set $S_1(a, b)$ and $S_2(a, b)$ in a chain graph, when $a = 1$ and $b = 3$. The minimum sample size in $S_1(a, b)$ determines the bias for estimating edge (a, b) , while the minimum sample size in $S_2(a, b)$ determines the variance for estimating edge (a, b) .

$\mathcal{T}^*, \mathcal{T}^{(n)*} \in \mathbb{R}^{p \times p \times p \times p}$ satisfy

$$\mathcal{T}_{j,k,j',k'}^* = \text{Cov}(X_j X_k, X_{j'} X_{k'}) = \Sigma_{j,j'}^* \Sigma_{k,k'}^* + \Sigma_{j,k'}^* \Sigma_{k,j'}^*$$

for $1 \leq j, k, j', k' \leq p$, and $(\mathcal{T}^{(n)*})_{j,k,j',k'} = \mathcal{T}_{j,k,j',k'}^* \frac{n_{j,k,j',k'}}{n_{j,k} n_{j',k'}}$, where $n_{j,k,j',k'} = |\{i : j, k, j', k' \in V_i\}|$ is the number of joint measurements for j, k, j', k' .

Assumption 2 (Sample size condition for accurate estimation).

$$n_1^{(a,b)} \geq C \frac{\|\Sigma^*\|_\infty^2}{\lambda_{\min}^2(\Sigma^*)} (\kappa_{\Sigma^*}^2 + \gamma_a + \gamma_b^{(a)}) (d_a + d_b + 1)^2 \log p,$$

Assumption 2 is similar to the sample size condition in Theorem 1, while the only difference lies that here $\min_k n_{j,k}$ needs to be large as long as $j \in \mathcal{N}_a \cup \overline{\mathcal{N}}_b^{(a)}$ instead of \mathcal{N}_a only, so that both $\hat{\theta}^{(a)}$ and $\hat{\Theta}_{b,:}^{(a)}$ are accurate estimators for $\theta^{(a)*}$ and $\Theta_{b,:}^{(a)*}$.

Assumption 3 (Sample size condition for normal approximation). $C_\varepsilon(\Sigma^*) (d_a + d_b + 1)^{2+\varepsilon} = o(n_2^{(a,b)})$ for some constant $\varepsilon > 0$, where $C_\varepsilon(\Sigma^*) = \left(\frac{C(1+2/\varepsilon)\|\Sigma^*\|_\infty}{\lambda_{\min}(\Sigma^*)} \right)^{2+\varepsilon}$.

Due to the erose measurements, establishing the Lyapunov condition is much more complicated than the same sample size setting. Assumption 3 is a technical assumption we need in this step so that the CLT can be applied to derive asymptotic normality result.

Assumption 4 (Sample size condition for controlling bias).

$$n_1^{(a,b)} \gg C^2(\Theta^*; a, b)(\kappa_{\Theta^*}^4 + \gamma_a + \gamma_b^{(a)})[(d_a + d_b + 1) \log p]^2 \frac{n_2^{(a,b)}}{n_1^{(a,b)}}, \quad (7)$$

where $C(\Theta^*; a, b) = \frac{C\kappa_{\Theta^*}^3 \|\Theta_{:,a}^*\|_1 \|\Theta_{:,b}^{(a)*}\|_1}{\min_{(j,k) \in \mathcal{S}_2(a,b)} |\Theta_{b,j}^{(a)*} \Theta_{a,k}^* + \Theta_{b,k}^{(a)*} \Theta_{a,j}^*|}$.

Remark 1. Rearranging (7), we can also write the this sample size condition as

$$n_1^{(a,b)} \gg C(\Theta^*; a, b)(\kappa_{\Theta^*}^2 + \sqrt{\gamma_a} + \sqrt{\gamma_b^{(a)}})[(d_a + d_b + 1) \log p] \sqrt{n_2^{(a,b)}}.$$

Remark 2. One may be confused when seeing $n_1^{(a,b)}$ both on the left and right hand side of (7). In fact, we present it this way in order to connect it to the same sample size setting where $n_2^{(a,b)} = n_1^{(a,b)} = n$, and thus (7) becomes $n \gg C^2(\Theta^*; a, b)\kappa_{\Theta^*}^4 [(d_a + d_b + 1) \log p]^2$. This is similar to the requirement in prior results on debiased lasso and debiased graphical lasso [45, 61, 24] with the same sample sizes, which requires $n \gg d^2 \log^2 p$. The additional price we paid for uneven sample sizes is reflected in the sample size ratios γ_a , $\gamma_b^{(a)}$ and $\frac{n_2^{(a,b)}}{n_1^{(a,b)}}$.

Remark 3 (Effect of γ_a , $\gamma_b^{(a)}$ and $\frac{n_2^{(a,b)}}{n_1^{(a,b)}}$). γ_a , $\gamma_b^{(a)}$ are the sample size ratios between the most well measured non-neighbor and the worst measured neighbor of a and b . These two quantities have a negative effect on our theory, as when the sample sizes for the non-neighbors are all much larger than the neighbors, the neighbors would suffer from much stronger regularization than non-neighbors. While for the sample size ratio $\frac{n_2^{(a,b)}}{n_1^{(a,b)}}$, note that when $n_2^{(a,b)}$ grows too much more quickly than $n_1^{(a,b)}$, the bias term would dominate the variance term and then the normal approximation of $\tilde{\theta}_b^{(a)}$ would not hold.

The following theorem establishes the asymptotic normality of $\tilde{\theta}_b^{(a)} + \frac{\Theta_{a,b}^*}{\Theta_{a,a}^*}$ under these three sample size assumptions, and Corollary 1 presents its direct consequence when all pairwise sample sizes are equal ($n_{i,j} = n$), with simplified sample size assumptions that is comparable to prior literature [45, 24].

Theorem 2 (Asymptotic Normality). Consider the model setting described in Section 1.1 and the debiased edge-wise statistic $\tilde{\theta}_b^{(a)}$ defined in (6). Suppose that $\lambda^{(a)}$ in (2) is chosen as

in Theorem 1, and $\lambda^{(a,b)}$ in (27) satisfies $\lambda_k^{(a,b)} \asymp \|\Sigma^*\|_\infty \frac{\|\Theta_{b,:}^{(a)*}\|_1}{\Theta_{b,b}^{(a)*}} \sqrt{\frac{\log p}{\min_{j \in [p]} n_{j,k}}}$. Then we have the following decomposition:

$$\tilde{\theta}_b^{(a)} = -\frac{\Theta_{a,b}^*}{\Theta_{a,a}^*} + B + E. \quad (8)$$

If Assumption 2 holds, then with probability at least $1 - Cp^{-c}$, $|B| \leq C(\Theta^*, \gamma_a, \gamma_b^{(a)}) \frac{(d_a + d_b + 1) \log p}{n_1^{(a,b)}}$, where $C(\Theta^*, \gamma_a, \gamma_b^{(a)}) = C\kappa_{\Sigma^*}(\kappa_{\Sigma^*}^2 + \sqrt{\gamma_a} + \sqrt{\gamma_b^{(a)}}) \|\Sigma^*\|_\infty^2 \|\Theta_{:,a}^*\|_1 \|\Theta_{:,b}^{(a)*}\|_1$. If Assumption 3 holds, $\sigma_n^{-1}(a,b)E \xrightarrow{d} \mathcal{N}(0,1)$ with $\sigma_n^2(a,b) = \frac{1}{\Theta_{aa}^{*2}} \mathcal{T}^{(n)*} \times_1 \Theta_{:,b}^{(a)*} \times_2 \Theta_{:,a}^* \times_3 \Theta_{:,b}^{(a)*} \times_4 \Theta_{:,a}^*$. Furthermore, if Assumptions 2-4 hold,

$$\sigma_n^{-1}(a,b) \left(\tilde{\theta}_b^{(a)} + \frac{\Theta_{a,b}^*}{\Theta_{aa}^*} \right) \xrightarrow{d} \mathcal{N}(0,1).$$

The proof of Theorem 2 is deferred to Section G of the Appendix.

Remark 4 (Bias-Variance decomposition). *As suggested by (8), the error of the debiased lasso estimator can be decomposed into a bias term (B) and a variance term (E), where B depends on the minimum pairwise sample size $n_1^{(a,b)}$ between any nodes and the neighbors of nodes a, b , while E depends only on the sample size $n_2^{(a,b)}$ for nodes within the neighborhoods of a, b (See Figure 3). When $C(\Theta^*, \gamma_a, \gamma_b^{(a)})$ is viewed as a constant, then $|B| \asymp \frac{(d_a + d_b + 1) \log p}{n_1^{(a,b)}}$, and the term E scales as the asymptotic standard deviation $\sigma_n(a,b)$, which is further characterized by Proposition 2.*

Proposition 2 (Variance characterization). *The variance term $\sigma_n^2(a,b)$ satisfies*

$$\begin{aligned} \sigma_n(a,b) &\leq \frac{\sqrt{2} \lambda_{\max}(\Sigma^*) \|\Theta_{:,b}^{(a)*}\|_2 \|\Theta_{:,a}^*\|_2}{\Theta_{a,a}^*} (n_2^{(a,b)})^{-\frac{1}{2}} \leq \sqrt{2} \kappa_{\Sigma^*}^2 (n_2^{(a,b)})^{-\frac{1}{2}}, \\ \sigma_n(a,b) &\geq \frac{\sqrt{2} \lambda_{\min}(\Sigma^*) \min_{(j,k) \in S_2(a,b)} \left| \Theta_{b,j}^{(a)*} \Theta_{a,k}^* + \Theta_{b,k}^{(a)*} \Theta_{a,j}^* \right|}{2\Theta_{a,a}^*} (n_2^{(a,b)})^{-\frac{1}{2}}. \end{aligned}$$

When $C_1 \leq \frac{\lambda_{\min}(\Sigma^*) \min_{(j,k) \in S_2(a,b)} \left| \Theta_{b,j}^{(a)*} \Theta_{a,k}^* + \Theta_{b,k}^{(a)*} \Theta_{a,j}^* \right|}{\Theta_{a,a}^*} \leq \kappa_{\Sigma^*}^2 \leq C_2$, Proposition 2 suggests that $\sigma_n(a,b) \asymp (n_2^{(a,b)})^{-1/2}$.

Corollary 1 (Normal Approximation with the Same Sample Size). *Consider the same model, edge-wise statistic and tuning parameters as in Theorem 2. When the pairwise sample sizes*

are all equal: $n_{j,k} = n$, then if

$$n \gg C^2(\Theta^*; a, b) \kappa_{\Theta^*}^4 (d_a + d_b + 1)^2 \log^2 p + C_\epsilon(\Sigma^*) (d_a + d_b + 1)^{2+\epsilon}$$

for some $\epsilon > 0$, we have $\sqrt{n} \left(\tilde{\theta}_b^{(a)} + \frac{\Theta_{a,b}^*}{\Theta_{aa}^*} \right) \xrightarrow{d} \mathcal{N} \left(0, \frac{\Theta_{a,a}^* \Theta_{b,b}^* - (\Theta_{a,b}^*)^2}{(\Theta_{a,a}^*)^2} \right)$. Here $C(\Theta^*; a, b)$ and $C_\epsilon(\Sigma^*)$ are as defined in Assumption 3 and 4, depending only on Σ^* and Θ^* .

Remark 5. Corollary 1 is a direct consequence of Theorem 2. If $d_a + d_b + 1 \leq (\log p)^c$ for some $c > 0$, the sample size condition is the same as the prior literature on debiased lasso and debiased graphical lasso [45, 24]. Note that Corollary 1 does not require all variables are measured simultaneously, and hence we can also apply it to the settings where only pairwise measurements or general size-constrained measurements are available [13].

3.2 Variance Estimation and Edge-wise Inference

In this section, we propose our GI-JOE method for edge-wise statistical inference. That is, we test the null hypothesis: $H_0 : \Theta_{a,b}^* = 0$ against $H_1 : \Theta_{a,b}^* \neq 0$. With the aid of Theorem 2, we still need to estimate the unknown variance $\sigma_n^2(a, b)$ so that we can construct a test statistic with known distribution under H_0 .

Recall the definition of $\sigma_n^2(a, b)$ in Theorem 2, and the fact that $\mathcal{T}_{j,k,j',k'}^* = \Sigma_{j,j'}^* \Sigma_{k,k'}^* + \Sigma_{j,k'}^* \Sigma_{k,j'}^*$, $(\mathcal{T}^{(n)*})_{j,k,j',k'} = \mathcal{T}_{j,k,j',k'}^* \frac{n_{j,k,j',k'}}{n_{j,k} n_{j',k'}}$, here we define an estimator $\hat{\sigma}_n^2(a, b)$ as follows:

$$\hat{\sigma}_n^2(a, b) = \hat{\mathcal{T}}^{(n)} \times_1 \hat{\Theta}_{b,:}^{(a)} \times_2 \hat{\theta}^{(a)} \times_3 \hat{\Theta}_{b,:}^{(a)} \times_4 \hat{\theta}^{(a)}, \quad (9)$$

where $\hat{\mathcal{T}}^{(n)}$ is an estimator for $\mathcal{T}^{(n)*}$: $(\hat{\mathcal{T}}^{(n)})_{j,k,j',k'} = (\hat{\Sigma}_{j,j'} \hat{\Sigma}_{k,k'} + \hat{\Sigma}_{j,k'} \hat{\Sigma}_{k,j'}) \frac{n_{j,k,j',k'}}{n_{j,k} n_{j',k'}}$; $\hat{\theta}^{(a)} \in \mathbb{R}^p$ serves as an estimate for $\frac{\Theta_{:,a}^*}{\Theta_{a,a}^*}$ and it satisfies $\hat{\theta}_a^{(a)} = 1$ and $\hat{\theta}_{\setminus a}^{(a)} = -\hat{\theta}_{\setminus a}^{(a)}$.

Assumption 5 (Sample size condition for variance estimation).

$$n_1^{(a,b)} \gg \frac{C^4(\Theta^*; a, b)}{\kappa_{\Theta^*}^4} (d_a + d_b + 1)^2 \log p \left(\frac{n_2^{(a,b)}}{n_1^{(a,b)}} \right)^2,$$

where $C(\Theta^*; a, b)$ is defined as in Assumption 4.

Proposition 3 (Estimation consistency of variance). *Under Assumptions 2, 4 and 5, if the tuning parameters are as specified in Theorem 2, then (9) satisfies $\frac{\widehat{\sigma}_n^{-1}(a,b)}{\sigma_n^{-1}(a,b)} \xrightarrow{p} 1$.*

Theorem 3 (Normal approximation with unknown variance). *With appropriately chosen tuning parameters as in Theorem 2, if Assumptions 2-5 hold, $\widehat{\sigma}_n^{-1}(a,b)(\widetilde{\theta}_b^{(a)} - \theta_b^{(a)*}) \xrightarrow{d} \mathcal{N}(0,1)$ for $\widehat{\sigma}_n^2(a,b)$ defined in (9) and $\widetilde{\theta}_b^{(a)}$ defined in (6).*

The proof of Theorem 3 is deferred to Section G of the Appendix. Theorem 3 suggests that for testing $H_0 : \Theta_{a,b}^* = 0$, we can use the test statistic $\widehat{z}(a,b) = \widehat{\sigma}_n^{-1}(a,b)\widetilde{\theta}_b^{(a)}$. For a given type I error α , we reject H_0 if $|\widehat{z}(a,b)| \geq z_{\alpha/2}$, where $z_{\alpha/2}$ is the $1 - \frac{\alpha}{2}$ quantile of standard Gaussian distribution. We can also construct a confidence interval for $\theta_b^{(a)*} = -\frac{\Theta_{a,b}^*}{\Theta_{a,a}^*}$:

$$\widehat{\mathcal{C}}_{\alpha}^{a,b} = [\widetilde{\theta}_b^{(a)} - z_{\alpha/2}\widehat{\sigma}_n(a,b), \widetilde{\theta}_b^{(a)} + z_{\alpha/2}\widehat{\sigma}_n(a,b)]. \quad (10)$$

Our full GI-JOE (edge-wise inference) procedure is summarized in Algorithm 1. The following Corollary characterizes the type I error and power of the GI-JOE approach.

Theorem 4 (Type I error and Power Analysis). *Consider the model setting described in Section 1.1 and let $p_{a,b}$ be the p -value given by Algorithm 1 for node pair (a,b) . If all conditions in Theorem 3 hold so that as $n, p \rightarrow \infty$, p, d_a, d_b and sample sizes $n_1^{(a,b)}, n_2^{(a,b)}$ scale as in Assumption 4 and Assumption 5, then the following holds:*

1. *Under the null hypothesis $H_0 : \Theta_{a,b}^* = 0$, $\lim_{n,p \rightarrow \infty} \mathbb{P}(p_{a,b} \leq \alpha) = \alpha$;*

2. *Under the alternative hypothesis $H_1 : \frac{\Theta_{a,b}^*}{\Theta_{a,a}^*} = \delta_n$,*

(a) *if $\lim_{n,p \rightarrow \infty} \frac{\delta_n}{\sigma_n(a,b)} = 0$, $\lim_{n,p \rightarrow \infty} \mathbb{P}(p_{a,b} \leq \alpha) = \alpha$;*

(b) *if $\lim_{n,p \rightarrow \infty} \frac{\delta_n}{\sigma_n(a,b)} = \delta$ for $\delta \neq 0$; $\lim_{n,p \rightarrow \infty} \mathbb{P}(p_{a,b} \leq \alpha) \geq \Phi(|\delta| - z_{\alpha/2})$, where $\Phi(\cdot)$ is the distribution function of standard Gaussian $\mathcal{N}(0,1)$;*

(c) *if $\lim_{n,p \rightarrow \infty} \frac{\delta_n}{\sigma_n(a,b)} = +\infty$, $\lim_{n,p \rightarrow \infty} \mathbb{P}(p_{a,b} \leq \alpha) = 1$.*

The proof of Theorem 4 is deferred to Section G of the Appendix. Theorem 4 suggests that when all conditions of Theorem 3 hold, the type I error of this test is asymptotically α .

Algorithm 1: GI-JOE: edge-wise inference

1 Input: Data set $\{x_{i,V_i} : V_i \subset [p]\}_{i=1}^n$, pairwise sample sizes $\{n_{j,k}\}_{j,k=1}^p$, node pair (a, b) for testing with $a \neq b$, significant level α

1. Compute the entry-wise estimate of the covariance matrix $\widehat{\Sigma} \in \mathbb{R}^{p \times p}$:

$$\widehat{\Sigma}_{j,k} = \frac{1}{n_{j,k}} \sum_{j,k \in V_i} x_{i,j} x_{i,k}$$

2. Project $\widehat{\Sigma}$ onto the positive semi-definite cone: compute $\widetilde{\Sigma}$ as in (11).

3. Perform neighborhood regression for node a : compute $\widehat{\theta}^{(a)}$ as in (2)

4. Estimate the debiasing matrix by performing neighborhood regression for node b upon nodes $[p] \setminus \{a, b\}$: compute $\widehat{\Theta}_{b,:}^{(a)}$ as in (28) and (27).

5. Debias the neighborhood lasso estimate: $\widetilde{\theta}_b^{(a)} = \widehat{\theta}_b^{(a)} - \widehat{\Theta}_{b,:}^{(a)} (\widehat{\Sigma} \widehat{\theta}^{(a)} - \widehat{\Sigma}_{:,a})$.

6. Estimate the variance: $\widehat{\sigma}_n^2 = \widehat{\mathcal{T}}^{(n)} \times_1 \widehat{\Theta}_{b,:}^{(a)} \times_2 \widehat{\theta}^{(a)} \times_3 \widehat{\Theta}_{b,:}^{(a)} \times_4 \widehat{\theta}^{(a)}$, where

$$(\widehat{\mathcal{T}}^{(n)})_{j,k,j',k'} = (\widehat{\Sigma}_{j,j'} \widehat{\Sigma}_{k,k'} + \widehat{\Sigma}_{j,k'} \widehat{\Sigma}_{k,j'}) \frac{n_{j,k,j',k'}}{n_{j,k} n_{j',k'}}$$

and $\widehat{\theta}^{(a)}$ is defined as $\widehat{\theta}_a^{(a)} = 1$ and $\widehat{\theta}_{\setminus a}^{(a)} = -\widehat{\theta}_{\setminus a}^{(a)}$.

7. Compute p -value $p_{a,b} = 2(1 - \Phi(\frac{\widetilde{\theta}_b^{(a)}}{\widehat{\sigma}_n(a,b)}))$ where $\Phi(\cdot)$ is the distribution function of standard Gaussian; confidence interval $\widehat{\mathbb{C}}_\alpha^{a,b} = [\widetilde{\theta}_b^{(a)} - z_{\alpha/2} \widehat{\sigma}_n(a,b), \widetilde{\theta}_b^{(a)} + z_{\alpha/2} \widehat{\sigma}_n(a,b)]$

Output: p -value $p_{a,b}$, confidence interval $\widehat{\mathbb{C}}_\alpha^{a,b}$ for $\theta_{a,b}^{(a)*} - \frac{\Theta_{a,b}^*}{\Theta_{a,a}^*}$.

Furthermore, as long as the signal strength $\frac{\Theta_{a,b}^*}{\Theta_{a,a}^*}$ shrinks no faster than $\sigma_n(a,b) \asymp (n_2^{(a,b)})^{-1/2}$, we can still reject the null with constant or high probability. The following theorem shows the validity of the confidence interval (10), a direct consequence of Theorem 3.

Theorem 5 (Coverage and Width of Confidence Intervals). *Under the same assumptions as in Theorem 4, the confidence interval $\widehat{\mathbb{C}}$ defined in (10) satisfies $\lim_{n,p \rightarrow \infty} \mathbb{P}(\theta_b^{(a)*} \in \widehat{\mathbb{C}}_\alpha^{a,b}) = 1 - \alpha$, $|\widehat{\mathbb{C}}_\alpha^{a,b}| \xrightarrow{p} 2z_{\alpha/2} \sigma_n(a,b)$, where $|\widehat{\mathbb{C}}_\alpha^{a,b}|$ is the width of the confidence interval.*

One might wonder whether it is possible to construct a valid confidence interval for $\Theta_{a,b}^*$, instead of $\frac{\Theta_{a,b}^*}{\Theta_{a,a}^*}$. In fact, one can estimate $\Theta_{a,a}^*$ by $\hat{\tau}^{(a)} := (\hat{\Sigma}_{a,a} - \hat{\Sigma}_{a,\setminus a} \tilde{\theta}_a^{(a)})^{-1}$ and then construct a confidence interval centered around $\hat{\tau}^{(a)} \tilde{\theta}_b^{(a)}$. However, to establish normal approximation result for $\hat{\tau}^{(a)} \tilde{\theta}_b^{(a)}$, the whole matrix $\hat{\Theta}^{(a)}$ has to be an accurate estimator for $\Theta^{(a)*}$ and hence it would be required that the neighborhood of all nodes are measured well.

4 FDR Control for Graph Inference with Erode Measurements

In many application scenarios, the inference of the full graph may be of more interest than the inference of one particular edge. Confronted with a multiple testing problem, we can simply apply the Holm's correction upon the p -values of all $\frac{p(p-1)}{2}$ node pairs (a, b) for $a < b$, and hence control the family-wise error rate. However, as this approach can be too conservative, here we also propose an FDR control procedure. We leverage the ideas from [26, 34] which consider the FDR control for the debiased lasso and Gaussian graphical models. In particular, for any $0 \leq \rho \leq 1$, let $R(\rho) = \sum_{i < j} \mathbb{1}_{\{p_{i,j} \leq \rho\}}$ be the number of significant edges when ρ is the threshold for p -values. Also define $t_p = (2 \log(p(p-1)/2) - 2 \log \log(p(p-1)/2))^{\frac{1}{2}}$, and if there exists $2(1 - \Phi(t_p)) \leq \rho \leq 1$ such that $\frac{p(p-1)\rho}{2R(\rho)\sqrt{1}} \leq \alpha$, the nominal level, then we would define $\rho_0 = \sup_{2(1 - \Phi(t_p)) \leq \rho \leq 1} \left\{ \rho : \frac{p(p-1)\rho}{2(R(\rho)\sqrt{1})} \leq \alpha \right\}$; otherwise, $\rho_0 = 2(1 - \Phi(\sqrt{2 \log(p(p-1)/2)})$. The significant edge set is then defined as $\tilde{E} = \{(j, k) : p_{j,k} \leq \rho_0\}$. This is similar to the Benjamini-Hochberg procedure with only an extra truncation step. The full procedure is summarized in Algorithm 2 in the Appendix.

In the following, we provide theoretical guarantees for our GI-JOE (FDR) approach. Define $\epsilon_i(a, b) = \sum_{j,k} (x_{i,j} x_{i,k} - \sum_{j,k}^* \frac{\delta_{j,k}^{(i)}}{n_{j,k}} \frac{\Theta_{j,b}^{(a)*} \Theta_{k,a}^* + \Theta_{k,b}^{(a)*} \Theta_{j,a}^*}{2\Theta_{a,a}^*})$ as the error for estimating edge (a, b) , contributed by the i th sample; $\xi_i(a, b)$ is the normalized error: $\xi_i(a, b) = \frac{\epsilon_i(a, b)}{\sigma_n(a, b)}$. One technical quantity that is useful in our proofs is $\alpha(\Theta^*, \{V_i\}_{i=1}^n) = \sup_{(a,b), (a',b')} \frac{\|\xi_i(a, b)\|_{\psi_1}^2 \vee \|\xi_i(a', b')\|_{\psi_1}^2}{\lambda_{\min}(\text{Cov}(\{\xi_i(a, b), \xi_i(a', b')\}))}$.

We want $\alpha(\Theta^*, \{V_i\}_{i=1}^n)$ to be not too large, similar to assuming $(\xi_i(a, b), \xi_i(a', b'))$ to be far from degenerate. Also define the covariance between the test statistics of different edges: $\sigma_n^2(a, b, a', b') = \frac{1}{\Theta_{a,a}^* \Theta_{a',a'}^*} \Gamma^{(n)*} \times_1 \Theta_{:,b}^{(a)*} \times_2 \Theta_{:,a}^* \times_3 \Theta_{:,b'}^{(a)*} \times_4 \Theta_{:,a'}^*$, and the correlation $\rho_n(a, b, a', b') = \frac{\sigma_n^2(a, b, a', b')}{\sigma_n(a, b) \sigma_n(a', b')}$.

Assumption 6. For any edge $(a, b) \in [p] \times [p]$, $n_2^{(a,b)} \geq \frac{C \|\Sigma^*\|_\infty^6 \alpha^2(\Theta^*, \{V_i\}_{i=1}^n)}{\lambda_{\min}^6(\Sigma^*)} (d+1)^6 (\log p)^6$, and $n_1^{(a,b)} \gg Cd^2 (\log p)^5 \log \log p \left(\frac{n_2^{(a,b)}}{n_1^{(a,b)}} \right)^2$, where $d = \max_{a \in [p]} d_a$.

Assumption 6 is stronger than the sample size requirements in Assumptions 4 and 5 for edge-wise inference, since the proof for asymptotically valid FDR control needs stronger normal approximation guarantees, especially at the tail.

Remark 6. When all variables are simultaneously measured with sample size n , Assumption 6 reduces to $n \geq C(d+1)^6 (\log p)^6$. This is a much weaker assumption than what is required in the literature of FDR control for graphical models [34]: $p \leq n^r$ for some constant $r > 0$. They used this assumption to show the tail probability of the test statistics can be well approximated by the Gaussian tail, while we weaken this assumption by using a different proof that exploits the properties of sub-exponential random variables. The sample size requirements in [26] on FDR control for debiased lasso is weaker than ours ($n \geq C(d+1)^6 (\log p)^6$), since they assume Gaussian noise instead of the sub-exponential noise we have here for estimating the covariance.

Assumption 7. For any $0 < \rho < 1$, $\gamma > 0$, let $\mathcal{A}_1(\rho) = \{(a, b, a', b') \in [p] \times [p] : \rho_n(a, b, a', b') > \rho\}$, and $\mathcal{A}_2(\rho, \gamma) = \{(a, b, a', b') \in [p] \times [p] : (\log p)^{-2-\gamma} < \rho_n(a, b, a', b') \leq \rho\}$. There exist $0 < \rho_0 < 1$ and $\gamma > 0$ such that, $|\mathcal{A}_1(\rho_0)| \leq Cp^2$, $|\mathcal{A}_2(\rho_0, \gamma)| \ll p^{\frac{4}{1+\rho_0}} (\log p)^{\frac{2\rho_0}{1+\rho_0} - \frac{1}{2}} (\log \log p)^{-\frac{1}{2}}$.

Assumption 7 enforces that that most edge-wise test statistics are only weakly correlated, and similar assumptions have also appeared in [34] and [26]. The main difference is that the correlations between our edge-wise statistics depend on the joint sample sizes of many quadruples and cannot be simplified. The following theorem suggests that our GI-JOE

(FDR) procedure can successfully control the false discovery proportion both in expectation and in probability, when the sample size requirements (Assumption 6) are satisfied for each pair and the correlations between most edges are weak.

Theorem 6 (Validity of FDR control). *Consider the GI-JOE (FDR) procedure described in Section 4 and suppose the significant edge set under a given nominal level α is given by \tilde{E} . Let $\text{FDP} = \frac{\sum_{(a,b) \in \mathcal{H}_0} \mathbb{1}_{\{(a,b) \in \tilde{E}\}}}{|\tilde{E}| \vee 1}$, where $\mathcal{H}_0 = \{(i, j) \in [p] \times [p] : \Theta_{i,j}^* = 0\}$; Also let $\text{FDR} = \mathbb{E}\text{FDP}$. If Assumptions 6 and 7 hold, then we have $\limsup_{n,p \rightarrow \infty} \text{FDR} \leq \alpha$, and for any $\epsilon > 0$, $\lim_{n,p \rightarrow \infty} \mathbb{P}(\text{FDP} > \alpha + \epsilon) = 0$.*

The proof of Theorem 6 can be found in Section G of the Appendix. This is the first theoretical guarantee for FDR control with erosely measured data. Although we still require sufficient pairwise sample sizes for all pairs of nodes, we allow $n_{j,k}$ to be of different order.

5 Empirical Studies

In this section, we present empirical studies to validate our GI-JOE approach for both edge-wise inference and full graph inference. We first verify the validity of our edge-wise inference procedure in Section 5.1; then we compare the graph selection performance using both our GI-JOE approaches and various baseline estimation and inference methods in Section 5.2 and 5.3. A real data example is included in Section 5.4.

5.1 Simulations for Edge-wise Inference: Validating Theory

Here, we investigate the type I error and power of GI-JOE for testing one node pair.

Data generation: To study the effect of different pairwise sample sizes, here we consider the pairwise measurement scenario. That is, for all $1 \leq i \leq n$, $V_i = \{j, k\}$ for some $j, k \in [p]$, and the i th sample $x_{i,V_i} \sim \mathcal{N}(0, \Sigma_{(j,k),(j,k)}^*)$ when the full covariance matrix is Σ^* . When the given node pair for inference is (a, b) , we set the pairwise sample size as

follows: $n_{j,k} = \sum_{i=1}^n \mathbb{1}_{\{j,k \in V_i\}} = n1$ if $(j, k) \in S_1(a, b) \setminus S_2(a, b)$, $n_{j,k} = n2$ if $(j, k) \in S_2(a, b)$, and $n_{j,k} = 50$ otherwise. The precision matrix $\Theta^* = \Sigma^{*-1}$ is generated with three graph structures: (i) Chain graph: $\Theta_{j,k}^* \neq 0$ if and only if $|j - k| \leq 1$; (ii) Multi-star graph: We set the number of stars to be 3, each having $\lfloor p/3 \rfloor$ nodes or $p - 2\lfloor p/3 \rfloor$ nodes; (iii) Erdős–Rényi graph: Each pair of nodes are connected with probability $\frac{3}{p-1}$ independently, so that the expected degree of each node is 3. Given the support set dictated by the graph structure, the non-zero off-diagonal elements of Θ^* are randomly generated from $U[0.6, 0.8]$. To study type I errors, we set the target node pair $a = 2$, $b = 4$, and $\Theta_{2,4}^* = 0$; to study power, we set $a = 2$, $b = 3$, and $\Theta_{2,3}^*$ is chosen from a list of different signal strengths. The diagonal elements of Θ^* are set to be the same positive value that ensures $\lambda_{\min}(\Theta^*) = 0.25$.

Some implementation details (e.g., tuning parameter selection) of our GI-JOE approach can be found in Section D.1 of the Appendix. Figure 4 summarizes the type I error rate and power averaged over 200 replicates when the confidence level is set as 0.95, under three graph structures. In the Type I error plot (a), we consider three network sizes $p = 50, 100, 200$, and a range of $n_1^{(a,b)}, n_2^{(a,b)}$. We can see that the type I error rates are close to 0.05 with moderately large, although differing, pairwise sample sizes. In the power plot, The dimension p is fixed as 200, sample sizes $n_2^{(a,b)} = n2 \in \{125, 250, 500\}$, $n_1^{(a,b)} = n1 \in n2/\{1, 1.2, 1.5\}$. The dependence of power on $\sqrt{n_2}\Theta_{a,b}^*$ is similar across different sample sizes regime, supporting our theoretical analysis in Theorem 4 .

5.2 Graph Selection Study and Comparison with Baselines

Now we study the graph selection performance of our GI-JOE (Holm) and GI-JOE (FDR) approaches under different error measurements, compared with some baselines. In particular, we consider four estimation methods and four inference methods. The estimation methods include standard plug-in methods [28, 37] with neighborhood lasso (Nlasso), graphical lasso (Glasso), CLIME, and the variant plug-in method described in Section 2 (Nlasso-JOE). The

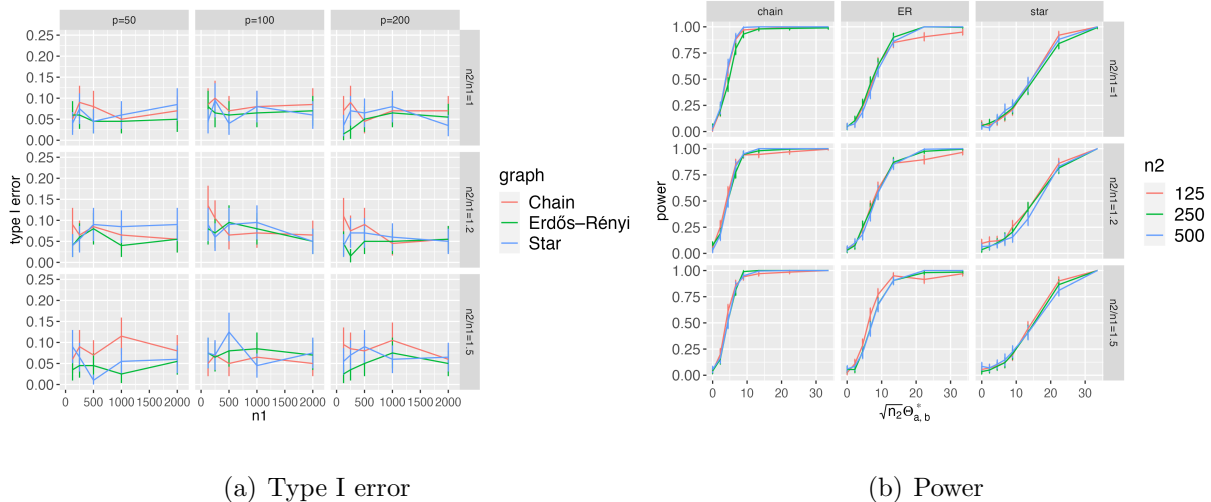


Figure 4: Type I error rates vs. sample size, and power vs. signal strength, averaged over 200 replicates when $\alpha = 0.05$, and the error bars represent the 95% confidence interval. The x -axis in (b) is $\sqrt{n_2^{(a,b)}} \Theta_{a,b}^*$, which determines the asymptotic power of our test given a fixed graph (see Theorem 4).

only difference between Nlasso-JOE and Nlasso is that we use different tuning parameters for each node that depend on its own sample sizes, as explained in Section 2. The inference methods include GI-JOE (Holm), GI-JOE (FDR), and also ad hoc implementations of the debiased graphical lasso [24]. Specifically, since there are no applicable inference methods designed for erose measurements, the only baseline we can implement is applying existing inference methods for simultaneous measurement settings and plug in the minimum pairwise sample size for computing the variance of each edge. This is not a method one would ever use in practice, since it is too conservative and has no theoretical guarantees, but we still present the results of such baselines, just to prove the concept that considering the different sample sizes over the graph is important. We choose the debiased graphical lasso instead of other graphical model inference methods since it is simpler to code up. Although [24] is only concerned with edge-wise inference, we still add a Holm’s correction and FDR control procedure on top of its edge-wise p -values for a fair comparison, and we denote these two procedures by DB-Glasso (Holm) and DB-Glasso (FDR). Some additional implementation details of these methods can be found in Section D.2 of the Appendix.

Data Generation: We fix the dimension $p = 200$, and consider the chain graph and star graph with 10 stars. We investigate the following three measurement scenarios: (i) The p nodes are divided into three sets of approximately the same size $(\lfloor \frac{p}{3} \rfloor, \lfloor \frac{p}{3} \rfloor, p - 2\lfloor \frac{p}{3} \rfloor)$. Nodes within each of the three sets are observed with probability $\sqrt{0.1}$, $\sqrt{0.5}$, and $\sqrt{0.9}$, independently. (ii) All nodes are independently missing, and the observed probability of each node j depends on the node degree in a positive way: $\mathbb{P}(j \in V_i) = 1 - 0.815^{d_j}$. (iii) The size of the jointly observed nodes is fixed as 20, and each node j is sampled with probability weight $1 - 0.815^{d_j}$. For each measurement scenario, we consider two different total sample sizes. Table 1 summarizes the F1 scores of our GI-JOE method and some other baseline estimation and inference methods, averaged over 20 independent runs (standard deviations included in parentheses). For both Nlasso and Nlasso-JOE, we present the results based on the AND rule; The results for OR rule and more detailed results on true positive rate, true negative rate, and true discovery rate can be found in Section E of the Appendix. In summary, among all different measurement scenarios, sample sizes, and graph structures, GI-JOE (FDR) is either the best or comparable to the best among all inference and estimation methods, in terms of the F1 score. The Nlasso-JOE is usually the best among the estimation methods, suggesting that using different tuning parameters that accommodate for the different pairwise sample sizes may be a simple yet effective trick.

5.3 Graph Selection Study Inspired by Real Data

Here we present some real data-inspired simulations, where either the graph structure or the measurement patterns are adopted from real neuroscience or gene expression data sets.

To obtain the real graph structure, we take a calcium imaging data set [30] from the Allen Institute, where the functional activities of $p = 227$ neurons in a mouse’s visual cortex are recorded. We focus on a recording session ($n = 8931$) where no external stimulus is presented to the mouse and estimate a graphical model among these 227 neurons. In the first

Chain graph						
Method	Measurement 1		Measurement 2		Measurement 3	
	n=600	n=800	n=1500	n=3000	n=20000	n=30000
Nlasso	0.62(0.18)	0.70(0.02)	0.31(0.01)	0.62(0.30)	0.41(0.01)	0.34(0.01)
Glasso	0.37(0.01)	0.35(0.01)	0.38(0.13)	0.59(0.01)	0.31(0.01)	0.47(0.21)
CLIME	0.40(0.04)	0.32(0.01)	0.44(0.01)	0.43(0.01)	0.27(0.00)	0.44(0.01)
Nlasso-JOE	0.64 (0.12)	0.91 (0.05)	0.61 (0.16)	0.89 (0.01)	0.68 (0.20)	0.88 (0.01)
DB-Glasso (Holm)	0.01(0.01)	0.05(0.02)	0.02(0.01)	0.70(0.02)	0.07(0.02)	0.42(0.03)
DB-Glasso (FDR)	0.02(0.01)	0.08(0.02)	0.04(0.02)	0.96(0.01)	0.23(0.13)	0.83(0.03)
GI-JOE (Holm)	0.80(0.01)	0.82(0.01)	0.54(0.07)	0.93(0.014)	0.51(0.08)	0.77(0.02)
GI-JOE (FDR)	0.84 (0.01)	0.88 (0.01)	0.85 (0.04)	0.97 (0.01)	0.82 (0.05)	0.93 (0.01)
10-Star graph						
Method	Measurement 1		Measurement 2		Measurement 3	
	n = 600	n = 800	n = 1500	n = 3000	n = 20000	n = 30000
Nlasso	0.35(0.11)	0.40(0.10)	0.25(0.01)	0.26(0.01)	0.28(0.01)	0.29(0.01)
Glasso	0.49(0.02)	0.47(0.01)	0.41(0.16)	0.49(0.02)	0.35(0.01)	0.39(0.25)
CLIME	0.25(0.01)	0.39(0.03)	0.19(0.01)	0.25(0.01)	0.28(0.03)	0.43(0.02)
Nlasso-JOE	0.82 (0.07)	0.86 (0.02)	0.72 (0.16)	0.70 (0.03)	0.80 (0.02)	0.90 (0.01)
DB-Glasso (Holm)	0.00(0.01)	0.00(0.01)	0.00(0.00)	0.00(0.00)	0.00(0.01)	0.04(0.01)
DB-Glasso (FDR)	0.00(0.01)	0.01(0.01)	0.00(0.00)	0.00(0.00)	0.01(0.01)	0.06(0.02)
GI-JOE (Holm)	0.62(0.03)	0.65(0.02)	0.68(0.09)	1.00 (0.00)	0.96(0.01)	0.97(0.01)
GI-JOE (FDR)	0.71 (0.02)	0.74 (0.01)	0.89 (0.03)	0.99(0.01)	0.98 (0.01)	0.98 (0.01)

Table 1: F1 scores of the graphs selected by estimation methods (first three) and inference methods (last four) across three measurement scenarios. The average sample size $\frac{1}{p^2} \sum_{j,k} n_{j,k}$ ranges from 50 to 350.

set of simulations, we generate data from this estimated graph, with the three measurement patterns introduced in Section 5.2. Similar to the experiments in Section 5.2, we present the F1-scores of our GI-JOE approaches and other baseline estimation and inference methods in Table 2, and either GI-JOE (Holm) or GI-JOE (FDR) performs the best or comparable to the best.

For the real measurement patterns, we take two publicly available single-cell RNA sequencing data sets [12, 11], and focus on the top 200 genes with highest variances. The

Method	Measurement 1		Measurement 2		Measurement 3	
	n = 8000	n = 12000	n = 5000	n = 8000	n = 80000	n = 120000
Nlasso	0.58(0.03)	0.69(0.02)	0.26(0.02)	0.32(0.02)	0.58(0.02)	0.69(0.02)
Glasso	0.54(0.02)	0.60(0.02)	0.29(0.02)	0.35(0.02)	0.66(0.03)	0.76(0.03)
CLIME	0.19(0.01)	0.72 (0.03)	0.29(0.02)	0.37(0.02)	0.43(0.02)	0.44(0.01)
Nlasso-JOE	0.64 (0.03)	0.70(0.16)	0.42 (0.03)	0.46 (0.03)	0.67 (0.02)	0.77 (0.02)
DB-Glasso (Holm)	0.22(0.02)	0.30(0.02)	0.05(0.01)	0.09(0.01)	0.23(0.02)	0.30(0.01)
DB-Glasso (FDR)	0.25(0.01)	0.39(0.06)	0.06(0.01)	0.11(0.01)	0.25(0.02)	0.41(0.06)
GI-JOE (Holm)	0.72(0.02)	0.82(0.02)	0.44(0.03)	0.60(0.02)	0.75(0.02)	0.83(0.02)
GI-JOE (FDR)	0.83 (0.02)	0.90 (0.02)	0.57 (0.03)	0.72 (0.03)	0.85 (0.02)	0.90 (0.02)

Table 2: F1 scores of estimation methods (first three) and inference methods (last four), across three simulated measurement scenarios, with the ground truth graph being the neuronal functional network estimated from a real calcium imaging data [30]. The average sample size $\frac{1}{p^2} \sum_{j,k} n_{j,k}$ ranges from around 500 to 5000.

chu and *darmanis* measurement patterns have pairwise sample sizes ranging from 0 to 1018 and from 5 to 366. The graphs for data generation are scale-free graphs and small-world graphs with 200 nodes. The F1-scores summarized in Table 3 also suggest the efficacy of the GI-JOE (FDR) approach. Visualizations of the real graph and measurement patterns, and specifics of the simulated graphs can be found in Section F of the Appendix.

5.4 Real Data Example: Application to Calcium Imaging Data

The two-photon calcium imaging technology can record in vivo functional activities of thousands of neurons [36, 44, 43], and such data sets can be used to understand the neuronal circuits with the help of graphical model techniques [57, 52, 47]. In this section, we investigate the potential of our GI-JOE approach on a real calcium imaging data set from the Allen Institute [30], which contains the functional recordings of $p = 227$ neurons in a mouse’s visual cortex, when different visual stimuli or no stimulus were presented to the mouse. Here, we focus on the raw fluorescence traces in one spontaneous session where there is no external stimulus. This session includes $n = 8931$ samples of the trace data associated with all 277

Method	<i>chu</i> measurement		<i>darmanis</i> measurement	
	scale-free graph	small-world graph	scale-free graph	small-world graph
Nlasso	0.54(0.25)	0.57(0.28)	0.31(0.02)	0.34(0.11)
Glasso	0.61 (0.19)	0.70(0.17)	0.59 (0.03)	0.49(0.10)
CLIME	0.41(0.08)	0.40(0.02)	0.26(0.04)	0.35(0.12)
Nlasso-JOE	0.61 (0.30)	0.92 (0.01)	0.51(0.03)	0.81 (0.01)
DB-Glasso (Holm)	0.00(0.00)	0.00(0.00)	0.00(0.00)	0.00(0.00)
DB-Glasso (FDR)	0.00(0.00)	0.00(0.00)	0.00(0.00)	0.00(0.00)
GI-JOE (Holm)	0.96 (0.01)	0.94 (0.01)	0.48(0.04)	0.63(0.02)
GI-JOE (FDR)	0.93(0.03)	0.92(0.02)	0.76 (0.03)	0.80 (0.01)

Table 3: F1 scores of estimation methods (first three) and inference methods (last four) with the ground truth graphs being a scale-free graph and a small-world graph with 200 nodes, under two real measurement patterns from single-cell RNA sequencing data sets (the *chu* data [11] and *darmanis* data [12]). Our GI-JOE methods always have the highest F1-scores, and GI-JOE (FDR) works better for the the *darmanis* measurement (average sample size 250) and GI-JOE (Holm) works better for the the *chu* measurement (average sample size 850).

neurons. We manually mask the data for some neurons to create erose measurements, and then validate our methods by comparing the tested graph based on masked data with the tested graph based on the full data set. In particular, the recorded neurons all lie on the same vertical plane in a mouse’s visual cortex (see Figure 5 for the physical locations of the neurons in x and y axis). To manually create erose measurements, we divide the neurons into three subsets based on their location on the x -axis (marked in different colors in Figure 5), and neurons in each subset are randomly observed with high ($\sqrt{0.9}$), moderate ($\sqrt{0.5}$), and low ($\sqrt{0.1}$) probabilities.

However, when inference methods are applied on the full data set, we find that the tested graph is always dense. This might be due to the huge amount of latent neurons in the mouse’s brain since latent variables are known to lead to dense graph structures in graphical models [52]. However, since most of these edges have small edge weights, here we consider testing if the edge weights are stronger than a threshold instead of testing if they are zero.

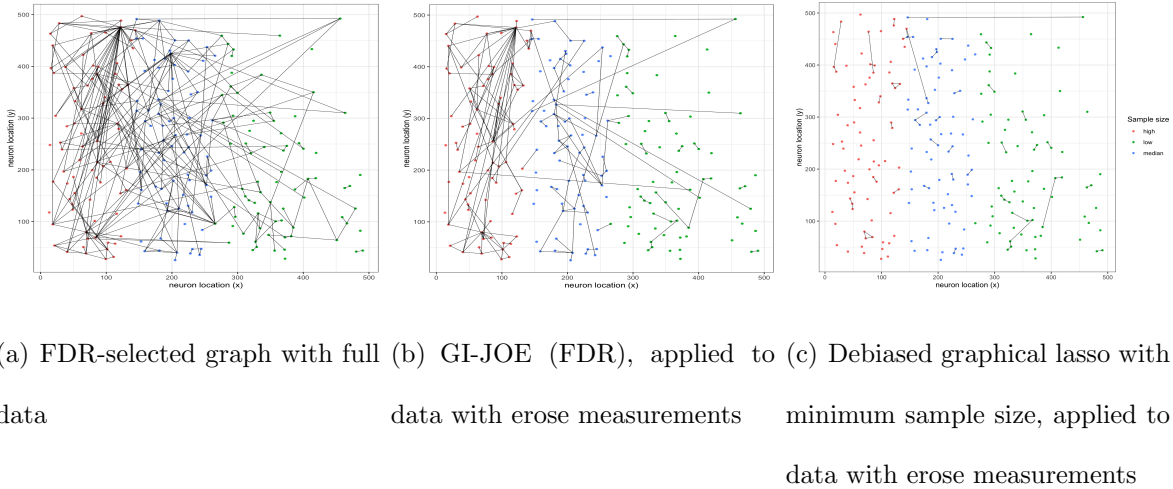


Figure 5: Tested functional connectivity graphs among neurons, using the Allen Brain Atlas data set. The neurons marked in red, blue, and green have high, moderate and low sample sizes. Our GI-JOE (FDR) approach works reasonably well, especially for red neurons, while the debiased graphical lasso with minimum sample size is too conservative to find any edge.

Specifically, for any node pair (a, b) , $H_{0,(a,b)} : \left| \frac{\Theta_{a,b}^*}{\Theta_{a,a}^*} \right| \leq 0.12$. Our GI-JOE approach can be directly extended to test such hypothesis and the detailed procedures are included in Section D of the Appendix. For validation purposes, we also apply a special version of our GI-JOE (FDR) approach on the full data set, where all pairwise sample sizes are equal. As suggested by Figure 5, our GI-JOE (FDR) approach works well, especially for the neuron set 1 (red) as they have larger sample sizes; it identifies the same hub neuron in set 1 as the tested graph (a) with the full data set. The specific F1-scores of each method for each set of neurons can be found in Section E of the Appendix.

6 Discussion

In this paper, we address the graphical model inference problem under the *erose* measurement setting, where irregular observational patterns lead to vastly different sample sizes for different node pairs. We propose a novel inference method, the *GI-JOE* (**G**raph **I**nference when **J**oint **O**bservations are **E**rose) approach, to quantify the different uncertainty levels

over the graph caused by the erose measurements, including both an edge-wise inference method and an FDR control procedure. When testing any given node pair (a, b) , we characterize its Type I error and power in terms of the sample sizes involving a, b 's neighbors; We also show that GI-JOE (FDR) can successfully control the FDR under appropriate conditions. Finally, through a number of synthetic data experiments and a real neuroscience data example, we validate the efficacy of our GI-JOE approach for different graph structures and measurement patterns.

Graph learning with erose measurements is commonly seen in practice but is understudied as a research problem, and there are still many open questions that could be investigated in the future. For instance, this paper focuses on the Gaussian graphical models, while it is also possible to extend the theory and methods to nonparanormal graphical models. Our current results are based on a variant of the neighborhood lasso, while one may also consider a variant of the graphical lasso or CLIME and investigate their potential in the erose measurement setting. Another practical but challenging setting not considered in this paper is data-dependent erose measurements, which requires novel methods and theory, since the sample covariance matrix would be biased in this setting and the plug-in type approach no longer works. Furthermore, erosely measured data sometimes take the form of a time series, and the temporal dependence could have an effect on the edge-wise variance computation, calling for new inference methodologies.

Acknowledgments

The authors gratefully acknowledge support by NSF NeuroNex-1707400, NIH 1R01GM140468, and NSF DMS-2210837. The authors also thank Gautam Dasarathy for helpful discussion during the preparation of this manuscript.

A Optimization Algorithm for the Weighted ℓ_∞ Norm Projection

We provide an ADMM algorithm to solve the following problem:

$$\tilde{\Sigma} = \arg \min_{\Sigma \succ 0} \max_{i,j} \sqrt{n_{ij}} |\Sigma_{ij} - \hat{\Sigma}_{ij}|. \quad (11)$$

Similar to [15], we introduce an additional variable $B \in \mathbb{R}^{p \times p}$, choose a small $\varepsilon > 0$ and solve

$$(\tilde{\Sigma}, \hat{B}) = \arg \min_{\Sigma \succeq \varepsilon I, B = \Sigma - \hat{\Sigma}} \max_{i,j} \sqrt{n_{ij}} |B_{ij}|.$$

Consider the augmented Lagrangian function of the objective above:

$$\begin{aligned} f(\Sigma, B, \Lambda) \\ = \frac{1}{2} \max_{i,j} \sqrt{n_{ij}} |B_{ij}| - \langle \Lambda, \Sigma - B - \hat{\Sigma} \rangle + \frac{1}{2\mu} \|\Sigma - B - \hat{\Sigma}\|_F^2, \end{aligned}$$

where $\Lambda \in \mathbb{R}^{p \times p}$ is the Lagrangian variable, and μ is a penalty parameter. Then the ADMM algorithm [5] takes the following steps at the i th iteration:

$$\Sigma^{(i+1)} = \arg \min_{\Sigma \succeq \varepsilon I} f(\Sigma, B^{(i)}, \Lambda^{(i)}), \quad (12)$$

$$B^{(i+1)} = \arg \min_B f(\Sigma^{(i+1)}, B, \Lambda^{(i)}), \quad (13)$$

$$\Lambda^{(i+1)} = \Lambda^{(i)} - \frac{\Sigma^{(i+1)} - B^{(i+1)} - \hat{\Sigma}}{\mu}. \quad (14)$$

Now we discuss how to solve (12) and (13). One can show that

$$\begin{aligned} \Sigma^{(i+1)} &= \arg \min_{\Sigma \succeq \varepsilon I} f(\Sigma, B^{(i)}, \Lambda^{(i)}) \\ &= \arg \min_{\Sigma \succeq \varepsilon I} \|\Sigma - B^{(i)} - \mu \Lambda^{(i)} - \hat{\Sigma}\|_F^2 \\ &= \mathcal{P}_{\mathcal{S}_\varepsilon^{++}}(B^{(i)} + \mu \Lambda^{(i)} + \hat{\Sigma}), \end{aligned}$$

where $\mathcal{P}_{\mathcal{S}_\varepsilon^{++}}(\cdot)$ is the projection operator upon $\mathcal{S}_\varepsilon^{++} = \{A \in \mathbb{R}^{p \times p} : A = A^\top, \lambda_{\min}(A) \geq \varepsilon\}$, w.r.t. the Frobenius norm. We can perform an eigenvalue thresholding to find this projection.

While for $B^{(i+1)}$, the following lemma shows how to solve (13):

Lemma 1. Let $\omega \in \mathbb{R}^{p \times p}$ with $\omega_{ij} = \sqrt{n_{ij}}$. The solution for (13) is:

$$B^{(i+1)} = \Sigma^{(i+1)} - \mu\Lambda^{(i)} - \widehat{\Sigma} - \mathcal{P}_{\mathbb{B}_{\omega^{-1},1}(\frac{\mu}{2})}(\Sigma^{(i+1)} - \mu\Lambda^{(i)} - \widehat{\Sigma}),$$

where $\mathcal{P}_{\mathbb{B}_{\omega^{-1},1}(\frac{\mu}{2})}(\cdot)$ is the projection operator upon the weighted ℓ_1 ball

$$\mathbb{B}_{\omega^{-1},1}(\frac{\mu}{2}) = \{A \in \mathbb{R}^{p \times p} : \sum_{i,j} \omega_{ij}^{-1} |A_{ij}| \leq \frac{\mu}{2}\},$$

w.r.t. the Frobenius norm.

Proof of Lemma 1. Let $A = \Sigma^{(i+1)} - \mu\Lambda^{(i)} - \widehat{\Sigma}$. First we can write

$$B^{(i+1)} = \arg \min_B \|B - A\|_F^2 + \mu \|\omega \circ B\|_\infty.$$

Due to the convexity of $g(B) = \|B - A\|_F^2 + \mu \|\omega \circ B\|_\infty$, it suffices to show that $0_{p \times p}$ is one sub-gradient of $g(B)$ at $\widehat{B} := A - \mathcal{P}_{\mathbb{B}_{\omega^{-1},1}(\frac{\mu}{2})}(A)$.

Let $\delta = \mathcal{P}_{\mathbb{B}_{\omega^{-1},1}(\mu/2)}(A)$, and $z = \frac{2}{\mu}\delta$. It is straightforward to verify that $(\nabla_B \|B - A\|_F^2)_{B=\widehat{B}} + \mu z = 0$, thus we only need to show that z is a sub-gradient of $\|\omega \circ B\|_\infty$ at $B = \widehat{B}$, that is, (i) $\|\omega^{-1} \circ z\|_1 \leq 1$ and (ii) $\langle \widehat{B}, z \rangle = \|\omega \circ \widehat{B}\|_\infty$.

First note that $\|\omega^{-1} \circ \delta\|_1 < \frac{\mu}{2}$ if and only if $\|\omega^{-1} \circ A\|_1 < \frac{\mu}{2}$, $\delta = A$ and $\widehat{B} = 0$, which implies $\|\omega^{-1} \circ z\|_1 < 1$ and $\langle \widehat{B}, z \rangle = \|\omega \circ \widehat{B}\|_\infty = 0$. Now we focus on the case where $\|\omega^{-1} \circ \delta\|_1 = \frac{\mu}{2}$. In this case, we can still easily verify (i) since $\|\omega^{-1} \circ z\|_1 = \frac{2}{\mu} \|\delta\|_{\omega^{-1},1} = 1$. While for (ii), note that by established results for projection on weighted ℓ_1 ball [41], there exists $c > 0$ such that $\delta_{ij} = \max\{|A_{ij}| - c\omega_{ij}^{-1}, 0\} \text{sgn}(A_{ij})$. Then one can show that $\|\omega \circ \widehat{B}\|_\infty = \max_{i,j} \omega_{ij} |A_{ij} - \delta_{ij}| = c$. Furthermore, $z_{ij} > 0$ implies $A_{ij} > c\omega_{ij}^{-1}$, and $z_{ij} < 0$ implies $A_{ij} < -c\omega_{ij}^{-1}$. Hence we have

$$\begin{aligned} \langle \widehat{B}, z \rangle &= \sum_{i,j} z_{ij} c \omega_{ij}^{-1} \text{sgn}(A_{ij}) \\ &= \sum_{i,j} c \omega_{ij}^{-1} |z_{ij}| \\ &= c \\ &= \|\omega \circ \widehat{B}\|_\infty. \end{aligned}$$

□

Hence solving for $B^{(i+1)}$ only requires the projection upon a weighted ℓ_1 ball, and this projection can be done by applying the algorithm proposed in [41]. We summarize the full ADMM algorithm for solving (11) in Algorithm A.

Algorithm 2: ADMM for weighted ℓ_∞ norm projection on positive semi-definite cone

1 Input: $\widehat{\Sigma}$, n_{ij} , $1 \leq i, j \leq p$, $\varepsilon > 0$, penalty parameter $\mu > 0$, initial values B_0 , Λ_0

2 $\omega_{ij} = \sqrt{n_{ij}}$;

3 **for** $i = 0, 1, \dots, K$ **do**

4 $\Sigma^{(i+1)} = \mathcal{P}_{\mathcal{S}_\varepsilon^{++}}(B^{(i)} + \widehat{\Sigma} + \mu\Lambda^{(i)});$

5 $A = \Sigma^{(i+1)} - \mu\Lambda^{(i)} - \widehat{\Sigma};$

6 $B^{(i+1)} = A - \mathcal{P}_{\mathbb{B}_{\omega,1}(\mu/2)}(A);$

7 $\Lambda^{(i+1)} = \Lambda^{(i)} - \frac{\Sigma^{(i+1)} - B^{(i+1)} - \widehat{\Sigma}}{\mu};$

8 **end for**

9 Output: $\Sigma^{(K+1)}$.

B Additional Theoretical Results and Discussion for Neighborhood Regression

Here, we discuss the consequences of the neighborhood recovery guarantee (Theorem 1).

Remark 7. *Theorem 1 suggests that, even when many pairs of nodes are only measured few times together, as long as the tuning parameters are chosen carefully w.r.t. the pairwise sample sizes, we are still able to recover the neighborhood of node a . In particular, we only need to collect sufficient samples for a pair of nodes if at least one node in this pair is a neighbor of a . This is not a trivial result, since the estimator (2) has to perform a selection from its neighbors and a large number of non-neighbors which are not measured well.*

For ease of presentation, here we have assumed that $n_{j,k} > 0, \forall j, k$ so that $\lambda_k^{(a)}$ is well defined. However, with a slight modification of our proof, the ℓ_2 and ℓ_1 error bounds in Theorem 1 would still hold even if $n_{j,k} = 0$ for some $j, k \in \overline{\mathcal{N}}_a^c$, and if we simply define

$$\lambda_j^{(a)} \asymp \|\Sigma^*\|_\infty \frac{\|\Theta_{:,a}^*\|_1}{\Theta_{a,a}^*} \sqrt{\frac{\log p}{\max\{1, \min_k n_{j,k}\}}}.$$

Remark 8 (Effect of differing sample sizes). *Theorem 1 also imposes a constraint on γ_a , the sample size ratio between the most well measured non-neighbor and the worst measured neighbor of a . This is due to that when the sample sizes for the non-neighbors are all much larger than the neighbors (large γ_a), the neighbors would suffer from much stronger regularization than non-neighbors.*

Remark 9 (Comparison with the literature). *When all pairwise sample sizes are all equal, $\gamma_a = 1$ and this requirement becomes $\min_{j \in \mathcal{N}_a} \min_{k \in [p]} n_{j,k} \geq C(\Sigma^*) d_a^2 \log p$, which is similar to the standard sample size requirement for neighborhood lasso in [35, 49], except for an additional factor d_a . This additional factor is due to technical challenges brought by non-simultaneous measurements of all variables.*

Theorem 7. *If the tuning parameters λ_j 's in the neighborhood regression estimator satisfy*

$$\lambda_j^{(a)} \asymp \|\Sigma^*\|_\infty \frac{\|\Theta_{:,a}^*\|_1}{\Theta_{a,a}^*} \sqrt{\frac{\log p}{\min_k n_{j,k}}},$$

$$\min_{j \in \mathcal{N}_a} \min_k n_{j,k} \geq \frac{C \|\Sigma^*\|_\infty^2 (\gamma_a + 1)}{\lambda_{\min}^2(\Sigma^*)} d_a^2 \log p,$$

then with probability at least $1 - Cp^{-c}$,

$$\|\widehat{\theta}^{(a)} - \theta^{(a)*}\|_2 \leq \frac{C \|\Sigma^*\|_\infty \|\Theta_{:,a}^*\|_1}{\lambda_{\min}(\Sigma^*) \Theta_{a,a}^*} \sqrt{\frac{d_a \log p}{\min_{j \in \mathcal{N}_a} \min_k n_{j,k}}},$$

$$\|\widehat{\theta}^{(a)} - \theta^{(a)*}\|_1 \leq \frac{C \|\Sigma^*\|_\infty (\sqrt{\gamma_a} + 1) \|\Theta_{:,a}^*\|_1}{\lambda_{\min}(\Sigma^*) \Theta_{a,a}^*} d_a \sqrt{\frac{\log p}{\min_{j \in \mathcal{N}_a} \min_k n_{j,k}}}.$$

One key sample size quantity in Theorem 7 is $\min_{j \in \mathcal{N}_a} \min_k n_{j,k}$, which is illustrated in Figure 6. With appropriately chosen regularization parameters $\lambda_j^{(a)}$ that reflect the corresponding sample sizes for each node, Theorem 7 shows that when $\min_{j \in \mathcal{N}_a} \min_k n_{j,k}$ is sufficiently large,

we can establish the both ℓ_2 and ℓ_1 consistency of the neighborhood lasso estimator $\widehat{\theta}^{(a)}$. The number of node pairs involved is $d_a p$, much smaller than the total number of node pairs p^2 when the degree of node a is small.

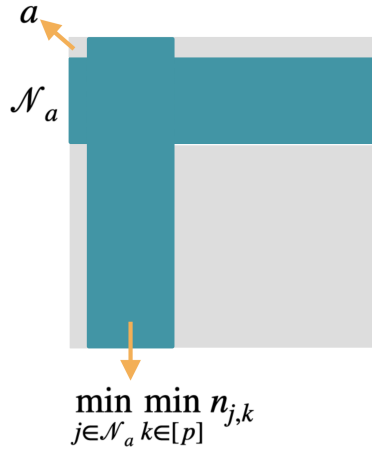


Figure 6: Illustration of node pairs whose pairwise sample sizes play key roles in the estimation error rate $\|\widehat{\theta}^{(a)} - \theta^{(a)*}\|_2$, $\|\widehat{\theta}^{(a)} - \theta^{(a)*}\|_2$.

C GI-JOE (FDR) Algorithm

We summarize our full GI-JOE (FDR) procedure in Algorithm 3. It calls the edge-wise inference algorithm for each node pair (a, b) for $1 \leq a < b \leq p$.

D Numerical Details

D.1 Tuning Parameter Selection in the Simulations on Edge-wise Inference

Our estimators $\widehat{\theta}^{(a)}$ and $\widehat{\Theta}_{b,:}^{(a)}$ depend on tuning parameters $\lambda_j^{(a)}$ and $\lambda_j^{(a,b)}$ for $1 \leq j \leq p$. Based on the theoretical scaling, we set $\lambda_j^{(a)} = \lambda_j^{(a,b)} = C_0 \sqrt{\frac{\log p}{\min_k n_{j,k}}}$, where C_0 is chosen based on neighborhood selection stability [33] over 20 random subsamplings, with the stability threshold set as 0.05, as suggested by [33]. For each random subsampling, each sample is

Algorithm 3: GI-JOE: FDR control

1 **Input:** Data set $\{x_{i,V_i} : V_i \subset [p]\}_{i=1}^n$, pairwise sample sizes $\{n_{j,k}\}_{j,k=1}^p$, significance level α

2 **for** $1 \leq a < b \leq p$ **do**

3 Run Algorithm 1 (edge-wise inference) in the main paper for node pair (a, b) and obtain p -value $p_{a,b}$

4 Sort the p -values of $m := \frac{p(p-1)}{2}$ pairs as $\mathbf{p}_{i_1} \leq \dots \leq \mathbf{p}_{i_m}$.

5 Let $k = m$, $t_p = (2 \log m - 2 \log \log m)^{\frac{1}{2}}$.

6 **while** $\mathbf{p}_{i_k} \geq 2(1 - \Phi(t_p))$ and $\mathbf{p}_{i_k} > \frac{\alpha k}{m}$ **do**

7 $k = k - 1$

8 **if** $\mathbf{p}_{i_k} < 2(1 - \Phi(t_p))$ **then**

9 $k = \arg \max_l \mathbf{p}_{i_l} \leq 2(1 - \Phi(\sqrt{2 \log m}))$.

10 **Output:** Set \tilde{E} of node pairs (a, b) associated with the k smallest p -values.

included with probability 0.8 independently. For each experimental setting, 200 independent replicates are run, but we only perform stability selection for one replicate and use the same tuning parameter for all 200 replicates.

D.2 Implementation Details in Graph Selection Comparison

Estimation Methods: For baseline plug-in type methods, we directly plug in the covariance matrix estimate $\tilde{\Sigma}$ (the positive semi-definite matrix solved by the ADMM algorithm) into the graphical lasso, neighborhood lasso, and CLIME algorithms to estimate the graph structure. This is slightly different from the original plug-in type methods where unbiased estimate $\hat{\Sigma}$ is in use. We choose $\tilde{\Sigma}$ to ensure convexity or algorithmic stability. We choose the tuning parameters for all methods using stability selection. 20 random subsamplings are used for Nlasso, Glasso, Nlasso-JOE, and 10 random subsamplings are used for CLIME

to save computational time. For each random subsampling, each sample is included with probability 0.8, and the stability threshold is 0.05.

Inference Methods: The inference methods include GI-JOE (Holm), GI-JOE (FDR), DB-Glasso (Holm), and DB-Glasso (FDR). For GI-JOE (Holm) and GI-JOE (FDR), the tuning parameters in the neighborhood regression problems are set as $\lambda_j^{(a)}, \lambda_j^{(a,b)} = C \sqrt{\frac{\log p}{\min_k n_{j,k}}}$, and the constant C is the same over the whole graph. We choose C by stability selection on the graph, with 20 random subsampling and stability threshold 0.05. For DB-Glasso (Holm) and DB-Glasso (FDR), we first plug in $\tilde{\Sigma}$ into graphical lasso to obtain an estimate $\hat{\Theta}$ of the precision matrix; then we compute the debiased graphical lasso statistic: $\hat{T} = 2\hat{\Theta} - \hat{\Theta}\tilde{\Sigma}\hat{\Theta}$. The variance of each edge (j, k) is estimated by $\frac{1}{\min_{j,k} n_{j,k}} \hat{\sigma}_{j,k}^2 = \hat{\Theta}_{j,j}\hat{\Theta}_{k,k} + \hat{\Theta}_{j,k}^2$, where we plug in the minimum pairwise sample size. Then we normalize the edge statistic to $\frac{\sqrt{\min_{j,k} n_{j,k}} \hat{T}_{j,k}}{\hat{\sigma}_{j,k}}$ and compute its p -value $p_{j,k} = 2(1 - \Phi(\frac{\sqrt{\min_{j,k} n_{j,k}} |\hat{T}_{j,k}|}{\hat{\sigma}_{j,k}}))$. Then we add Holm's correction and FDR control procedure on top of these edge-wise p -values, similar to what GI-JOE (Holm) and GI-JOE (FDR).

D.3 Testing against a Threshold

Suppose we would like to test the hypothesis $H_{0,(a,b)} : |\frac{\Theta_{a,b}^*}{\Theta_{a,a}^*}| \leq \epsilon$ for some positive value ϵ . We propose to find the p -value for $H_{0,(a,b)}$ as follows: $p_{a,b} = \min\{1, 2(1 - \Phi(\frac{|\tilde{\theta}_b^{(a)}| - \epsilon}{\hat{\sigma}_n(a,b)})\}$. Now we show that the validity of this p -value is directly implied by our current theoretical results. Note that under $H_{0,(a,b)}$, for any $t > 0$,

$$\begin{aligned} & \mathbb{P}\left(\frac{|\tilde{\theta}_b^{(a)}| - \epsilon}{\hat{\sigma}_n(a,b)} > t\right) \\ & \leq \mathbb{P}\left(\frac{|\tilde{\theta}_b^{(a)}| - |\frac{\Theta_{a,b}^*}{\Theta_{a,a}^*}|}{\hat{\sigma}_n(a,b)} > t\right) \\ & \leq \mathbb{P}\left(\frac{|\tilde{\theta}_b^{(a)} + \frac{\Theta_{a,b}^*}{\Theta_{a,a}^*}|}{\hat{\sigma}_n(a,b)} > t\right) \rightarrow 2(1 - \Phi(t)), \end{aligned}$$

where the last line is due to Theorem 3 in the main paper. After getting the p -values for all node pairs, we can further apply the Holm’s correction and the FDR control procedure upon these $\frac{p(p-1)}{2}$ p -values.

E Additional Empirical Results

In this section, we present some additional empirical results, including the detailed true positive rates (TPR), true negative rates (TNR), true discovery rate (TDR) and F1 scores in the graph selection studies (Table 4-14). Specifically, TPR is the ratio of selected true edges and total number of true edges; TNR is the ratio of unselected nonedges and total number of nonedges; TDR is the ratio of selected true edges and selected edges. In summary, estimation methods tend to be much more liberal (higher TPR but lower TDR) while inference methods are more conservative (higher TDR but lower TPR). The debiased graphical lasso methods with minimum sample size are often too conservative and select no edge at all, hence their TDR are sometimes NA.

Method	$n = 600$				$n = 800$			
	TPR	TNR	TDR	F1 score	TPR	TNR	TDR	F1 score
Nlasso (AND)	0.977(0.012)	0.984(0.016)	0.475(0.172)	0.619(0.181)	0.991(0.007)	0.991(0.001)	0.537(0.019)	0.697(0.016)
Nlasso (OR)	0.986(0.008)	0.973(0.011)	0.289(0.064)	0.443(0.082)	0.996(0.004)	0.975(0.001)	0.285(0.009)	0.443(0.011)
Glasso	0.993(0.005)	0.966(0.001)	0.228(0.008)	0.371(0.010)	0.999(0.002)	0.963(0.001)	0.214(0.005)	0.352(0.006)
CLIME	0.975(0.010)	0.971(0.004)	0.254(0.30)	0.402(0.036)	0.991(0.005)	0.957(0.002)	0.189(0.008)	0.317(0.011)
Nlasso-JOE (AND)	0.961(0.021)	0.989(0.005)	0.499(0.174)	0.641(0.118)	0.966(0.015)	0.998(0.002)	0.867(0.082)	0.911(0.053)
Nlasso-JOE (OR)	0.979(0.013)	0.929(0.027)	0.170(0.152)	0.267(0.177)	0.982(0.012)	0.986(0.012)	0.867(0.082)	0.911(0.053)
DB-Glasso (Holm)	0.007(0.004)	1.000(0.000)	NA	0.013(0.008)	0.028(0.011)	1.000(0.000)	1.000(0.000)	0.078(0.021)
DB-Glasso (FDR)	0.009(0.005)	1.000(0.000)	NA	0.017 (0.010)	0.041(0.011)	1.000(0.000)	1.000(0.000)	0.078(0.021)
GI-JOE (Holm)	0.667(0.011)	1.000(1.13e-05)	1.000(0.002)	0.800(0.008)	0.699(0.010)	1.000(1.55e-05)	0.999(0.002)	0.822(0.007)
GI-JOE (FDR)	0.747(0.015)	1.000(1.73e-4)	0.962(0.021)	0.841(0.012)	0.815(0.018)	1.000(9.5e-05)	0.966(0.011)	0.884(0.011)

Table 4: Graph selection results on chain graph, measurement scenario 1.

Method	$n = 1500$				$n = 3000$			
	TPR	TNR	TDR	F1 score	TPR	TNR	TDR	F1 score
Nlasso (AND)	0.997(0.003)	0.955(0.002)	0.183(0.005)	0.310(0.007)	1.000(0.000)	0.978(0.022)	0.514(0.313)	0.621(0.297)
Nlasso (OR)	0.997(0.003)	0.965(0.001)	0.221(0.005)	0.362(0.007)	1.000(0.000)	0.978(0.013)	0.376(0.145)	0.530(0.158)
Glasso	0.998(0.003)	0.964(0.011)	0.245(0.113)	0.382(0.125)	1.000(0.000)	0.986(0.001)	0.417(0.014)	0.588(0.014)
CLIME	0.996(0.005)	0.974(0.001)	0.282(0.011)	0.439(0.013)	1.000(0.000)	0.973(0.001)	0.272(0.008)	0.427(0.010)
Nlasso-JOE (AND)	0.991(0.008)	0.986(0.007)	0.462(0.203)	0.608(0.158)	1.000(0.000)	0.998(0.000)	0.806(0.015)	0.893 (0.009)
Nlasso-JOE (OR)	0.996(0.005)	0.954(0.021)	0.250(0.200)	0.368(0.210)	1.000(0.000)	0.990(0.001)	0.501(0.015)	0.668(0.013)
DB-Glasso (Holm)	0.009(0.007)	1.000(0.000)	NA	0.017(0.013)	0.539(0.029)	1.000(0.000)	1.000(0.000)	0.700(0.024)
DB-Glasso (FDR)	0.020(0.011)	1.000(0.000)	1.000(0.000)	0.038(0.021)	0.925(0.018)	1.000(1.55e-05)	0.999(0.002)	0.960(0.010)
GI-JOE (Holm)	0.377(0.070)	1.000(1.55e-05)	0.999(0.005)	0.544(0.072)	0.863(0.023)	1.000(1.13e-05)	1.000(0.001)	0.926(0.014)
GI-JOE (FDR)	0.761(0.065)	1.000(9.76e-05)	0.959(0.013)	0.848(0.042)	0.983(0.005)	1.000(1.45e-04)	0.958(0.013)	0.971(0.007)

Table 5: Graph selection results on chain graph, measurement scenario 2.

Method	$n = 20000$				$n = 30000$			
	TPR	TNR	TDR	F1 score	TPR	TNR	TDR	F1 score
Nlasso (AND)	0.997(0.004)	0.971(0.001)	0.258(0.010)	0.410(0.012)	0.999(0.002)	0.961(0.002)	0.205(0.007)	0.340(0.010)
Nlasso (OR)	0.997(0.004)	0.949(0.002)	0.164(0.004)	0.281(0.006)	1.000(0.001)	0.956(0.002)	0.185(0.006)	0.312(0.008)
Glasso	0.999(0.002)	0.954(0.002)	0.180(0.005)	0.305(0.007)	0.999(0.002)	0.969(0.019)	0.328(0.194)	0.466(0.207)
CLIME	0.996(0.004)	0.947(0.001)	0.158(0.003)	0.273(0.005)	0.999(0.002)	0.975(0.001)	0.283(0.008)	0.441(0.010)
Nlasso-JOE (AND)	0.987(0.010)	0.988(0.009)	0.562(0.255)	0.683(0.204)	0.996 (0.004)	0.997(0.000)	0.790(0.022)	0.881(0.014)
Nlasso-JOE (OR)	0.993(0.007)	0.966(0.027)	0.368(0.248)	0.491(0.263)	0.998(0.002)	0.992(0.001)	0.551(0.021)	0.710(0.018)
DB-Glasso (Holm)	0.036(0.013)	1.000(0.000)	1.000(0.000)	0.070(0.024)	0.263(0.027)	1.000(0.000)	1.000(0.000)	0.416(0.034)
DB-Glasso (FDR)	0.137(0.082)	1.000(0.000)	1.000(0.000)	0.232(0.125)	0.706(0.045)	1.000(1.85e-05)	0.999(0.003)	0.827(0.031)
GI-JOE (Holm)	0.348(0.078)	1.000(1.13e-05)	0.999(0.003)	0.512(0.085)	0.630(0.028)	1.000(1.55e-05)	0.999(0.002)	0.773 (0.021)
GI-JOE (FDR)	0.721(0.076)	1.000(1.87e-04)	0.951(0.024)	0.818(0.050)	0.914(0.013)	1.000(2.08e-04)	0.950(0.020)	0.931(0.012)

Table 6: Graph selection results on chain graph, measurement scenario 3.

Method	$n = 600$				$n = 800$			
	TPR	TNR	TDR	F1 score	TPR	TNR	TDR	F1 score
Nlasso (AND)	0.778(0.041)	0.969(0.016)	0.235(0.099)	0.348(0.111)	0.833(0.027)	0.974(0.013)	0.266(0.078)	0.396(0.096)
Nlasso (OR)	0.920(0.017)	0.960(0.013)	0.193(0.049)	0.317(0.066)	0.949(0.015)	0.963(0.006)	0.201 (0.024)	0.332(0.033)
Glasso	0.993(0.006)	0.981(0.001)	0.329(0.014)	0.494(0.016)	0.997(0.004)	0.979(0.001)	0.312(0.012)	0.475(0.015)
CLIME	0.833(0.019)	0.952(0.003)	0.144(0.008)	0.246(0.012)	0.836(0.025)	0.976(0.003)	0.251(0.024)	0.385 (0.030)
Nlasso-JOE (AND)	0.759(0.031)	0.999(0.003)	0.897(0.126)	0.815(0.073)	0.821(0.017)	0.999(0.000)	0.913(0.035)	0.864(0.021)
Nlasso-JOE (OR)	0.972(0.017)	0.991(0.014)	0.603(0.114)	0.736(0.122)	0.989(0.007)	0.993(0.001)	0.584(0.026)	0.734(0.021)
DB-Glasso (Holm)	0.001(0.002)	1.000(0.001)	NA	0.003(0.005)	0.002(0.003)	1.000(0.000)	NA	0.004(0.005)
DB-Glasso (FDR)	0.001(0.002)	1.000(0.000)	NA	0.003(0.005)	0.004(0.003)	1.000(0.000)	NA	0.007(0.007)
GI-JOE (Holm)	0.444(0.032)	1.000(1.13e-05)	0.999(0.003)	0.615(0.032)	0.486(0.019)	1(0.000)	1.000 (0.000)	0.654(0.017)
GI-JOE (FDR)	0.570(0.021)	1.000(1.23e-04)	0.951(0.021)	0.713(0.020)	0.604(0.014)	1.000(0.000)	0.954(0.025)	0.739(0.013)

Table 7: Graph selection results on star graph, measurement scenario 1.

Method	$n = 1500$				$n = 3000$			
	TPR	TNR	TDR	F1 score	TPR	TNR	TDR	F1 score
Nlasso (AND)	0.867(0.020)	0.951(0.001)	0.144(0.005)	0.247(0.008)	0.948(0.017)	0.950(0.001)	0.153(0.004)	0.263(0.006)
Nlasso (OR)	0.975(0.012)	0.954(0.001)	0.170(0.004)	0.289(0.006)	1.000(0.001)	0.957(0.009)	0.187(0.027)	0.314(0.040)
Glasso	1.000(0.001)	0.967(0.017)	0.274(0.131)	0.414(0.156)	1.000(0.000)	0.980(0.001)	0.327(0.013)	0.493(0.015)
CLIME	0.290(0.025)	0.983(0.001)	0.140(0.010)	0.189(0.014)	0.888(0.023)	0.951(0.001)	0.147(0.004)	0.253(0.006)
Nlasso-JOE (AND)	0.594(0.152)	1.000(0.000)	0.973(0.017)	0.723(0.157)	0.535(0.031)	1.000(0.000)	1.000(0.000)	0.697(0.026)
Nlasso-JOE (OR)	0.952(0.003)	0.988(0.004)	0.465(0.170)	0.611(0.118)	1.000(0.000)	0.999(0.000)	0.942(0.015)	0.970(0.008)
DB-Glasso (Holm)	0.000(0.000)	1.000(0.000)	NA	0.000(0.000)	0.000(0.000)	1.000(0.000)	NA	0.000(0.000)
DB-Glasso (FDR)	0.000(0.000)	1.000(0.000)	NA	0.000(0.000)	0.000(0.000)	1.000(0.000)	NA	0.000(0.000)
GI-JOE (Holm)	0.523(0.119)	1.000(0.000)	1.000(0.000)	0.680(0.088)	0.997(0.004)	1.000(0.000)	1.000(0.001)	0.998(0.002)
GI-JOE (FDR)	0.816(0.050)	1.000(0.000)	0.988(0.007)	0.893(0.029)	1.000(0.000)	1.000(0.000)	0.976(0.010)	0.988(0.005)

Table 8: Graph selection results on star graph, measurement scenario 2.

Method	$n = 8000$				$n = 12000$			
	TPR	TNR	TDR	F1 score	TPR	TNR	TDR	F1 score
Nlasso (AND)	0.923(0.020)	0.954(0.001)	0.162(0.005)	0.275(0.007)	0.954(0.012)	0.956(0.001)	0.174(0.005)	0.294(0.007)
Nlasso (OR)	0.999(0.002)	0.952(0.001)	0.166(0.003)	0.284(0.004)	1.000(0.000)	0.957(0.001)	0.184(0.004)	0.311(0.006)
Glasso	1.000(0.000)	0.965(0.001)	0.213(0.004)	0.351(0.006)	1.000(0.000)	0.960(0.017)	0.285(0.281)	0.392(0.248)
CLIME	0.898(0.026)	0.956(0.007)	0.168(0.021)	0.282(0.030)	0.942(0.014)	0.976(0.002)	0.275(0.022)	0.425(0.024)
Nlasso-JOE (AND)	0.659(0.020)	1.000(0.000)	1.000(0.002)	0.794(0.015)	0.821(0.023)	1.000(0.000)	1.000(0.001)	0.901(0.014)
Nlasso-JOE (OR)	1.000(0.000)	1.000(0.000)	0.962(0.008)	0.981(0.004)	1.000(0.000)	0.999(0.000)	0.946(0.018)	0.972(0.010)
DB-Glasso (Holm)	0.001(0.004)	1.000(0.000)	NA	0.003(0.007)	0.018(0.007)	1.000(0.000)	0.988(0.056)	0.035(0.014)
DB-Glasso (FDR)	0.003(0.005)	1.000(0.000)	NA	0.006(0.010)	0.032(0.011)	1.000(0.000)	0.983(0.056)	0.061(0.021)
GI-JOE (Holm)	0.922(0.017)	1.000(0.000)	1.000(0.001)	0.959(0.010)	0.941(0.017)	1.000(0.000)	1.000(0.000)	0.969(0.009)
GI-JOE (FDR)	0.991(0.008)	1.000(0.000)	0.968(0.016)	0.979(0.008)	0.994(0.005)	1.000(0.000)	0.962(0.014)	0.977(0.008)

Table 9: Graph selection results on star graph, measurement scenario 3.

F The Graphs and Measurement Patterns in Real Data-inspired Simulations

In Section 5.3 of the main paper, we present simulation results (i) when the underlying graph for data generation is estimated from a real calcium imaging data set; and (ii) when the measurement patterns are the same as the ones in two single-cell RNA sequencing data sets. We present here the estimated graph structure from neuroscience and the measurement patterns from gene expression data in Figure 7 and Figure 8.

Method	$n = 8000$				$n = 12000$			
	TPR	TNR	TDR	F1 score	TPR	TNR	TDR	F1 score
Nlasso (AND)	0.550(0.028)	0.998(0.000)	0.611(0.033)	0.579(0.027)	0.713(0.028)	0.998(0.000)	0.662(0.026)	0.686(0.021)
Nlasso (OR)	0.623(0.030)	0.998(0.000)	0.601(0.027)	0.612(0.025)	0.782(0.024)	0.998(0.000)	0.648(0.026)	0.709(0.021)
Glasso	0.736(0.024)	0.994(0.000)	0.427(0.019)	0.540(0.020)	0.864(0.015)	0.994(0.000)	0.461(0.019)	0.601(0.016)
CLIME	0.931(0.020)	0.954(0.001)	0.104(0.003)	0.187(0.006)	0.684(0.034)	0.999(0.000)	0.757(0.035)	0.718(0.029)
Nlasso-JOE (AND)	0.482(0.029)	1.000(0.000)	0.959(0.017)	0.641(0.026)	0.568(0.166)	1.000(0.000)	0.974(0.017)	0.700(0.157)
Nlasso-JOE (OR)	0.693(0.028)	0.999(0.000)	0.859(0.030)	0.767(0.023)	0.746(0.187)	0.999(0.000)	0.894(0.059)	0.792(0.123)
DB-Glasso (Holm)	0.126(0.010)	1.000(0.000)	1.000(0.000)	0.224(0.016)	0.178(0.012)	1.000(0.000)	1.000(0.000)	0.302(0.017)
DB-Glasso (FDR)	0.142(0.009)	1.000(0.000)	0.998(0.010)	0.249(0.014)	0.247(0.046)	1.000(0.000)	0.999(0.006)	0.394(0.059)
GI-JOE (Holm)	0.558(0.024)	1.000(0.000)	1.000(0.000)	0.716(0.020)	0.703(0.027)	1.000(0.000)	0.998(0.004)	0.825(0.018)
GI-JOE (FDR)	0.734(0.029)	1.000(0.000)	0.948(0.024)	0.827(0.023)	0.851(0.020)	1.000(0.000)	0.949(0.023)	0.897(0.015)

Table 10: Graph selection results with the ground truth graph being the neuronal functional network estimated from a real calcium imaging data [30], measurement scenario 1.

Method	$n = 5000$				$n = 8000$			
	TPR	TNR	TDR	F1 score	TPR	TNR	TDR	F1 score
Nlasso (AND)	0.468(0.039)	0.988(0.001)	0.182(0.016)	0.262(0.022)	0.586(0.033)	0.988(0.001)	0.219(0.019)	0.318 (0.021)
Nlasso (OR)	0.466(0.034)	0.990(0.001)	0.202(0.017)	0.282(0.023)	0.591(0.029)	0.990(0.001)	0.244(0.019)	0.346(0.023)
Glasso	0.492(0.036)	0.989(0.001)	0.210(0.018)	0.295(0.023)	0.613(0.031)	0.989(0.001)	0.250(0.020)	0.355(0.024)
CLIME	0.370(0.026)	0.993(0.000)	0.242(0.021)	0.292(0.022)	0.537(0.024)	0.992(0.001)	0.284(0.022)	0.371(0.022)
Nlasso-JOE (AND)	0.523(0.043)	0.994(0.001)	0.353(0.042)	0.419(0.029)	0.315(0.069)	1.000(0.001)	0.935(0.099)	0.461(0.027)
Nlasso-JOE (OR)	0.719(0.047)	0.982(0.002)	0.183(0.020)	0.291(0.024)	0.465(0.073)	0.999(0.003)	0.855(0.146)	0.585(0.051)
DB-Glasso (Holm)	0.027(0.004)	1.000(0.000)	1.000(0.000)	0.053(0.007)	0.049(0.005)	1.000(0.000)	1.000(0.000)	0.094(0.009)
DB-Glasso (FDR)	0.029(0.003)	1.000(0.000)	1.000(0.000)	0.056(0.005)	0.056(0.008)	1.000(0.000)	1.000(0.000)	0.107(0.014)
GI-JOE (Holm)	0.281(0.021)	1.000(0.000)	0.999(0.005)	0.438(0.026)	0.425(0.021)	1.000(0.000)	0.999(0.003)	0.596(0.020)
GI-JOE (FDR)	0.408(0.031)	1.000(0.000)	0.945(0.027)	0.569(0.031)	0.580(0.033)	1.000(0.000)	0.953(0.019)	0.720(0.027)

Table 11: Graph selection results with the ground truth graph being the neuronal functional network estimated from a real calcium imaging data [30], measurement scenario 2.

Generation of scale-free and small-world graphs: The scale-free graph is generated from the Barabasi-Albert model with 200 nodes, and for each new node sequentially added to the model, one edge between it and the existing nodes is randomly created. The small-world graph is generated from the Watts-Strogatz model with degree 2 and rewiring probability 0.5.

Method	$n = 80000$				$n = 120000$			
	TPR	TNR	TDR	F1 score	TPR	TNR	TDR	F1 score
Nlasso (AND)	0.440(0.018)	1.000(0.000)	0.846(0.034)	0.579(0.016)	0.573(0.025)	1.000(0.000)	0.879(0.029)	0.694(0.022)
Nlasso (OR)	0.508(0.017)	0.999(0.000)	0.850(0.035)	0.635(0.015)	0.654(0.026)	1.000(0.000)	0.884(0.027)	0.751(0.021)
Gllasso	0.620(0.035)	0.999(0.000)	0.714(0.034)	0.663(0.029)	0.765(0.034)	0.999(0.000)	0.759(0.041)	0.762(0.034)
CLIME	0.891(0.031)	0.987(0.000)	0.284(0.011)	0.430(0.015)	0.959(0.015)	0.986(0.000)	0.288(0.007)	0.443(0.009)
Nlasso-JOE (AND)	0.513(0.026)	1.000(0.000)	0.974(0.015)	0.672(0.022)	0.639(0.030)	1.000(0.000)	0.982(0.009)	0.774(0.022)
Nlasso-JOE (OR)	0.735(0.035)	1.000(0.000)	0.924(0.015)	0.818(0.023)	0.851(0.027)	1.000(0.000)	0.920(0.022)	0.884(0.022)
DB-Glasso (Holm)	0.127(0.012)	1.000(0.000)	1.000(0.000)	0.225(0.019)	0.175(0.010)	1.000(0.000)	1.000(0.000)	0.298(0.014)
DB-Glasso (FDR)	0.144(0.010)	1.000(0.000)	1.000(0.000)	0.251(0.016)	0.260(0.043)	1.000(0.000)	0.999(0.005)	0.411(0.055)
GI-JOE (Holm)	0.595(0.029)	1.000(0.000)	0.998(0.003)	0.745(0.023)	0.713(0.023)	1.000(0.000)	0.997(0.002)	0.831(0.016)
GI-JOE (FDR)	0.769(0.036)	1.000(0.000)	0.951(0.018)	0.850(0.024)	0.855(0.025)	1.000(0.000)	0.947(0.018)	0.899(0.015)

Table 12: Graph selection results with the ground truth graph being the neuronal functional network estimated from a real calcium imaging data [30], measurement scenario 3.

Method	<i>chu</i> measurement				<i>darmanis</i> measurement			
	TPR	TNR	TDR	F1 score	TPR	TNR	TDR	F1 score
Nlasso (AND)	0.996(0.004)	0.974(0.020)	0.408(0.252)	0.536(0.252)	0.899(0.026)	0.961(0.005)	0.189(0.018)	0.312(0.024)
Nlasso (OR)	0.997(0.003)	0.970(0.021)	0.343(0.187)	0.483(0.206)	0.912(0.022)	0.959(0.002)	0.185(0.009)	0.307(0.014)
Gllasso	0.551(0.314)	0.999(0.001)	0.823(0.051)	0.606(0.189)	0.529(0.036)	0.997(0.001)	0.672(0.046)	0.591(0.031)
CLIME	0.998(0.003)	0.969(0.011)	0.260(0.051)	0.410(0.067)	0.908(0.028)	0.947(0.008)	0.152(0.035)	0.259(0.043)
Nlasso-JOE (AND)	0.509(0.342)	1.000(0.000)	1.000(0.000)	0.610(0.301)	0.343(0.026)	1.000(0.000)	0.994(0.015)	0.510(0.029)
Nlasso-JOE (OR)	0.593(0.327)	0.999(0.000)	0.915(0.018)	0.670(0.242)	0.514(0.035)	0.999(0.000)	0.805(0.048)	0.626(0.033)
DB-Glasso (Holm)	0.000(0.000)	1.000(0.000)	NA	0.000(0.000)	0.000(0.000)	1.000(0.000)	NA	0.000(0.000)
DB-Glasso (FDR)	0.000(0.000)	1.000(0.000)	NA	0.000(0.000)	0.000(0.000)	1.000(0.000)	NA	0.000(0.000)
GI-JOE (Holm)	0.928(0.011)	1.000(0.000)	0.997(0.006)	0.961(0.006)	0.318(0.032)	1.000(0.000)	0.999(0.003)	0.481(0.037)
GI-JOE (FDR)	0.964(0.006)	0.999(0.001)	0.894(0.053)	0.926(0.027)	0.621(0.035)	1.000(0.000)	0.971(0.017)	0.758(0.029)

Table 13: Graph selection results with the ground truth graph being a scale-free graph with 200 nodes, under two real measurement patterns from single-cell RNA sequencing data sets (the *chu* data [11] and *darmanis* data [12]).

Method	<i>chu</i> measurement				<i>darmanis</i> measurement			
	TPR	TNR	TDR	F1 score	TPR	TNR	TDR	F1 score
Nlasso (AND)	0.997(0.003)	0.975(0.022)	0.457(0.288)	0.574(0.281)	0.953(0.018)	0.960(0.008)	0.213(0.113)	0.339(0.114)
Nlasso (OR)	0.999(0.003)	0.973(0.020)	0.372(0.199)	0.512(0.216)	0.965(0.015)	0.964(0.007)	0.222(0.072)	0.356(0.080)
Glasso	0.983(0.021)	0.990(0.007)	0.579(0.234)	0.701(0.172)	0.936(0.017)	0.980(0.004)	0.341(0.120)	0.492(0.098)
CLIME	0.999(0.002)	0.969(0.002)	0.247(0.013)	0.395(0.016)	0.947(0.018)	0.958(0.018)	0.218(0.094)	0.345(0.118)
Nlasso-JOE (AND)	0.912(0.043)	0.999(0.000)	0.939(0.043)	0.924(0.008)	0.757(0.020)	0.999(0.000)	0.881(0.019)	0.814(0.014)
Nlasso-JOE (OR)	0.935(0.023)	0.996(0.002)	0.746(0.152)	0.820(0.078)	0.860(0.016)	0.992(0.001)	0.518(0.024)	0.646(0.018)
DB-Glasso (Holm)	0.000(0.000)	1.000(0.000)	NA	0.000(0.000)	0.000(0.000)	1.000(0.000)	NA	0.000(0.000)
DB-Glasso (FDR)	0.000(0.000)	1.000(0.000)	NA	0.000(0.000)	0.000(0.000)	1.000(0.000)	NA	0.000(0.000)
GI-JOE (Holm)	0.903(0.013)	1.000(0.000)	0.986(0.009)	0.942(0.007)	0.460(0.024)	1.000(0.000)	0.999(0.002)	0.630(0.022)
GI-JOE (FDR)	0.941(0.007)	0.999(0.000)	0.908(0.035)	0.924(0.017)	0.691(0.020)	1.000(0.000)	0.958(0.015)	0.802(0.014)

Table 14: Graph selection results with the ground truth graph being a small-world graph with 200 nodes, under two real measurement patterns from single-cell RNA sequencing data sets (the *chu* data [11] and *darmanis* data [12]).

Method	Neuron set 1				Neuron set 2				Neuron set 3			
	TPR	TNR	TDR	F1	TPR	TNR	TDR	F1	TPR	TNR	TDR	F1
GI-JOE(FDR)	0.725	0.996	0.879	0.795	0.595	0.999	0.922	0.723	0.396	1.000	0.950	0.559
GI-JOE(Holm)	0.583	0.998	0.921	0.714	0.405	1.000	0.970	0.571	0.333	1.000	1.000	0.500
DB-Glasso(FDR)	0.142	1.000	1.000	0.248	0.177	1.000	0.933	0.298	0.333	1.000	0.941	0.492
DB-Glasso(Holm)	0.133	1.000	1.000	0.235	0.139	1.000	1.000	0.244	0.250	1.000	1.000	0.400

Table 15: Comparison of the tested sub-graph on a real calcium imaging data set, when the sub-graph only consists of neurons in one of the three sets. Neuron set 1, 2, 3 are observed with high, median and low probabilities, respectively. For neuron set 3, all methods don't work well due to the small sample sizes, while for neuron sets 1 and 2, GI-JOE approaches have much higher true positive rate and F1-scores than the debiased graphical lasso with minimum sample size.

Method	TPR	TNR	TDR	F1
GI-JOE(FDR)	0.494	0.999	0.884	0.634
GI-JOE(Holm)	0.374	1.000	0.934	0.534
DB-Glasso(FDR)	0.150	1.000	0.962	0.260
DB-Glasso(Holm)	0.124	1.000	1.000	0.220

Table 16: Comparison of the tested full graph on a real calcium imaging data set.

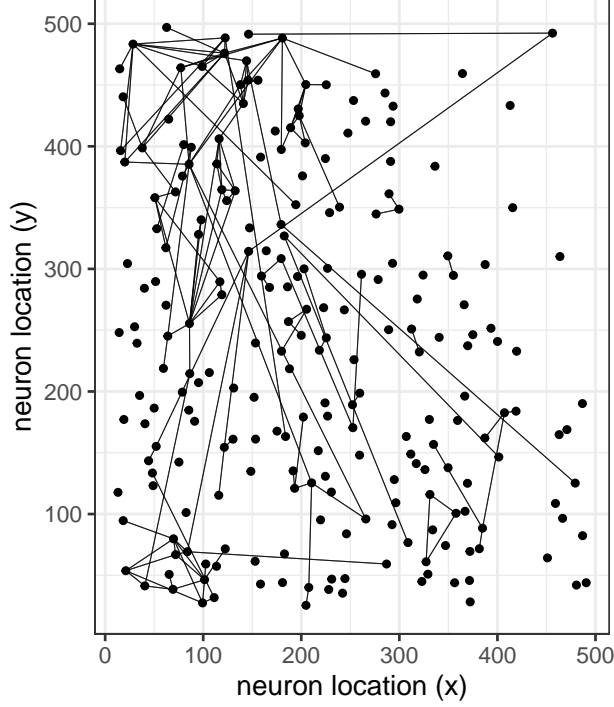


Figure 7: The estimated graph from the calcium imaging data set [30]. We generate data from this graph in our first set of simulations presented in Section 5.3.

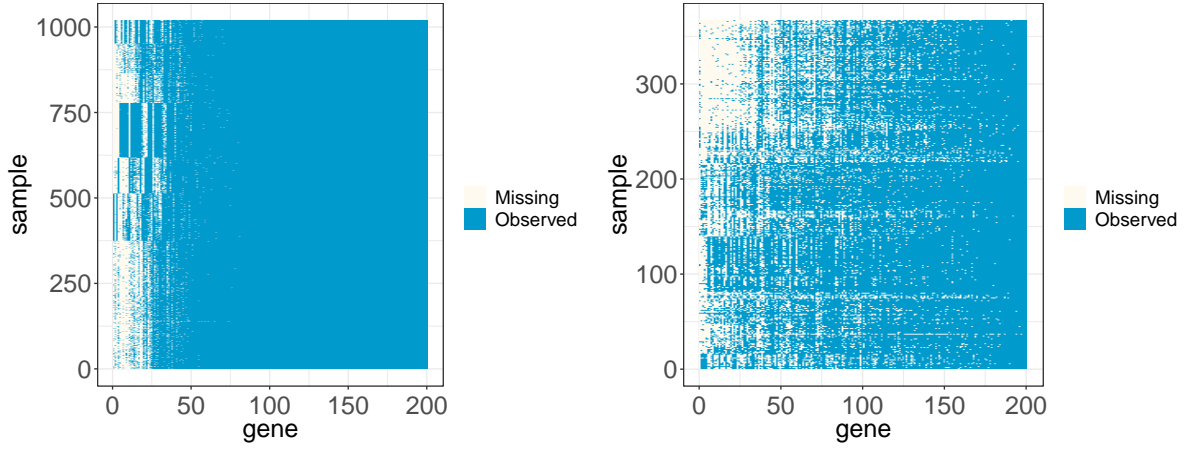
G Proofs

G.1 Proof of Theorem 1 and Theorem 7

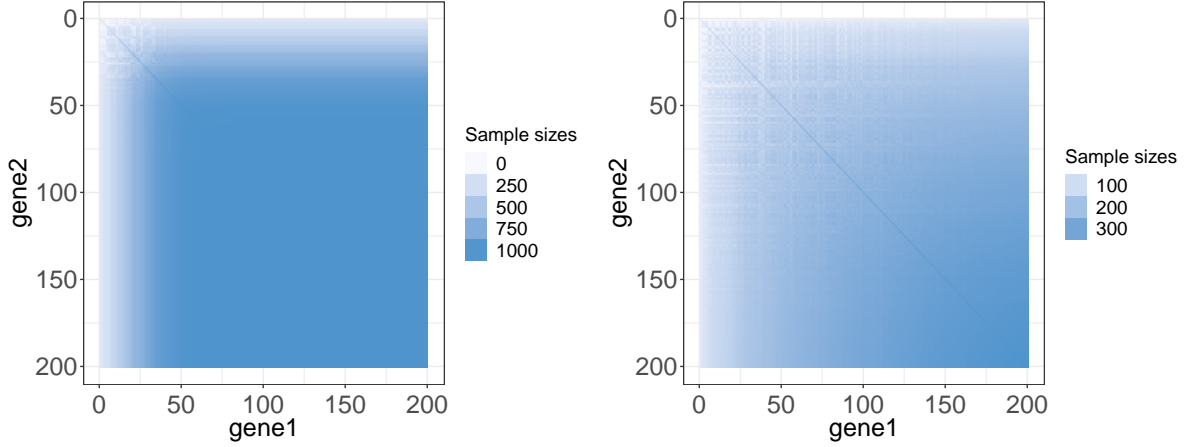
Proof of Theorem 1. We first would like to show that there is no false positive: $\hat{\theta}_{(\mathcal{N}_a)^c} = 0$;

While the second step is to show no false negative in \mathcal{N}_a . Let

$$\tilde{\theta} = \arg \min_{\theta_{(\mathcal{N}_a)^c} = 0} \frac{1}{2} \theta^\top \tilde{\Sigma} \theta - \tilde{\Sigma}_{:,a} \theta + \|\lambda \circ \theta\|_1,$$



(a) Observational patterns



(b) Pairwise sample sizes

Figure 8: Observational patterns and pairwise sample sizes of two real scRNA-seq data sets [11, 12], including top 200 genes with the highest variances. The pairwise sample sizes range from 0 to 1018 (*chu* data, left) and from 5 to 366 (*darmanis*, right). These are the observational patterns used in our second set of simulations presented in Section 5.3.

$\tilde{\Delta} = \tilde{\theta} - \theta^*$, then since $\tilde{\Sigma}$ is positive semi-definite, $\hat{\theta}$ exists and satisfies the KKT condition,

$$\tilde{\Sigma}_{\mathcal{N}_a, \mathcal{N}_a} \Delta_{\mathcal{N}_a} + \tilde{\Sigma}_{\mathcal{N}_a, \mathcal{N}_a} \theta_{\mathcal{N}_a}^* - \tilde{\Sigma}_{\mathcal{N}_a, a} + \lambda_{\mathcal{N}_a} \circ \tilde{Z}_{\mathcal{N}_a} = 0, \quad (15)$$

$$\text{where } \tilde{Z}_j = \begin{cases} \text{sgn}(\tilde{\theta}_j), & j \in \mathcal{N}_a, \tilde{\theta}_j \neq 0 \\ \in [-1, 1], & j \in \mathcal{N}_a, \tilde{\theta}_j = 0. \end{cases} \quad \text{Define } \tilde{Z}_j, j \in \overline{\mathcal{N}}_a^c \text{ to satisfy}$$

$$\tilde{\Sigma}_{\overline{\mathcal{N}}_a^c, \mathcal{N}_a} \Delta_{\mathcal{N}_a} + \tilde{\Sigma}_{\overline{\mathcal{N}}_a^c, \mathcal{N}_a} \theta_{\mathcal{N}_a}^* - \tilde{\Sigma}_{\overline{\mathcal{N}}_a^c, a} + \lambda_{\overline{\mathcal{N}}_a^c} \circ \tilde{Z}_{\overline{\mathcal{N}}_a^c}, \quad (16)$$

and we would like to show $\|\tilde{Z}_{\mathcal{N}_a^c}\|_\infty \leq 1$. By (15) and (16), we have that

$$\begin{aligned} \tilde{Z}_{\mathcal{N}_a^c} &= \frac{1}{\lambda_{\mathcal{N}_a^c}} \circ \left[\tilde{\Sigma}_{\mathcal{N}_a^c, a} - \tilde{\Sigma}_{\mathcal{N}_a^c, \mathcal{N}_a} \theta_{\mathcal{N}_a}^* \right. \\ &\quad \left. - \tilde{\Sigma}_{\mathcal{N}_a^c, \mathcal{N}_a} (\tilde{\Sigma}_{\mathcal{N}_a, \mathcal{N}_a})^{-1} (\tilde{\Sigma}_{\mathcal{N}_a, a} - \tilde{\Sigma}_{\mathcal{N}_a, \mathcal{N}_a} \theta_{\mathcal{N}_a}^* - \lambda_{\mathcal{N}_a} \circ \tilde{Z}_{\mathcal{N}_a}) \right] \end{aligned}$$

In the following we first bound $|\tilde{\Sigma}_{j,a} - \tilde{\Sigma}_{j,\mathcal{N}_a} \theta_{\mathcal{N}_a}^*|$ for any $j \neq a$, then bound $\left\| \tilde{\Sigma}_{\mathcal{N}_a^c, \mathcal{N}_a} (\tilde{\Sigma}_{\mathcal{N}_a, \mathcal{N}_a})^{-1} \right\|_\infty$.

Let $\widehat{W} = \tilde{\Sigma} - \Sigma^*$, then we have

$$\begin{aligned} \left| \tilde{\Sigma}_{j,a} - \tilde{\Sigma}_{j,\mathcal{N}_a} \theta_{\mathcal{N}_a}^* \right| &= \left| \Sigma_{j,a}^* - \Sigma_{j,\mathcal{N}_a}^* \theta_{\mathcal{N}_a}^* + \widehat{W}_{j,a} - \widehat{W}_{j,\mathcal{N}_a} \theta_{\mathcal{N}_a}^* \right| \\ &= \left| \widehat{W}_{j,a} - \widehat{W}_{j,\mathcal{N}_a} \theta_{\mathcal{N}_a}^* \right|, \end{aligned} \tag{17}$$

where the last equation is due to the definition

$$\theta_{\mathcal{N}_a}^* = (\Sigma_{\setminus a, \setminus a}^*)^{-1} \Sigma_{\setminus a, a}^*.$$

By Proposition 1, with probability at least $1 - p^{-c}$,

$$|\widehat{W}_{ij}| \leq C \|\Sigma^*\|_\infty \sqrt{\frac{\log p}{n_{ij}}}$$

holds for all $1 \leq i, j \leq p$. Hence

$$\left| \tilde{\Sigma}_{j,a} - \tilde{\Sigma}_{j,\mathcal{N}_a} \theta_{\mathcal{N}_a}^* \right| \leq \|\widehat{W}_{j, \overline{\mathcal{N}_a}}\|_\infty (\kappa_1 + 1) \leq \frac{\gamma \lambda_j}{4} \tag{18}$$

for $j \neq a$.

On the other hand, for any $j \in \overline{\mathcal{N}_a^c}$,

$$\begin{aligned} &\|(\tilde{\Sigma}_{\mathcal{N}_a, \mathcal{N}_a})^{-1} \tilde{\Sigma}_{\mathcal{N}_a, j}\|_1 \\ &\leq \|(\Sigma_{\mathcal{N}_a, \mathcal{N}_a}^*)^{-1} \Sigma_{\mathcal{N}_a, j}^*\|_1 + d_a \left\| (\tilde{\Sigma}_{\mathcal{N}_a, \mathcal{N}_a})^{-1} \right\|_\infty \left\| \tilde{\Sigma}_{\mathcal{N}_a, j} - \Sigma_{\mathcal{N}_a, j}^* \right\|_\infty \\ &\quad + d_a \|(\tilde{\Sigma}_{\mathcal{N}_a, \mathcal{N}_a})^{-1} - (\Sigma_{\mathcal{N}_a, \mathcal{N}_a}^*)^{-1}\|_\infty \|\Sigma_{\mathcal{N}_a, j}^*\|_1 \\ &\leq 1 - \gamma + \kappa_3 d_a \|(\tilde{\Sigma}_{\mathcal{N}_a, \mathcal{N}_a})^{-1} - (\Sigma_{\mathcal{N}_a, \mathcal{N}_a}^*)^{-1}\|_\infty \\ &\quad + C d_a \left(\kappa_2 + d_a \left\| (\tilde{\Sigma}_{\mathcal{N}_a, \mathcal{N}_a})^{-1} - (\Sigma_{\mathcal{N}_a, \mathcal{N}_a}^*)^{-1} \right\|_\infty \right) \\ &\quad * \max_{i \in \mathcal{N}_a} \|\Sigma^*\|_\infty \sqrt{\frac{\log p}{n_{ij}}} \\ &\leq 1 - \frac{5\gamma}{6} + \left(\kappa_3 + \frac{\gamma}{6\kappa_2} \right) d_a \|(\tilde{\Sigma}_{\mathcal{N}_a, \mathcal{N}_a})^{-1} - (\Sigma_{\mathcal{N}_a, \mathcal{N}_a}^*)^{-1}\|_\infty. \end{aligned} \tag{19}$$

Since

$$\begin{aligned}
\left\| \left(\Sigma_{\mathcal{N}_a, \mathcal{N}_a}^* \right)^{-1} \widehat{W}_{\mathcal{N}_a, \mathcal{N}_a} \right\|_{\infty} &\leq \left\| \left(\Sigma_{\mathcal{N}_a, \mathcal{N}_a}^* \right)^{-1} \right\|_{\infty} \left\| \widehat{W}_{\mathcal{N}_a, \mathcal{N}_a} \right\|_{\infty} \\
&\leq \kappa_2 d_a \left\| \widehat{W}_{\mathcal{N}_a, \mathcal{N}_a} \right\|_{\infty} \\
&\leq C \kappa_2 d_a \max_{i, j \in \mathcal{N}_a} \left\| \Sigma^* \right\|_{\infty} \sqrt{\frac{\log p}{n_{ij}}} \\
&\leq \frac{1}{2},
\end{aligned}$$

where the last line is due to the sample size requirement in Theorem 1. Thus the following matrix expansion holds:

$$\begin{aligned}
&\left(\widetilde{\Sigma}_{\mathcal{N}_a, \mathcal{N}_a} \right)^{-1} - \left(\Sigma_{\mathcal{N}_a, \mathcal{N}_a}^* \right)^{-1} \\
&= \left(\Sigma_{\mathcal{N}_a, \mathcal{N}_a}^* + \widehat{W}_{\mathcal{N}_a, \mathcal{N}_a} \right)^{-1} - \left(\Sigma_{\mathcal{N}_a, \mathcal{N}_a}^* \right)^{-1} \\
&= \sum_{k=1}^{\infty} (-1)^k \left[\left(\Sigma_{\mathcal{N}_a, \mathcal{N}_a}^* \right)^{-1} \widehat{W}_{\mathcal{N}_a, \mathcal{N}_a} \right]^k \left(\Sigma_{\mathcal{N}_a, \mathcal{N}_a}^* \right)^{-1} \\
&= - \left(\Sigma_{\mathcal{N}_a, \mathcal{N}_a}^* \right)^{-1} \widehat{W}_{\mathcal{N}_a, \mathcal{N}_a} J \left(\Sigma_{\mathcal{N}_a, \mathcal{N}_a}^* \right)^{-1}.
\end{aligned} \tag{20}$$

Here $J = \sum_{k=0}^{\infty} (-1)^k \left[\left(\Sigma_{\mathcal{N}_a, \mathcal{N}_a}^* \right)^{-1} \widehat{W}_{\mathcal{N}_a, \mathcal{N}_a} \right]^k$ and satisfies $\left\| J \right\|_{\infty} \leq \sum_{k=0}^{\infty} \left(\frac{1}{2} \right)^k = 2$. Hence we have

$$\begin{aligned}
&\left\| \left(\widetilde{\Sigma}_{\mathcal{N}_a, \mathcal{N}_a} \right)^{-1} - \left(\Sigma_{\mathcal{N}_a, \mathcal{N}_a}^* \right)^{-1} \right\|_{\infty} \\
&\leq 2 \kappa_2^2 \left\| \widehat{W}_{\mathcal{N}_a, \mathcal{N}_a} \right\|_{\infty} \\
&\leq 2C \kappa_2^2 \left\| \Sigma^* \right\|_{\infty} \max_{i, j \in \mathcal{N}_a} \sqrt{\frac{\log p}{n_{ij}}} \\
&\leq \min \left\{ \frac{\kappa_2}{s}, \frac{\gamma}{6\kappa_3 s} \right\}.
\end{aligned} \tag{21}$$

Combining (21) and (19) implies

$$\left\| \left(\widetilde{\Sigma}_{\mathcal{N}_a, \mathcal{N}_a} \right)^{-1} \widetilde{\Sigma}_{\mathcal{N}_a, j} \right\|_1 \leq 1 - \frac{\gamma}{2}. \tag{22}$$

By (17), (18), (22), we have

$$\begin{aligned}
&\left\| \widetilde{Z}_{\overline{\mathcal{N}}_a^c} \right\|_{\infty} \\
&\leq \frac{\gamma}{4} + \left(1 - \frac{\gamma}{2} \right) \frac{\max_{j \in \mathcal{N}_a} \lambda_j}{\min_{j \in \overline{\mathcal{N}}_a^c} \lambda_j} \\
&\leq c\gamma + \left(1 - \frac{\gamma}{2} \right) \sqrt{\gamma_a} \\
&\leq \leq 1,
\end{aligned}$$

where the last inequality is due to the condition on γ_a .

Now we only need to upper bound $\|\Delta_{\mathcal{N}_a}\|_\infty$. Based on (15), (18) and (21), it is straightforward to see that

$$\|\Delta_{\mathcal{N}_a}\|_\infty \leq 2\kappa_2(1 + \frac{\gamma}{4}) \max_{j \in \mathcal{N}_a} \lambda_j \leq \frac{\theta_{\min}^*}{2},$$

which implies that $\{j : \hat{\theta}_j \neq 0\} = \mathcal{N}_a$ and $\text{sgn}(\hat{\theta}_j) = \text{sgn}(\theta_j^*) = \text{sgn}(\Theta_{ja}^*)$. \square

Proof of Theorem 7. By the definition of $\hat{\theta}^{(a)}$, we have

$$\begin{aligned} & \frac{1}{2} \hat{\theta}^{(a)\top} \tilde{\Sigma} \hat{\theta}^{(a)} - \tilde{\Sigma}_{a,:} \hat{\theta}^{(a)} + \sum_{j=1}^p \lambda_j^{(a)} |\hat{\theta}_j^{(a)}| \\ & \leq \frac{1}{2} \theta^{(a)*\top} \tilde{\Sigma} \hat{\theta}^{(a)*} - \tilde{\Sigma}_{a,:} \theta^{(a)*} + \sum_{j=1}^p \lambda_j^{(a)} |\theta_j^{(a)*}|, \end{aligned}$$

which implies

$$\begin{aligned} & \frac{1}{2} (\hat{\theta}^{(a)} - \theta^{(a)*})^\top \tilde{\Sigma} (\hat{\theta}^{(a)} - \theta^{(a)*}) \\ & \leq (\tilde{\Sigma}_{:,a} - \tilde{\Sigma} \theta^{(a)*})^\top (\hat{\theta}^{(a)} - \theta^{(a)*}) + \sum_{j=1}^p \lambda_j^{(a)} (|\theta_j^{(a)*}| - |\hat{\theta}_j^{(a)}|) \\ & \leq \sum_{j=1}^p \|\tilde{\Sigma}_{j,:} - \Sigma_{j,:}^*\|_\infty (\|\theta^{(a)*}\|_1 + 1) |\hat{\theta}_j^{(a)} - \theta_j^{(a)*}| + \sum_{j=1}^p \lambda_j^{(a)} (|\theta_j^{(a)*}| - |\hat{\theta}_j^{(a)}|) \end{aligned} \quad (23)$$

$$= \sum_{j=1}^p \|\tilde{\Sigma}_{j,:} - \Sigma_{j,:}^*\|_\infty \frac{\|\Theta_{:,a}^*\|_1}{\Theta_{a,a}^*} |\hat{\theta}_j^{(a)} - \theta_j^{(a)*}| + \sum_{j=1}^p \lambda_j^{(a)} (|\theta_j^{(a)*}| - |\hat{\theta}_j^{(a)}|). \quad (24)$$

The following lemma provides an upper bound for $\|\tilde{\Sigma}_{j,:} - \Sigma_{j,:}^*\|_\infty$:

Lemma 2 (Entry-wise error bounds for $\hat{\Sigma} - \Sigma^*$ and $\tilde{\Sigma}$). *With probability at least $1 - p^{-c}$, for $1 \leq i, j \leq p$,*

$$\begin{aligned} |\hat{\Sigma}_{i,j} - \Sigma_{i,j}^*| & \leq C \|\Sigma^*\|_\infty \sqrt{\frac{\log p}{n_{i,j}}}, \\ |\tilde{\Sigma}_{i,j} - \Sigma_{i,j}^*| & \leq C \|\Sigma^*\|_\infty \sqrt{\frac{\log p}{n_{i,j}}}. \end{aligned}$$

Lemma 2 suggests that

$$\|\tilde{\Sigma}_{j,:} - \Sigma_{j,:}^*\|_\infty (\|\theta^{(a)*}\|_1 + 1) \leq C \|\Sigma^*\|_\infty \frac{\|\Theta_{:,a}^*\|_1}{\Theta_{a,a}^*} \sqrt{\frac{\log p}{\min_k n_{j,k}}} \leq \frac{\lambda_j^{(a)}}{2}$$

with high probability. Together with (24), we have

$$\begin{aligned}
& \frac{1}{2}(\widehat{\theta}^{(a)} - \theta^{(a)*})^\top \widetilde{\Sigma}(\widehat{\theta}^{(a)} - \theta^{(a)*}) \\
& \leq \sum_{j=1}^p \frac{\lambda_j}{2} |\widehat{\theta}_j^{(a)} - \theta_j^{(a)*}| + \lambda_j^{(a)} (|\theta_j^{(a)*}| - |\widehat{\theta}_j^{(a)}|) \\
& \leq \sum_{j \in \mathcal{N}_a} \frac{3}{2} \lambda_j^{(a)} |\widehat{\theta}_j^{(a)} - \theta_j^{(a)*}| - \sum_{j \in \overline{\mathcal{N}}_a^c} \frac{1}{2} \lambda_j^{(a)} |\widehat{\theta}_j^{(a)} - \theta_j^{(a)*}|,
\end{aligned}$$

where $\mathcal{N}_a = \{j \neq a : \Theta_{j,a}^* \neq 0\} = \{j : \theta_j^{(a)*} \neq 0\}$ and $\overline{\mathcal{N}}_a = \{a\} \cup \mathcal{N}_a$. By construction, $\widetilde{\Sigma}$ is positive semi-definite, which implies that

$$\sum_{j \in \overline{\mathcal{N}}_a^c} \lambda_j^{(a)} |\widehat{\theta}_j^{(a)} - \theta_j^{(a)*}| \leq 3 \sum_{j \in \mathcal{N}_a} \lambda_j^{(a)} |\widehat{\theta}_j^{(a)} - \theta_j^{(a)*}|. \quad (25)$$

Our next step is to show a lower bound of the L.H.S. of the inequality above. Let $\Delta = \widehat{\theta}^{(a)} - \theta^{(a)*}$. First note that

$$\frac{1}{2} \Delta^\top \widetilde{\Sigma} \Delta \geq \frac{1}{2} \|\Delta\|_2^2 \lambda_{\min}(\Sigma^*) - \frac{1}{2} |\Delta^\top (\widetilde{\Sigma} - \Sigma^*) \Delta|,$$

where the latter term can be further bounded as follows:

$$\begin{aligned}
|\Delta^\top (\widetilde{\Sigma} - \Sigma^*) \Delta| & \leq \sum_{j,k} \lambda_j^{(a)} |\Delta_j| \left| \frac{\widetilde{\Sigma}_{j,k} - \Sigma_{j,k}^*}{\lambda_j^{(a)}} \right| |\Delta_k| \\
& \leq \left(\sum_{j=1}^p \lambda_j^{(a)} |\Delta_j| \right) \|\Delta\|_1 \max_{j,k} \left| \frac{\widetilde{\Sigma}_{j,k} - \Sigma_{j,k}^*}{\lambda_j^{(a)}} \right| \\
& \leq \frac{\Theta_{a,a}^*}{2 \|\Theta_{:,a}^*\|_1} \left(\sum_{j=1}^p \lambda_j^{(a)} |\Delta_j| \right) \|\Delta\|_1,
\end{aligned}$$

where the last line is due to Lemma 2. By (25),

$$\begin{aligned}
\|\Delta\|_1 & = \sum_{j \in \mathcal{N}_a} |\Delta_j| + \sum_{j \in \overline{\mathcal{N}}_a^c} |\Delta_j| \\
& \leq \sum_{j \in \mathcal{N}_a} |\Delta_j| + \frac{1}{\min_{j \in \overline{\mathcal{N}}_a^c} \lambda_j^{(a)}} \sum_{j \in \overline{\mathcal{N}}_a^c} \lambda_j^{(a)} |\Delta_j| \\
& \leq \sum_{j \in \mathcal{N}_a} |\Delta_j| + \frac{3 \max_{j \in \mathcal{N}_a} \lambda_j^{(a)}}{\min_{j \in \overline{\mathcal{N}}_a^c} \lambda_j^{(a)}} \sum_{j \in \mathcal{N}_a} |\Delta_j| \\
& \leq (3\sqrt{\gamma_a} + 1) \sqrt{d_a} \|\Delta\|_2,
\end{aligned} \quad (26)$$

and

$$\begin{aligned}
\sum_{j=1}^p \lambda_j^{(a)} |\Delta_j| &\leq 4 \sum_{j \in \mathcal{N}_a} \lambda_j^{(a)} |\Delta_j| \\
&\leq 4 \max_{j \in \mathcal{N}_a} \lambda_j^{(a)} \sqrt{d_a} \|\Delta\|_2 \\
&\leq \frac{C \|\Sigma^*\|_\infty \|\Theta_{:,a}^*\|_1}{\Theta_{a,a}^*} \sqrt{\frac{d_a \log p}{\min_{j \in \mathcal{N}_a} \min_k n_{j,k}}} \|\Delta\|_2.
\end{aligned}$$

Hence we can further bound the term above as follows:

$$\begin{aligned}
&|\Delta^\top (\tilde{\Sigma} - \Sigma^*) \Delta| \\
&\leq C \|\Sigma^*\|_\infty \sqrt{\frac{d_a^2 \log p}{\min_{j \in \mathcal{N}_a} \min_k n_{j,k}}} (\sqrt{\gamma_a} + 1) \|\Delta\|_2^2 \\
&\leq \frac{\lambda_{\min}(\Sigma^*)}{2} \|\Delta\|_2^2,
\end{aligned}$$

where the last line is due to our condition that

$$\min_{j \in \mathcal{N}_a} \min_k n_{j,k} \geq C \frac{C \|\Sigma^*\|_\infty^2 (\gamma_a + 1)}{\lambda_{\min}^2(\Sigma^*)} d_a^2 \log p.$$

Therefore,

$$\begin{aligned}
\|\Delta\|_2^2 &\leq \frac{6}{\lambda_{\min}(\Sigma^*)} \sum_{j \in \mathcal{N}_a} \lambda_j^{(a)} |\Delta_j| \\
&\leq \frac{C \|\Sigma^*\|_\infty \|\Theta_{:,a}^*\|_1}{\lambda_{\min}(\Sigma^*) \Theta_{a,a}^*} \sqrt{\frac{d_a \log p}{\min_{j \in \mathcal{N}_a} \min_k n_{j,k}}} \|\Delta\|_2,
\end{aligned}$$

which implies

$$\|\Delta\|_2 \leq \frac{C \|\Sigma^*\|_\infty \|\Theta_{:,a}^*\|_1}{\lambda_{\min}(\Sigma^*) \Theta_{a,a}^*} \sqrt{\frac{d_a \log p}{\min_{j \in \mathcal{N}_a} \min_k n_{j,k}}}.$$

While for the ℓ_1 norm error, one can apply (26) to obtain that

$$\|\Delta\|_1 \leq \frac{C \|\Sigma^*\|_\infty (\sqrt{\gamma_a} + 1) \|\Theta_{:,a}^*\|_1}{\lambda_{\min}(\Sigma^*) \Theta_{a,a}^*} \sqrt{\frac{d_a^2 \log p}{\min_{j \in \mathcal{N}_a} \min_k n_{j,k}}},$$

$$\begin{aligned}
\sum_{j=1}^p \lambda_j^{(a)} |\Delta_j| &\leq 4 \sum_{j \in \mathcal{N}_a} \lambda_j^{(a)} |\Delta_j| \\
&\leq \frac{C \|\Sigma^*\|_\infty^2 \|\Theta_{:,a}^*\|_1^2}{\lambda_{\min}(\Sigma^*) (\Theta_{a,a}^*)^2} \frac{d_a \log p}{\min_{j \in \mathcal{N}_a} \min_k n_{j,k}}.
\end{aligned}$$

□

G.2 Proof of Theorem 2

We start by presenting the following lemma that guarantees the estimation performance of $\widehat{\Theta}^{(a)}$ and hence helps establish our normal approximation result of the debiased neighborhood lasso. Define the sample size ratio for node j as

$$\gamma_j^{(a)} = \frac{\max_{i \in \overline{\mathcal{N}}_j^{(a)c}} \min_k n_{i,k}}{\min_{i \in \mathcal{N}_j^{(a)}} \min_k n_{i,k}}.$$

Also recall the neighborhood lasso estimator used for debiasing:

$$\begin{aligned} \widehat{\theta}^{(a,b)} &= \arg \min_{\theta \in \mathbb{R}^p, \theta_a = \theta_b = 0} \frac{1}{2} \theta^\top \widetilde{\Sigma} \theta - \widetilde{\Sigma}_{b,\cdot} \theta + \sum_{k=1}^p \lambda_k^{(a,b)} |\theta_k|, \\ \widehat{\tau}^{(a,b)} &= (\widetilde{\Sigma}_{b,b} - \widetilde{\Sigma}_{b,\cdot} \widehat{\theta}^{(a,b)})^{-1}, \end{aligned} \tag{27}$$

Lemma 3. *If the tuning parameters $\lambda_k^{(a,j)}$'s in (27) satisfy*

$$\begin{aligned} \lambda_k^{(a,j)} &\asymp \|\Sigma^*\|_\infty \frac{\|\Theta_{j,\cdot}^{(a)*}\|_1}{\Theta_{j,j}^{(a)*}} \sqrt{\frac{\log p}{\min_{i \in [p]} n_{i,k}}}, \\ \min_{i \in \overline{\mathcal{N}}_j^{(a)}} \min_{k \in [p]} n_{i,k} &\geq \frac{C \|\Sigma^*\|_\infty^2 (\gamma_j^{(a)} + \kappa_{\Sigma^*}^2)}{\lambda_{\min}^2(\Sigma^*)} d_j^{(a)2} \log p, \end{aligned}$$

then with probability at least $1 - Cp^{-c}$,

$$\begin{aligned} \|\widehat{\Theta}_{j,\cdot}^{(a)} - \Theta_{j,\cdot}^{(a)*}\|_2 &\leq \frac{C \kappa_{\Sigma^*} \|\Sigma^*\|_\infty}{\lambda_{\min}(\Sigma^*)} \|\Theta_{j,\cdot}^{(a)*}\|_1 \sqrt{\frac{d_j^{(a)} \log p}{\min_{k \in \overline{\mathcal{N}}_k^{(a)}} \min_{i \in [p]} n_{i,k}}}, \\ \|\widehat{\Theta}_{j,\cdot}^{(a)} - \Theta_{j,\cdot}^{(a)*}\|_1 &\leq \frac{C(\kappa_{\Sigma^*} + \sqrt{\gamma_j^{(a)}}) \|\Sigma^*\|_\infty}{\lambda_{\min}(\Sigma^*)} \|\Theta_{j,\cdot}^{(a)*}\|_1 d_j^{(a)} \sqrt{\frac{\log p}{\min_{k \in \overline{\mathcal{N}}_j^{(a)}} \min_{i \in [p]} n_{i,k}}}, \\ \|\widehat{\Theta}_{j,\cdot}^{(a)} - \Theta_{j,\cdot}^{(a)*}\|_{\lambda^{(a,j)},1} &\leq \frac{C \kappa_{\Sigma^*} \|\Sigma^*\|_\infty^2}{\lambda_{\min}(\Sigma^*)} \frac{\|\Theta_{j,\cdot}^{(a)*}\|_1^2}{\Theta_{j,j}^{(a)*}} \frac{d_j^{(a)} \log p}{\min_{k \in \overline{\mathcal{N}}_k^{(a)}} \min_{i \in [p]} n_{i,k}}. \end{aligned}$$

Proof of Lemma 3. By the definition of $\widehat{\Theta}^{(a)}$:

$$\widehat{\Theta}_{b,\setminus b}^{(a)} = -\widehat{\tau}^{(a,b)} \widehat{\theta}_{\setminus b}^{(a,b)}, \quad \widehat{\Theta}_{b,b}^{(a)} = \widehat{\tau}^{(a,b)}, \tag{28}$$

we have

$$\begin{aligned}
& \|\widehat{\Theta}_{j,:}^{(a)} - \Theta_{j,:}^{(a)*}\| \\
& \leq |\widehat{\tau}^{(a,j)} - \tau^{(a,j)*}| \frac{\|\Theta_{j,:}^{(a)*}\|}{\Theta_{j,j}^{(a)*}} + \tau^{(a,j)*} \|\widehat{\theta}^{(a,j)} - \theta^{(a,j)*}\| \\
& \quad + |\widehat{\tau}^{(a,j)} - \tau^{(a,j)*}| \|\widehat{\theta}^{(a,j)} - \theta^{(a,j)*}\|,
\end{aligned} \tag{29}$$

where $\|\cdot\|$ can either be ℓ_2 norm $\|\cdot\|_2$, ℓ_1 norm $\|\cdot\|_1$, or the weighted ℓ_1 norm $\|\cdot\|_{\lambda^{(a,j)},1}$ defined as $\|\theta\|_{\lambda^{(a,j)},1} = \sum_{k=1}^p \lambda_k^{(a,j)} |\theta_k|$, and

$$\begin{aligned}
\tau^{(a,j)*} &= \Theta_{j,j}^{(a)*} = (\Sigma_{j,j}^* - \Sigma_{j,\{a,j\}}^* (\Sigma_{\{a,j\},\{a,j\}}^*)^{-1} \Sigma_{\{a,j\},j}^*)^{-1}, \\
\theta^{(a,j)*} &= (\Sigma_{\{a,j\},\{a,j\}}^*)^{-1} \Sigma_{\{a,j\},j}^*.
\end{aligned}$$

For $\|\widehat{\theta}^{(a,j)} - \theta^{(a,j)*}\|_2$, $\|\widehat{\theta}^{(a,j)} - \theta^{(a,j)*}\|_1$, and $\|\widehat{\theta}^{(a,j)} - \theta^{(a,j)*}\|_{\lambda^{(a,j)},1}$, we can bound them by the same arguments as the proof of Theorem 7. The only difference lies that we substitute Σ^* and $\widetilde{\Sigma}$ by $\Sigma_{\setminus a, \setminus a}^*$ and $\widetilde{\Sigma}_{\setminus a, \setminus a}$, and hence with probability at least $1 - Cp^{-c}$, we have

$$\begin{aligned}
\|\widehat{\theta}^{(a,j)} - \theta^{(a,j)*}\|_2 &\leq \frac{C\|\Sigma^*\|_\infty}{\lambda_{\min}(\Sigma^*)} \frac{\|\Theta_{j,:}^{(a)*}\|_1}{\Theta_{j,j}^{(a)*}} \sqrt{\frac{d_j^{(a)} \log p}{\min_{k \in \mathcal{N}_k^{(a)}} \min_{i \in [p]} n_{i,k}}}, \\
\|\widehat{\theta}^{(a,j)} - \theta^{(a,j)*}\|_1 &\leq \frac{C\|\Sigma^*\|_\infty (\sqrt{\gamma_j^{(a)}} + 1)}{\lambda_{\min}(\Sigma^*)} \frac{\|\Theta_{j,:}^{(a)*}\|_1}{\Theta_{j,j}^{(a)*}} \sqrt{\frac{d_j^{(a)2} \log p}{\min_{k \in \mathcal{N}_j^{(a)}} \min_{i \in [p]} n_{i,k}}}, \\
\|\widehat{\theta}^{(a,j)} - \theta^{(a,j)*}\|_{\lambda^{(a,j)},1} &\leq \frac{C\|\Sigma^*\|_\infty^2}{\lambda_{\min}(\Sigma^*)} \frac{\|\Theta_{j,:}^{(a)*}\|_1^2}{(\Theta_{j,j}^{(a)*})^2} \frac{d_j^{(a)} \log p}{\min_{k \in \mathcal{N}_k^{(a)}} \min_{i \in [p]} n_{i,k}}.
\end{aligned} \tag{30}$$

While for $|\widehat{\tau}^{(a,j)} - \tau^{(a,j)*}|$, we have

$$|\widehat{\tau}^{(a,j)} - \tau^{(a,j)*}| \leq |\widehat{\tau}^{(a,j)} \tau^{(a,j)*}| |(\widehat{\tau}^{(a,j)})^{-1} - (\tau^{(a,j)*})^{-1}|, \tag{31}$$

and by the definition of $\widehat{\tau}^{(a,j)}$,

$$\begin{aligned}
|(\widehat{\tau}^{(a,j)})^{-1} - (\tau^{(a,j)*})^{-1}| &= |\widetilde{\Sigma}_{j,j} - \Sigma_{j,j}^*| + |(\widetilde{\Sigma}_{j,:} - \Sigma_{j,:}^*) \widehat{\theta}^{(a,j)}| \\
&\quad + |\Sigma_{j,:}^* (\widehat{\theta}^{(a,j)} - \theta^{(a,j)*})| \\
&\leq \|(\widetilde{\Sigma} - \Sigma^*)_{j,:}\|_\infty (1 + \|\theta^{(a,j)*}\|_1 + \|\widehat{\theta} - \theta^{(a,j)*}\|_1) \\
&\quad + \|\Sigma_{j,:}^*\|_2 \|\widehat{\theta}^{(a,j)} - \theta^{(a,j)*}\|_2.
\end{aligned}$$

Since $\|\theta^{(a,j)*}\|_1 + 1 = \frac{\|\Theta_{j,:}^{(a)*}\|_1}{\Theta_{j,j}^{(a)*}}$, $\|\widehat{\theta}^{(a,j)} - \theta^{(a,j)*}\|_1 \leq \frac{\|\Theta_{j,:}^{(a)*}\|_1}{\Theta_{j,j}^{(a)*}}$ due to (30) and the sample size condition in Lemma 3, and $\|\Sigma_{j,:}^*\|_2 \geq \lambda_{\min}(\Sigma^*)$, the error term $|(\widehat{\tau}^{(a,j)})^{-1} - (\tau^{(a,j)*})^{-1}|$ can be further bounded by

$$|(\widehat{\tau}^{(a,j)})^{-1} - (\tau^{(a,j)*})^{-1}| \quad (32)$$

$$\leq \frac{C\|\Sigma^*\|_\infty\|\Sigma_{j,:}^*\|_2\|\Theta_{j,:}^{(a)*}\|_1}{\lambda_{\min}(\Sigma^*)\Theta_{j,j}^{(a)*}} \sqrt{\frac{d_j^{(a)} \log p}{\min_{k \in \mathcal{N}_j^{(a)}} \min_{i \in [p]} n_{i,k}}} \quad (33)$$

$$\leq \frac{C\kappa_{\Sigma^*}\|\Sigma^*\|_\infty}{\lambda_{\min}(\Sigma^*)\Theta_{j,j}^{(a)*}} \sqrt{\frac{d_j^{(a)2} \log p}{\min_{k \in \mathcal{N}_j^{(a)}} \min_{i \in [p]} n_{i,k}}} \quad (34)$$

$$\leq \frac{1}{2\tau^{(a,j)*}}, \quad (35)$$

where the last line is due to the fact that $\|\Theta_{j,:}^{(a)*}\|_1 \leq \sqrt{d_j^{(a)}}\|\Theta_{j,:}^{(a)*}\|_2 \leq \sqrt{d_j^{(a)}}\lambda_{\max}(\Theta^{(a)*}) \leq \sqrt{d_j^{(a)}}\lambda_{\min}^{-1}(\Sigma^*)$, $\|\Sigma_{j,:}^*\|_2 \leq \lambda_{\max}(\Sigma^*)$, and the sample size condition in Lemma 3. Plug in (32) into (31), one can show that

$$\begin{aligned} & |\widehat{\tau}^{(a,j)} - \tau^{(a,j)*}| \\ & \leq C(\tau^{(a,j)*})^2 \frac{\|\Sigma^*\|_\infty\|\Sigma_{j,:}^*\|_2\|\Theta_{j,:}^{(a)*}\|_1}{\lambda_{\min}(\Sigma^*)\Theta_{j,j}^{(a)*}} \sqrt{\frac{d_j^{(a)} \log p}{\min_{k \in \mathcal{N}_j^{(a)}} \min_{i \in [p]} n_{i,k}}} \\ & = \frac{C\|\Sigma^*\|_\infty\|\Sigma_{j,:}^*\|_2\Theta_{j,j}^{(a)*}\|\Theta_{j,:}^{(a)*}\|_1}{\lambda_{\min}(\Sigma^*)} \sqrt{\frac{d_j^{(a)} \log p}{\min_{k \in \mathcal{N}_j^{(a)}} \min_{i \in [p]} n_{i,k}}}, \end{aligned}$$

and

$$\begin{aligned} |\widehat{\tau}^{(a,j)} - \tau^{(a,j)*}| & \leq \frac{1}{2}\widehat{\tau}^{(a,j)} \\ & \leq \frac{1}{2}[(\tau^{(a,j)*})^{-1} - |(\widehat{\tau}^{(a,j)})^{-1} - (\tau^{(a,j)*})^{-1}|]^{-1} \leq \tau^{(a,j)*}. \end{aligned}$$

Therefore, combining the bound above with (30) and (29), we have

$$\begin{aligned}
\|\widehat{\Theta}_{j,:}^{(a)} - \Theta_{j,:}^{(a)*}\|_2 &\leq C \frac{\|\Sigma^*\|_\infty \|\Sigma_{j,:}^*\|_2 \|\Theta_{j,:}^{(a)*}\|_1 \|\Theta_{j,:}^{(a)*}\|_2}{\lambda_{\min}(\Sigma^*)} \sqrt{\frac{d_j^{(a)} \log p}{\min_{k \in \overline{\mathcal{N}}_j^{(a)}} \min_{i \in [p]} n_{i,k}}} \\
&\quad + \frac{C \|\Sigma^*\|_\infty}{\lambda_{\min}(\Sigma^*)} \|\Theta_{j,:}^{(a)*}\|_1 \sqrt{\frac{d_j^{(a)} \log p}{\min_{k \in \mathcal{N}_k^{(a)}} \min_{i \in [p]} n_{i,k}}} \\
&\leq \frac{C \kappa_{\Sigma^*} \|\Sigma^*\|_\infty}{\lambda_{\min}(\Sigma^*)} \|\Theta_{j,:}^{(a)*}\|_1 \sqrt{\frac{d_j^{(a)} \log p}{\min_{k \in \overline{\mathcal{N}}_k^{(a)}} \min_{i \in [p]} n_{i,k}}},
\end{aligned}$$

where the last line is due to that $\|\Sigma_{j,:}^*\|_2 \leq \lambda_{\max}(\Sigma^*)$ and $\|\Theta_{j,:}^{(a)*}\|_2 \leq \lambda_{\min}^{-1}(\Sigma^*)$;

$$\begin{aligned}
\|\widehat{\Theta}_{j,:}^{(a)} - \Theta_{j,:}^{(a)*}\|_1 &\leq C \frac{\|\Sigma^*\|_\infty \|\Sigma_{j,:}^*\|_2 \|\Theta_{j,:}^{(a)*}\|_1^2}{\lambda_{\min}(\Sigma^*)} \sqrt{\frac{d_j^{(a)} \log p}{\min_{k \in \overline{\mathcal{N}}_j^{(a)}} \min_{i \in [p]} n_{i,k}}} \\
&\quad + \frac{C \|\Sigma^*\|_\infty (\sqrt{\gamma_j^{(a)}} + 1)}{\lambda_{\min}(\Sigma^*)} \|\Theta_{j,:}^{(a)*}\|_1 \sqrt{\frac{d_j^{(a)2} \log p}{\min_{k \in \mathcal{N}_k^{(a)}} \min_{i \in [p]} n_{i,k}}} \\
&\leq \frac{C \|\Sigma^*\|_\infty \|\Theta_{j,:}^{(a)*}\|_1}{\lambda_{\min}(\Sigma^*)} (\kappa_{\Sigma^*} + \sqrt{\gamma_j^{(a)}}) d_j^{(a)} \sqrt{\frac{\log p}{\min_{k \in \overline{\mathcal{N}}_j^{(a)}} \min_{i \in [p]} n_{i,k}}},
\end{aligned}$$

where we have applied the fact that $\|\Theta_{j,:}^{(a)*}\|_1 \leq \sqrt{d_j^{(a)}} \|\Theta_{j,:}^{(a)*}\|_2$. While for the $\|\cdot\|_{\lambda^{(a,j)},1}$ error,

note that

$$\frac{\|\Theta_{j,:}^{(a)*}\|_{\lambda^{(a,j)},1}}{\Theta_{j,j}^{(a)*}} \leq \frac{\|\Sigma^*\|_\infty \|\Theta_{j,:}^{(a)*}\|_1^2}{(\Theta_{j,j}^{(a)*})^2} \sqrt{\frac{\log p}{\min_{k \in \overline{\mathcal{N}}_j^{(a)}} \min_{i \in [p]} n_{i,k}}},$$

and hence we have

$$\begin{aligned}
\|\widehat{\Theta}_{j,:}^{(a)} - \Theta_{j,:}^{(a)*}\|_{\lambda^{(a,j)},1} &\leq C \frac{\|\Sigma^*\|_\infty^2 \|\Sigma_{j,:}^*\|_2 \|\Theta_{j,:}^{(a)*}\|_1^3}{\lambda_{\min}(\Sigma^*) \Theta_{j,j}^{(a)*}} \frac{\sqrt{d_j^{(a)} \log p}}{\min_{k \in \overline{\mathcal{N}}_j^{(a)}} \min_{i \in [p]} n_{i,k}} \\
&\quad + \frac{C \|\Sigma^*\|_\infty^2 \|\Theta_{j,:}^{(a)*}\|_1^2}{\lambda_{\min}(\Sigma^*) \Theta_{j,j}^{(a)*}} \frac{d_j^{(a)} \log p}{\min_{k \in \mathcal{N}_k^{(a)}} \min_{i \in [p]} n_{i,k}} \\
&\leq C \kappa_{\Sigma^*} \frac{\|\Sigma^*\|_\infty^2 \|\Theta_{j,:}^{(a)*}\|_1^2}{\lambda_{\min}(\Sigma^*) \Theta_{j,j}^{(a)*}} \frac{d_j^{(a)} \log p}{\min_{k \in \mathcal{N}_k^{(a)}} \min_{i \in [p]} n_{i,k}}.
\end{aligned}$$

□

Proof of Theorem 2. First we start with some algebra to decompose $\tilde{\theta}_b^{(a)} - \theta_b^{(a)*} = \tilde{\theta}_b^{(a)} + \frac{\Theta_{a,b}^*}{\Theta_{a,a}^*}$ into terms B and E . Here we applied the fact that $\theta_{\setminus a}^{(a)*} = -\Theta_{a,a}^{*-1}\Theta_{:,a}^*$. By definition (6),

$$\begin{aligned}\tilde{\theta}_b^{(a)} - \theta_b^{(a)*} &= \hat{\theta}_b^{(a)} - \theta_b^{(a)*} - \hat{\Theta}_{b,:}^{(a)}(\hat{\Sigma}\hat{\theta}^{(a)} - \hat{\Sigma}_{:,a}) \\ &= (\Theta_{b,:}^{(a)*}\Sigma^* - \hat{\Theta}_{b,:}^{(a)}\hat{\Sigma})(\hat{\theta}^{(a)} - \theta^{(a)*}) - \hat{\Theta}_{b,:}^{(a)}(\hat{\Sigma}\theta^{(a)*} - \hat{\Sigma}_{:,a}) \\ &= (\Theta_{b,:}^{(a)*}\Sigma^* - \hat{\Theta}_{b,:}^{(a)}\hat{\Sigma})(\hat{\theta}^{(a)} - \theta^{(a)*}) + \Theta_{a,a}^{*-1}(\hat{\Theta}_{b,:}^{(a)} - \Theta_{b,:}^{(a)*})(\hat{\Sigma} - \Sigma^*)\Theta_{:,a}^* \\ &\quad + \Theta_{a,a}^{*-1}\Theta_{b,:}^{(a)*}(\hat{\Sigma} - \Sigma^*)\Theta_{:,a}^*,\end{aligned}$$

where the second line is due to that $(\Theta_{b,:}^{(a)*}\Sigma^*)_{\setminus a} = e_b^\top$, and the third line holds since $\hat{\Sigma}\theta^{(a)*} - \hat{\Sigma}_{:,a} = -\Theta_{a,a}^{*-1}\hat{\Sigma}\Theta_{:,a}^*$, and $\hat{\Theta}_{b,:}^{(a)}\Sigma^*\Theta_{:,a}^* = \hat{\Theta}_{b,:}^{(a)}e_a = 0$. Let

$$B = (\Theta_{b,:}^{(a)*}\Sigma^* - \hat{\Theta}_{b,:}^{(a)}\hat{\Sigma})(\hat{\theta}^{(a)} - \theta^{(a)*}) + \Theta_{a,a}^{*-1}(\hat{\Theta}_{b,:}^{(a)} - \Theta_{b,:}^{(a)*})(\hat{\Sigma} - \Sigma^*)\Theta_{:,a}^*, \quad (36)$$

and $E = \Theta_{a,a}^{*-1}\Theta_{b,:}^{(a)*}(\hat{\Sigma} - \Sigma^*)\Theta_{:,a}^*$. We will show an upper bound for $|B|$ and a normal approximation for E .

G.2.1 Bounding the bias term B

We first further decompose the bias term B and upper bound it by functions of estimation errors $\hat{\theta}^{(a)} - \theta^{(a)*}$ and $\hat{\Theta}_{b,:}^{(a)} - \Theta_{b,:}^{(a)*}$. One can show that

$$\begin{aligned}& \left| (\Theta_{b,:}^{(a)*}\Sigma^* - \hat{\Theta}_{b,:}^{(a)}\hat{\Sigma})(\hat{\theta}^{(a)} - \theta^{(a)*}) \right| \\ &= \left| \Theta_{b,:}^{(a)*}(\Sigma^* - \hat{\Sigma})(\hat{\theta}^{(a)} - \theta^{(a)*}) + (\Theta_{b,:}^{(a)*} - \hat{\Theta}_{b,:}^{(a)})\Sigma^*(\hat{\theta}^{(a)} - \theta^{(a)*}) \right. \\ &\quad \left. + (\Theta_{b,:}^{(a)*} - \hat{\Theta}_{b,:}^{(a)})(\hat{\Sigma} - \Sigma^*)(\hat{\theta}^{(a)} - \theta^{(a)*}) \right| \\ &\leq \|\Theta_{b,:}^{(a)*}\|_1 \|\Sigma_{\overline{N}_b^{(a)},:}^* - \hat{\Sigma}_{\overline{N}_b^{(a)},:}\|_\infty \|\hat{\theta}^{(a)} - \theta^{(a)*}\|_1 \\ &\quad + \|\Sigma^*\| \|\Theta_{b,:}^{(a)*} - \hat{\Theta}_{b,:}^{(a)}\|_2 \|\hat{\theta}^{(a)} - \theta^{(a)*}\|_2 \\ &\quad + \sum_{j,k} |\hat{\Sigma}_{j,k} - \Sigma_{j,k}^*| \|\hat{\Theta}_{b,j}^{(a)} - \Theta_{b,j}^*\| |\hat{\theta}_k^{(a)} - \theta_k^{(a)*}|.\end{aligned}$$

Since

$$\begin{aligned}\overline{N}_b^{(a)} &= \{j : \Theta_{b,j}^{(a)*} \neq 0\} = \{j : \Theta_{b,j}^* - \frac{\Theta_{a,b}^*\Theta_{a,j}^*}{\Theta_{a,a}^*} \neq 0\} \\ &\subseteq \{j : \Theta_{b,j}^* \neq 0\} \cup \{j \neq a : \Theta_{a,j}^* \neq 0\} = \mathcal{N}_a \cup \overline{N}_b,\end{aligned}$$

we have $d_b^{(a)} \leq d_a + d_b + 1$, and hence the sample size condition in Theorem 7 and Lemma 3 can be implied by Assumption 2. By Lemma 2, Lemma 3 and Theorem 7, one can show that

$$\begin{aligned}
& \|\Theta_{b,:}^{(a)*}\|_1 \|\Sigma_{\overline{\mathcal{N}}_b^{(a)},:}^* - \widehat{\Sigma}_{\overline{\mathcal{N}}_b^{(a)},:}\|_\infty \|\widehat{\theta}^{(a)} - \theta^{(a)*}\|_1 \\
& \leq C \kappa_{\Sigma^*} (\sqrt{\gamma_a} + 1) \|\Sigma^*\|_\infty^2 \|\Theta_{b,:}^{(a)*}\|_1 \|\Theta_{:,a}^*\|_1 \frac{(d_a + d_b + 1) \log p}{\min_{j \in \mathcal{N}_a \cup \overline{\mathcal{N}}_b^{(a)}} \min_{k \in [p]} n_{j,k}}, \\
& \|\Sigma^*\| \|\Theta_{b,:}^{(a)*} - \widehat{\Theta}_{b,:}^{(a)}\|_2 \|\widehat{\theta}^{(a)} - \theta^{(a)*}\|_2 \\
& \leq C \kappa_{\Sigma^*}^3 \|\Sigma^*\|_\infty^2 \|\Theta_{:,a}^*\|_1 \|\Theta_{:,b}^{(a)*}\|_1 \frac{(d_a + d_b + 1) \log p}{\min_{j \in \mathcal{N}_a \cup \overline{\mathcal{N}}_b^{(a)}} \min_k n_{j,k}}, \\
& \sum_{j,k} |\widehat{\Sigma}_{j,k} - \Sigma_{j,k}^*| |\widehat{\Theta}_{b,j}^{(a)} - \Theta_{b,j}^*| |\widehat{\theta}_k^{(a)} - \theta_k^{(a)*}| \\
& \leq \frac{C \Theta_{a,a}^*}{\|\Theta_{:,a}^*\|_1} \|\widehat{\Theta}_{b,:}^{(a)} - \Theta_{b,:}^{(a)*}\|_2 \sum_{k=1}^p \lambda_k^{(a)} |\widehat{\theta}_k^{(a)} - \theta_k^{(a)*}| \\
& \leq \frac{C \kappa_{\Sigma^*}^2 \|\Sigma^*\|_\infty^3}{\lambda_{\min}(\Sigma^*)} \|\Theta_{:,a}^*\|_1 \|\Theta_{:,b}^{(a)*}\|_1 \left(\frac{(d_a + d_b + 1) \log p}{\min_{j \in \mathcal{N}_a \cup \overline{\mathcal{N}}_b^{(a)}} \min_{k \in [p]} n_{j,k}} \right)^{\frac{3}{2}}.
\end{aligned} \tag{37}$$

Here $\kappa_{\Sigma^*} = \frac{\lambda_{\max}(\Sigma^*)}{\lambda_{\min}(\Sigma^*)}$, and we have applied the fact that $\Theta_{a,a}^* \geq \lambda_{\max}^{-1}(\Sigma^*)$, $\|\Theta_{:,b}^{(a)*}\|_2 \leq \lambda_{\min}^{-1}(\Sigma^*)$. Also noting that we have the condition

$$\frac{(d_a + d_b + 1) \log p}{n_1^{(a,b)}} \leq \frac{C \lambda_{\min}^2(\Sigma^*)}{\|\Sigma^*\|_\infty^2},$$

suggesting the upper bound for the third term in (37) can be dominated by the second term.

Hence we have

$$\begin{aligned}
& \left| (\Theta_{b,:}^{(a)*} \Sigma^* - \widehat{\Theta}_{b,:}^{(a)} \widehat{\Sigma})(\widehat{\theta}^{(a)} - \theta^{(a)*}) \right| \\
& \leq C \kappa_{\Sigma^*} (\kappa_{\Sigma^*}^2 + \sqrt{\gamma_a}) \|\Sigma^*\|_\infty^2 \|\Theta_{:,a}^*\|_1 \|\Theta_{:,b}^{(a)*}\|_1 \frac{(d_a + d_b + 1) \log p}{n_1^{(a,b)}}.
\end{aligned}$$

While for the second term in (36), one can show that

$$\begin{aligned}
& |\Theta_{a,a}^{*-1} (\widehat{\Theta}_{b,:}^{(a)} - \Theta_{b,:}^{(a)*}) (\widehat{\Sigma} - \Sigma^*) \Theta_{:,a}^*| \\
& \leq \frac{\|\Theta_{:,a}^*\|_1}{\Theta_{a,a}^*} \|\widehat{\Theta}_{b,:}^{(a)} - \Theta_{b,:}^{(a)*}\|_1 \|\widehat{\Sigma}_{:, \overline{\mathcal{N}}_a} - \Sigma_{:, \overline{\mathcal{N}}_a}^*\|_\infty \\
& \leq C \kappa_{\Sigma^*} (\kappa_{\Sigma^*} + \sqrt{\gamma_b^{(a)}}) \|\Sigma^*\|_\infty^2 \|\Theta_{:,a}^*\|_1 \|\Theta_{b,:}^{(a)*}\|_1 \frac{(d_a + d_b + 1) \log p}{n_1^{(a,b)}}.
\end{aligned}$$

Therefore, with probability at least $1 - Cp^{-c}$,

$$|B| \leq C_1(\Theta^*) \frac{(d_a + d_b + 1) \log p}{n_1^{(a,b)}},$$

with $C_1(\Theta^*) = C\kappa_{\Sigma^*}(\kappa_{\Sigma^*}^2 + \sqrt{\gamma_a} + \sqrt{\gamma_b^{(a)}})\|\Sigma^*\|_\infty^2\|\Theta_{:,a}^*\|_1\|\Theta_{:,b}^{(a)*}\|_1$.

G.2.2 Normal approximation of term E

Let $\delta^{(i)}, N \in \mathbb{R}^{p \times p}$ such that $\delta_{j,k}^{(i)} = \mathbb{1}_{\{j,k \in V_i\}}$ and $N_{j,k} = n_{j,k}$. Then we can write $\widehat{\Sigma} = \sum_{i=1}^n x_i x_i^\top \circ \delta^{(i)} \oslash N$, where \circ represents Hadamard product and \oslash represents Hadamard division. With a little abuse of notation, when $N_{j,k} = 0$, we let $\frac{\delta_{j,k}^{(i)}}{N_{j,k}} = 0$. To apply the central limit theorem and establish the normal approximation result, here we rewrite E as follows:

$$E = \sum_{i=1}^n \Theta_{a,a}^{*-1} \Theta_{b,:}^{(a)*} [(x_i x_i^\top - \Sigma^*) \circ \delta^{(i)} \oslash N] \Theta_{:,a}^*.$$

Here we applied the fact that $(\sum_{i=1}^n \Sigma^* \circ \delta^{(i)} \oslash N)_{j,k} = \Sigma_{j,k}^*$ as long as $N_{j,k} > 0$, and

$\min_{j \in \overline{\mathcal{N}}_a, k \in \overline{\mathcal{N}}_b^{(a)}} n_{j,k} > 0$. Since the n terms inside the summation are independent, we can apply the central limit theorem. The variance $\sigma_n^2(a, b)$ can be calculated as follows:

$$\begin{aligned} \sigma_n^2(a, b) &= \Theta_{a,a}^{*-2} \sum_{i=1}^n \mathbb{E}(\Theta_{b,:}^{(a)*} [(x_i x_i^\top - \Sigma^*) \circ \delta^{(i)} \oslash N] \Theta_{:,a}^*)^2 \\ &= \Theta_{a,a}^{*-2} \sum_{i=1}^n \text{Var} \left(\sum_{j,k} \Theta_{b,j}^{(a)*} \Theta_{k,a}^* \delta_{j,k}^{(i)} n_{j,k}^{-1} x_{i,j} x_{i,k} \right) \\ &= \Theta_{a,a}^{*-2} \sum_{j,k,j',k'} \frac{\Theta_{b,j}^{(a)*} \Theta_{k,a}^* \Theta_{b,j'}^{(a)*} \Theta_{k',a}^*}{n_{j,k} n_{j',k'}} \mathcal{T}_{j,k,j',k'}^* \sum_{i=1}^n \delta_{j,k}^{(i)} \delta_{j',k'}^{(i)} \\ &= \frac{1}{(\Theta_{a,a}^*)^2} \mathcal{T}^{(n)*} \times_1 \Theta_{:,b}^{(a)*} \times_2 \Theta_{:,a}^* \times_3 \Theta_{:,b}^{(a)*} \times_4 \Theta_{:,a}^*, \end{aligned}$$

where we used the definition

$$\mathcal{T}_{j,k,j',k'}^* = \text{Cov}(x_{i,j} x_{i,k}, x_{i,j'} x_{i,k'}) = \Sigma_{j,j'}^* \Sigma_{k,k'}^* + \Sigma_{j,k'}^* \Sigma_{k,j'}^*$$

on the third line, and $\mathcal{T}_{j,k,j',k'}^{(n)*} = \mathcal{T}_{j,k,j',k'}^* \frac{n_{j,k,j',k'}}{n_{j,k} n_{j',k'}}$. In the following, we will verify the Lyapunov's condition so that we can apply the central limit theorem.

Define $U, U^{(\delta,i)}, \epsilon^{(i)} \in \mathbb{R}^{p \times p}$ by

$$U_{j,k} = \frac{\Theta_{j,b}^{(a)*} \Theta_{k,a}^* + \Theta_{k,b}^{(a)*} \Theta_{j,a}^*}{2\Theta_{a,a}^*},$$

$U_{j,k}^{(\delta,i)} = U_{j,k} \frac{\delta_{j,k}^{(i)}}{n_{j,k}}$, and $\epsilon_{j,k}^{(i)} = x_{i,j}x_{i,k} - \Sigma_{j,k}^*$. Then we can write $E = \sum_{i=1}^n \langle U^{(\delta,i)}, \epsilon^{(i)} \rangle$. Now we will show that $\sum_{i=1}^n \mathbb{E} |\langle U^{(\delta,i)}, \epsilon^{(i)} \rangle|^{2+\delta} = o(\sigma_n^{2+\delta}(a,b))$ for $\delta = \frac{4}{\varepsilon} > 0$. First we bound the sub-exponential norm $\|\cdot\|_{\psi_1}$ of $\langle U^{(\delta,i)}, \epsilon^{(i)} \rangle$, which is defined in Definition 1. One can show that

$$\left\| \sum_{j,k} U_{j,k}^{(\delta,i)} \epsilon_{j,k}^{(i)} \right\|_{\psi_1} \leq \sum_{j,k} |U_{j,k}| \frac{\delta_{j,k}^{(i)}}{n_{j,k}} \|x_{i,j}x_{i,k} - \Sigma_{j,k}^*\|_{\psi_1} \leq C \sum_{j,k} |U_{j,k}| \frac{\delta_{j,k}^{(i)}}{n_{j,k}} \|\Sigma^*\|_{\infty}.$$

Then by the definition of the norm $\|\cdot\|_{\psi_1}$, we have

$$\begin{aligned} & \sum_{i=1}^n \mathbb{E} |\langle U^{(\delta,i)}, \epsilon^{(i)} \rangle|^{2+\delta} \\ & \leq \sum_{i=1}^n (C(2+\delta)\|\Sigma^*\|_{\infty})^{2+\delta} \left(\sum_{j,k} |U_{j,k}| \delta_{j,k}^{(i)} n_{j,k}^{-1} \right)^{2+\delta} \\ & \leq (C(2+\delta)\|\Sigma^*\|_{\infty})^{2+\delta} \left(\sum_{j,k} |U_{j,k}|^2 n_{j,k}^{-1} \right)^{1+\delta/2} \sum_{i=1}^n \left(\sum_{j \in \bar{\mathcal{N}}_b^{(a)}, k \in \bar{\mathcal{N}}_a} \delta_{j,k}^{(i)} n_{j,k}^{-1} \right)^{1+\delta/2}, \end{aligned}$$

where the third line is due to the Cauchy-Schwarz inequality and the fact that $U_{j,k} \neq 0$ only when $j \in \bar{\mathcal{N}}_b^{(a)}$, $k \in \bar{\mathcal{N}}_a$. In addition, for the third term in the multiplication on the third line, we have

$$\begin{aligned} & \sum_{i=1}^n \left(\sum_{j \in \bar{\mathcal{N}}_b^{(a)}, k \in \bar{\mathcal{N}}_a} \delta_{j,k}^{(i)} n_{j,k}^{-1} \right)^{1+\delta/2} \\ & = (d_a + d_b + 1)^{2+\delta} \sum_{i=1}^n \left(\frac{1}{(d_a + d_b + 1)^2} \sum_{j \in \bar{\mathcal{N}}_b^{(a)}, k \in \bar{\mathcal{N}}_a} \delta_{j,k}^{(i)} n_{j,k}^{-1} \right)^{1+\delta/2} \quad (38) \\ & \leq (d_a + d_b + 1)^{\delta} \sum_{i=1}^n \sum_{j \in \bar{\mathcal{N}}_b^{(a)}, k \in \bar{\mathcal{N}}_a} \delta_{j,k}^{(i)} n_{j,k}^{-(1+\delta/2)} \\ & \leq (d_a + d_b + 1)^{2+\delta} (n_2^{(a,b)})^{-\delta/2}, \end{aligned}$$

where the third line is due to Jensen's inequality and the fact that $g(x) = x^{2+\delta}$ is a convex function; the fourth line is due to that $\sum_{i=1}^n \delta_{j,k}^{(i)} = n_{j,k}$, $|\bar{\mathcal{N}}_b^{(a)}|, |\bar{\mathcal{N}}_a| \leq d_a + d_b + 1$, and

$n_2^{(a,b)} = \min_{j \in \bar{\mathcal{N}}_a, k \in \bar{\mathcal{N}}_b^{(a)}} n_{j,k}, n_{j,k} = n_{k,j}$. On the other hand, we can lower bound $\sigma_n^2(a, b)$ as follows:

$$\begin{aligned} \sigma_n^2(a, b) &= \sum_{i=1}^n \mathbb{E} \langle U^{(\delta,i)}, \epsilon^{(i)} \rangle^2 \\ &= \sum_{i=1}^n \sum_{j,j',k,k'} \mathcal{T}_{j,k,j',k'}^* U_{j,k}^{(\delta,i)} U_{j',k'}^{(\delta,i)} \\ &= \sum_{i=1}^n \sum_{j,j'} \Sigma_{j,j'}^* U_{j,:}^{(\delta,i)} \Sigma^*(U_{j',:}^{(\delta,i)})^\top + \sum_{j,k'} \Sigma_{j,k'}^* U_{j,:}^{(\delta,i)} \Sigma^* U_{:,k'}^{(\delta,i)}. \end{aligned}$$

Due to the symmetry of $U^{(\delta,i)}$, we further have

$$\begin{aligned} \sigma_n^2(a, b) &= 2 \sum_{i=1}^n \langle \Sigma^*, U^{(\delta,i)} \Sigma^*(U^{(\delta,i)}) \rangle \\ &= 2 \sum_{i=1}^n \|\Sigma^* \frac{1}{2} U^{(\delta,i)} \Sigma^* \frac{1}{2}\|_F^2 \\ &\geq 2 \lambda_{\min}^2(\Sigma^*) \sum_{j,k} U_{j,k}^2 n_{j,k}^{-1}. \end{aligned}$$

Therefore, combining the upper bounds for $\sum_{i=1}^n \mathbb{E} |\langle U^{(\delta,i)}, \epsilon^{(i)} \rangle|^{2+\delta}$ and $\sigma_n^{2+\delta}(a, b)$ leads to the following:

$$\begin{aligned} \frac{\sum_{i=1}^n \mathbb{E} |\langle U^{(\delta,i)}, \epsilon^{(i)} \rangle|^{2+\delta}}{\sigma_n^{2+\delta}(a, b)} &\leq \left(\frac{C(2+\delta) \|\Sigma^*\|_\infty}{\lambda_{\min}(\Sigma^*)} \right)^{2+\delta} (d_a + d_b + 1)^{2+\delta} (n_2^{(a,b)})^{-\delta/2} \\ &\leq C_\epsilon^{\delta/2}(\Sigma^*) (d_a + d_b + 1)^{2+\delta} (n_2^{(a,b)})^{-\delta/2}. \end{aligned}$$

Since $\delta = \frac{4}{\epsilon}$, $C_\epsilon(\Sigma^*) (d_a + d_b + 1)^{2+\epsilon} = o(n_2(a, b))$, the inequality above implies

$$\sum_{i=1}^n \mathbb{E} |\langle U^{(\delta,i)}, \epsilon^{(i)} \rangle|^{2+\delta} = o(\sigma_n^{2+\delta}(a, b)).$$

Now we can apply the central limit theorem to obtain the following convergence in distribution result:

$$\sigma_n^{-1}(a, b) E \xrightarrow{d} \mathcal{N}(0, 1).$$

G.2.3 Normal Approximation Result

Now that we have proved an upper bound for B and the convergence in distribution result for E , a combination of these two results can lead to our final claim. To see this, note that

$$\sigma_n^{-1}(a, b) \left(\theta_b^{(a)} + \frac{\Theta_{a,b}^*}{\Theta_{a,a}^*} \right) = \frac{B}{\sigma_n(a, b)} + \sigma_n^{-1}(a, b)E.$$

As shown earlier,

$$\begin{aligned} |B| &\leq C_1(\Theta^*) \frac{(d_a + d_b + 1) \log p}{n_1^{(a,b)}} \\ &\leq C \kappa_{\Sigma^*} (\kappa_{\Sigma^*}^2 + \sqrt{\gamma_a} + \sqrt{\gamma_b^{(a)}}) \lambda_{\max}^2(\Sigma^*) \|\Theta_{:,a}^*\|_1 \|\Theta_{:,b}^{(a)*}\|_1 \frac{(d_a + d_b + 1) \log p}{n_1^{(a,b)}}, \end{aligned}$$

and

$$\begin{aligned} \sigma_n(a, b) &\geq \sqrt{2} \lambda_{\min}(\Sigma^*) \sqrt{\sum_{j,k} |U_{j,k}|^2 n_{j,k}^{-1}} \\ &\geq \frac{\sqrt{2} \lambda_{\min}(\Sigma^*) \min_{(j,k) \in S_2(a,b)} \left| \Theta_{b,j}^{(a)*} \Theta_{a,k}^* + \Theta_{b,k}^{(a)*} \Theta_{a,j}^* \right|}{2 \Theta_{a,a}^* \sqrt{n_2^{(a,b)}}} \\ &\geq \frac{\sqrt{2}}{2} \lambda_{\min}^2(\Sigma^*) \frac{\min_{(j,k) \in S_2(a,b)} \left| \Theta_{b,j}^{(a)*} \Theta_{a,k}^* + \Theta_{b,k}^{(a)*} \Theta_{a,j}^* \right|}{\sqrt{n_2^{(a,b)}}}. \end{aligned}$$

Hence

$$\left| \frac{B}{\sigma_n(a, b)} \right| \leq C(\Theta^*; a, b) (\kappa_{\Theta^*}^2 + \sqrt{\gamma_a} + \sqrt{\gamma_b^{(a)}}) \frac{(d_a + d_b + 1) \log p}{\sqrt{n_1^{(a,b)}}} \sqrt{\frac{n_2^{(a,b)}}{n_1^{(a,b)}}},$$

where

$$C(\Theta^*; a, b) = \frac{C \kappa_{\Theta^*}^3 \|\Theta_{:,a}^*\|_1 \|\Theta_{:,b}^{(a)*}\|_1}{\min_{(j,k) \in S_2(a,b)} \left| \Theta_{b,j}^{(a)*} \Theta_{a,k}^* + \Theta_{b,k}^{(a)*} \Theta_{a,j}^* \right|}$$

and $\kappa_{\Theta^*} = \frac{\lambda_{\max}(\Theta^*)}{\lambda_{\min}(\Theta^*)} = \frac{\lambda_{\max}(\Sigma^*)}{\lambda_{\min}(\Sigma^*)} = \kappa_{\Sigma^*}$. When Assumptions 2-4 hold, $\left| \frac{B}{\sigma_n(a, b)} \right| = o(1)$, and

hence

$$\sigma_n^{-1}(a, b) \left(\theta_b^{(a)} + \frac{\Theta_{a,b}^*}{\Theta_{a,a}^*} \right) \xrightarrow{d} \mathcal{N}(0, 1).$$

□

Proof of Proposition 2. As has been shown in the proof of Theorem 2,

$$\begin{aligned}\sigma_n(a, b) &= \sqrt{2} \left(\sum_{i=1}^n \|\Sigma^{*\frac{1}{2}} U^{(\delta, i)} \Sigma^{*\frac{1}{2}}\|_F^2 \right)^{\frac{1}{2}} \\ &\geq \sqrt{2} \lambda_{\min}(\Sigma^*) \frac{\min_{(j, k) \in S_2(a, b)} \left| \Theta_{b, j}^{(a)*} \Theta_{a, k}^* + \Theta_{b, k}^{(a)*} \Theta_{a, j}^* \right|}{2\Theta_{a, a}^* \sqrt{n_2^{(a, b)}}}.\end{aligned}$$

Similarly, for the upper bound, one has

$$\begin{aligned}\sigma_n^2(a, b) &= 2 \sum_{i=1}^n \|\Sigma^{*\frac{1}{2}} U^{(\delta, i)} \Sigma^{*\frac{1}{2}}\|_F^2 \\ &\leq 2\lambda_{\max}^2(\Sigma^*) \sum_{(j, k) \in S_2(a, b)} U_{j, k}^2 n_{j, k}^{-1} \\ &\leq \lambda_{\max}^2(\Sigma^*) \frac{2\|\Theta_{:, b}^{(a)*}\|_2^2 \|\Theta_{:, a}^*\|_2^2}{(\Theta_{a, a}^*)^2} (n_2^{(a, b)})^{-1},\end{aligned}$$

one can show that

$$\begin{aligned}\sigma_n^2(a, b) &\leq \sum_{i=1}^n 2\lambda_{\max} \left(\Sigma_{\mathcal{N}_a, \mathcal{N}_a}^* \otimes \Sigma_{\mathcal{N}_b^{(a)}, \mathcal{N}_b^{(a)}}^* \right) \|U^{(\delta, i)}\|_F^2 \\ &\leq 2\lambda_{\max}^2(\Sigma^*) \sum_{j, k} |U_{j, k}|^2 n_{j, k}^{-1} \\ &\leq \frac{2\lambda_{\max}^2(\Sigma^*) \|\Theta_{:, b}^{(a)*}\|_2^2 \|\Theta_{:, a}^*\|_2^2}{(\Theta_{a, a}^*)^2 n_2^{(a, b)}} \\ &\leq 2\kappa_{\Sigma^*}^4 (n_2^{(a, b)})^{-1}.\end{aligned}$$

□

G.3 Proof of Proposition 3: Consistency of Variance Estimator

First we define the following 4th order tensors that would be useful in our subsequent proof:

$\widehat{\mathcal{T}}, \mathcal{U}^*, \widehat{\mathcal{U}}, \mathcal{N} \in \mathbb{R}^{p \times p \times p \times p}$ that satisfy

$$\begin{aligned}\widehat{\mathcal{T}}_{j, k, j', k'} &= \widehat{\Sigma}_{j, j'} \widehat{\Sigma}_{k, k'}, \\ \mathcal{U}_{j, k, j', k'}^* &= \Theta_{b, j}^{(a)*} \bar{\theta}_k^{(a)} \Theta_{b, j'}^{(a)*} \bar{\theta}_{k'}^{(a)}, \\ \widehat{\mathcal{U}}_{j, k, j', k'} &= \widehat{\Theta}_{b, j}^{(a)} \widehat{\theta}_k^{(a)} \widehat{\Theta}_{b, j'}^{(a)} \widehat{\theta}_{k'}^{(a)}, \\ \mathcal{N}_{j, k, j', k'} &= \frac{n_{j, k, j', k'}}{n_{j, k} n_{j', k'}},\end{aligned}$$

where $\bar{\theta}^{(a)*} = \frac{\Theta_{:,a}^*}{\Theta_{a,a}^*}$. Also recall the definition of tensor $\widehat{\mathcal{T}}^{(n)}$, then we can rewrite $\widehat{\sigma}_n^2(a, b)$ as follows

$$\widehat{\sigma}_n^2(a, b) = 2\langle \widehat{\mathcal{T}} \circ \mathcal{N}, \widehat{\mathcal{U}} \rangle = 2\langle \widehat{\mathcal{T}}, \widehat{\mathcal{U}} \circ \mathcal{N} \rangle.$$

Define $\mathcal{E}_1 = 2(\widehat{\mathcal{T}} - \mathcal{T}^*)$, $\mathcal{E}_2 = \widehat{\mathcal{U}} - \mathcal{U}^*$, then the estimation error for variance $\sigma_n^2(a, b)$ can be decomposed as follows:

$$\widehat{\sigma}_n^2(a, b) - \sigma_n^2(a, b) = \underbrace{\langle \mathcal{E}_1 \circ \mathcal{N}, \mathcal{U}^* \rangle}_{\text{I}} + \underbrace{2\langle \mathcal{T}^*, \mathcal{E}_2 \circ \mathcal{N} \rangle}_{\text{II}} + \underbrace{\langle \mathcal{E}_1 \circ \mathcal{N}, \mathcal{E}_2 \rangle}_{\text{III}},$$

To establish the consistency of the variance estimator $\widehat{\sigma}_n^2(a, b)$, we bound the three terms above separately.

G.3.1 Bounding Error Term I

First we provide an entry-wise estimation error bound for the 4th order moment \mathcal{T}^* .

Lemma 4 (Entry-wise error bound for \mathcal{E}_1). *With probability at least $1 - Cp^{-c}$,*

$$|(\mathcal{E}_1)_{j,k,j',k'}| \leq C\|\Sigma^*\|_\infty^2 \left(\sqrt{\frac{\log p}{n_{j,j'}}} + \sqrt{\frac{\log p}{n_{k,k'}}} + \frac{\log p}{\sqrt{n_{j,j'}n_{k,k'}}} \right).$$

Then by the definition of I, one can show that with probability at least $1 - Cp^{-c}$,

$$\begin{aligned} |\text{I}| &\leq C\|\Sigma^*\|_\infty^2 \sum_{j,k,j',k'} \left(\frac{\sqrt{n_{j,k,j',k'} \log p}}{n_{j,k}n_{j',k'}} + \frac{\log p}{n_{j,k}n_{j',k'}} \right) \mathcal{U}_{j,k,j',k'}^* \\ &\leq C\|\Sigma^*\|_\infty^2 \|\mathcal{U}^*\|_1 \max_{j,j' \in \overline{\mathcal{N}}_b^{(a)}, k,k' \in \overline{\mathcal{N}}_a} \left(\frac{\sqrt{\log p}}{n_{j,k}\sqrt{n_{j',k'}}} + \frac{\log p}{n_{j,k}n_{j',k'}} \right) \\ &\leq C\|\Sigma^*\|_\infty^2 \|\mathcal{U}^*\|_1 \left(\frac{\sqrt{\log p}}{(n_2^{(a,b)})^{3/2}} + \frac{\log p}{(n_2^{(a,b)})^2} \right) \end{aligned}$$

where the second line is due to that $\mathcal{U}_{j,k,j',k'}^*$ is only nonzero for $j, j' \in \overline{\mathcal{N}}_b^{(a)}$, $k, k' \in \overline{\mathcal{N}}_a$.

G.3.2 Bounding Error Term II

Since $|\text{II}| \leq 2\|\mathcal{T}^*\|_\infty \|\mathcal{E} \circ \mathcal{N}\|_1 \leq 2\|\Sigma^*\|_\infty^2 \|\mathcal{E} \circ \mathcal{N}\|_1$, we will show an upper bound for $\|\mathcal{E} \circ \mathcal{N}\|_1$

in the following. By definition,

$$\mathcal{E} \circ \mathcal{N} = [\widehat{\Theta}_{b,:}^{(a)} \otimes \widehat{\theta}^{(a)} \otimes \widehat{\Theta}_{b,:}^{(a)} \otimes \widehat{\theta}^{(a)} - \Theta_{b,:}^{(a)*} \otimes \bar{\theta}^{(a)*} \otimes \Theta_{b,:}^{(a)*} \otimes \bar{\theta}^{(a)*}] \circ \mathcal{N}.$$

The following lemma provides a general upper bound for kronecker products.

Lemma 5. Consider vectors $u^{(1)}, \dots, u^{(4)}, \epsilon^{(1)}, \dots, \epsilon^{(4)} \in \mathbb{R}^p$. Let $i_l = 2\lceil l/2 \rceil - \mathbb{1}_{\{l \text{ is even}\}}$. If for all $1 \leq j \leq 4$,

$$\sum_{j=1}^p \left| \frac{\epsilon_j^{(l)}}{\sqrt{\min_k n_{j,k}}} \right| \leq \frac{C_1 \|u^{(l)}\|_1}{\sqrt{\min_{j \in \text{supp}(u^{(l)})} \min_k n_{j,k}}}, \quad \|\epsilon^{(l)}\|_1 \leq C_1 \|u^{(l)}\|_1$$

for some universal constant C_1 , then we have

$$\begin{aligned} & \|[(u^{(1)} + \epsilon^{(1)}) \otimes (u^{(2)} + \epsilon^{(2)}) \otimes (u^{(3)} + \epsilon^{(3)}) \otimes (u^{(4)} + \epsilon^{(4)}) \\ & \quad - u^{(1)} \otimes u^{(2)} \otimes u^{(3)} \otimes u^{(4)}] \circ \mathcal{N}\|_1 \\ & \leq C_2 \sum_{l=1}^4 \left[\sum_{j=1}^p \frac{|\epsilon_j^{(l)}|}{\sqrt{\min_k n_{j,k}}} \frac{\|u^{(i_l)}\|_1}{\sqrt{\min_{j \in \text{supp}(u^{(l)})} \min_k n_{j,k}}} \prod_{m \neq l, i_l} \|u^{(m)}\|_1 \right], \end{aligned}$$

where C_2 is also a universal constant.

We can apply Lemma 5 with $u^{(1)} = u^{(3)} = \Theta_{b,:}^{(a)*}$, $u^{(2)} = u^{(4)} = \bar{\theta}^{(a)*}$, $\epsilon^{(1)} = \epsilon^{(3)} = \widehat{\Theta}_{b,:}^{(a)} - \Theta_{b,:}^{(a)*}$, $\epsilon^{(2)} = \epsilon^{(4)} = \widehat{\theta}^{(a)} - \bar{\theta}^{(a)*} = -\widehat{\theta}^{(a)} + \theta^{(a)*}$. By Lemma 3,

$$\begin{aligned} \|\epsilon^{(1)}\|_1 & \leq \frac{C(\kappa_{\Sigma^*} + \sqrt{\gamma_b^{(a)}}) \|\Sigma^*\|_\infty \|\Theta_{b,:}^{(a)*}\|_1 d_b^{(a)} \sqrt{\frac{\log p}{\min_{k \in \mathcal{N}_b^{(a)}} \min_{i \in [p]} n_{i,k}}}}{\lambda_{\min}(\Sigma^*)} \\ & \leq C \|\Theta_{b,:}^{(a)*}\|_1 = C \|u^{(1)}\|_1, \end{aligned}$$

where we have applied the sample size condition in Assumption 2. In addition, Lemma 3 implies

$$\begin{aligned} \sum_{j=1}^p \frac{|\epsilon_j^{(1)}|}{\sqrt{\min_k n_{j,k}}} & \leq \frac{C \kappa_{\Sigma^*} \|\Sigma^*\|_\infty \|\Theta_{b,:}^{(a)*}\|_1 d_b^{(a)} \sqrt{\log p}}{\lambda_{\min}(\Sigma^*) \min_{k \in \mathcal{N}_k^{(a)}} \min_{i \in [p]} n_{i,k}} \\ & \leq \frac{\|u^{(1)}\|_1}{\sqrt{\min_{k \in \mathcal{N}_k^{(a)}} \min_{i \in [p]} n_{i,k}}}. \end{aligned}$$

Furthermore, Theorem 7 suggests that

$$\begin{aligned} \|\epsilon^{(2)}\|_1 & \leq \frac{C(\sqrt{\gamma_a} + 1) \|\Sigma^*\|_\infty \|\Theta_{a,:}^*\|_1 d_a \sqrt{\frac{\log p}{\min_{j \in \mathcal{N}_a} \max_k n_{j,k}}}}{\lambda_{\min}(\Sigma^*) \Theta_{a,a}^*} \\ & \leq \frac{C \|\Theta_{a,:}^*\|_1}{\Theta_{a,a}^*}, \end{aligned}$$

$$\begin{aligned} \sum_{j=1}^p \frac{|\epsilon_j^{(2)}|}{\sqrt{\min_k n_{j,k}}} &\leq \frac{C \|\Sigma^*\|_\infty \|\Theta_{a,:}^*\|_1}{\lambda_{\min}(\Sigma^*) \Theta_{a,a}^*} \frac{d_a \sqrt{\log p}}{\min_{j \in \mathcal{N}_a} \min_k n_{j,k}} \\ &\leq \frac{\|u^{(2)}\|_1}{\sqrt{\min_{k \in \mathcal{N}_a} \min_{i \in [p]} n_{i,k}}}. \end{aligned}$$

Therefore,

$$\|\mathcal{E} \circ \mathcal{N}\|_1 \leq \frac{C \kappa_{\Sigma^*} \|\Sigma^*\|_\infty \|\Theta_{b,:}^{(a)*}\|_1^2 \|\theta^{(a)*}\|_1^2 (d_a + d_b + 1) \sqrt{\log p}}{\lambda_{\min}(\Sigma^*) (n_1^{(a,b)})^{3/2}},$$

which further implies that

$$|\text{III}| \leq \frac{C \kappa_{\Sigma^*} \|\Sigma^*\|_\infty^3 \|\Theta_{b,:}^{(a)*}\|_1^2 \|\theta^{(a)*}\|_1^2 (d_a + d_b + 1) \sqrt{\log p}}{\lambda_{\min}(\Sigma^*) (n_1^{(a,b)})^{3/2}}.$$

G.3.3 Bounding Error Term III

By Lemma 4, one can bound III as follows:

$$\begin{aligned} \text{III} &\leq C \|\Sigma^*\|_\infty^2 \sum_{j,k,j',k'} \left(\frac{\sqrt{(\log p) n_{j,k,j',k'}}}{n_{j,k} n_{j',k'}} + \frac{\log p}{n_{j,k} n_{j',k'}} \right) |(\mathcal{E}_2)_{j,k,j',k'}| \\ &\leq C \|\Sigma^*\|_\infty^2 \sqrt{\log p} \sum_{j,k,j',k'} \frac{\sqrt{n_{j,k,j',k'}}}{n_{j,k} n_{j',k'}} |(\mathcal{E}_2)_{j,k,j',k'}| \\ &\quad + C \|\Sigma^*\|_\infty^2 \log p \sum_{j,k,j',k'} \frac{|(\mathcal{E}_2)_{j,k,j',k'}|}{n_{j,k} n_{j',k'}} \\ &\leq C \|\Sigma^*\|_\infty^2 \sqrt{\log p} \|\mathcal{E}_2 \circ \mathcal{N}^{(1)}\|_1 + C \|\Sigma^*\|_\infty^2 \log p \|\mathcal{E}_2 \circ \mathcal{N}^{(2)}\|_1, \end{aligned}$$

where $\mathcal{N}^{(1)}, \mathcal{N}^{(2)} \in \mathbb{R}^{p \times p \times p \times p}$ satisfy $\mathcal{N}_{j,k,j',k'}^{(1)} = \frac{\sqrt{n_{j,k,j',k'}}}{n_{j,k} n_{j',k'}}$ and $\mathcal{N}_{j,k,j',k'}^{(2)} = \frac{1}{n_{j,k} n_{j',k'}}$. By

Lemma 12 (a similar result to Lemma 5 but with $\mathcal{N}^{(1)}$ and $\mathcal{N}^{(2)}$), we have

$$\begin{aligned} \|\mathcal{E} \circ \mathcal{N}^{(1)}\|_1 &\leq \frac{C \kappa_{\Sigma^*} \|\Sigma^*\|_\infty \|\Theta_{b,:}^{(a)*}\|_1^2 \|\theta^{(a)*}\|_1^2 (d_a + d_b + 1) \sqrt{\log p}}{\lambda_{\min}(\Sigma^*) (n_1^{(a,b)})^2}, \\ \|\mathcal{E} \circ \mathcal{N}^{(2)}\|_1 &\leq \frac{C \kappa_{\Sigma^*} \|\Sigma^*\|_\infty \|\Theta_{b,:}^{(a)*}\|_1^2 \|\theta^{(a)*}\|_1^2 (d_a + d_b + 1) \sqrt{\log p}}{\lambda_{\min}(\Sigma^*) (n_1^{(a,b)})^{5/2}}. \end{aligned}$$

Therefore,

$$\text{III} \leq \frac{C \kappa_{\Sigma^*} \|\Sigma^*\|_\infty^3 \|\Theta_{b,:}^{(a)*}\|_1^2 \|\theta^{(a)*}\|_1^2 (d_a + d_b + 1) \log p}{\lambda_{\min}(\Sigma^*) (n_1^{(a,b)})^2}.$$

Combining the upper bounds for I, II, and III, and applying Assumptions 2 and 4, one can show that

$$\begin{aligned} & |\widehat{\sigma}_n^2(a, b) - \sigma_n^2(a, b)| \\ & \leq \frac{C\kappa_{\Sigma^*} \|\Sigma^*\|_\infty^3 \|\Theta_{b,:}^{(a)*}\|_1^2 \|\Theta_{:,a}^*\|_1^2 (d_a + d_b + 1) \sqrt{\log p}}{\lambda_{\min}(\Sigma^*) (\Theta_{a,a}^*)^2 (n_1^{(a,b)})^{3/2}}. \end{aligned}$$

To interpret the bound above, note that $\|\Sigma^*\|_\infty^2 \|\Theta_{b,:}^{(a)*}\|_1^2 \frac{\|\Theta_{:,a}^*\|_1^2}{(\Theta_{a,a}^*)^2}$ can be viewed as an upper bound for $|\langle \mathcal{T}^*, \mathcal{U}^* \rangle| \leq \|\mathcal{T}^*\|_\infty \|\mathcal{U}^*\|_1$, $\frac{\kappa_{\Sigma^*} \|\Sigma^*\|_\infty (d_a + d_b + 1) \sqrt{\log p}}{\lambda_{\min}(\Sigma^*) (n_1^{(a,b)})^{3/2}}$ is the error brought by estimating $\mathcal{U}^* = \Theta_{b,:}^{(a)*} \otimes \bar{\theta}^{(a)*} \otimes \Theta_{b,:}^{(a)*} \otimes \bar{\theta}^{(a)*}$, which dominates the error brought by estimating \mathcal{T}^* . As have been shown in the proof of Theorem 2,

$$\sigma_n^2(a, b) \geq \frac{\lambda_{\min}^2(\Sigma^*) \min_{(j,k) \in S_2(a,b)} \left| \Theta_{b,j}^{(a)*} \Theta_{a,k}^* + \Theta_{b,k}^{(a)*} \Theta_{a,j}^* \right|^2}{2(\Theta_{a,a}^*)^2 n_2^{(a,b)}},$$

which implies

$$\begin{aligned} & \frac{|\widehat{\sigma}_n^2(a, b) - \sigma_n^2(a, b)|}{\sigma_n^2(a, b)} \\ & \leq \frac{C^2(\Theta^*; a, b) (d_a + d_b + 1) n_2^{(a,b)} \sqrt{\log p}}{\kappa_{\Theta^*}^2 (n_1^{(a,b)})^{3/2}} \tag{39} \\ & =: \varepsilon_n. \end{aligned}$$

By Assumption 5, $\lim_{n \rightarrow \infty} \varepsilon_n = 0$. Note that when $\varepsilon_n \leq \frac{1}{2}$, with probability at least $1 - Cp^{-c}$, one has

$$\begin{aligned} |\widehat{\sigma}_n(a, b) - \sigma_n(a, b)| & \leq \frac{\widehat{\sigma}_n^2(a, b) - \sigma_n^2(a, b)}{2\sqrt{\sigma_n^2(a, b) - |\widehat{\sigma}_n^2(a, b) - \sigma_n^2(a, b)|}} \\ & \leq \frac{\varepsilon_n \sigma_n(a, b)}{2\sqrt{1 - \varepsilon_n}}, \end{aligned}$$

and hence,

$$\begin{aligned} \left| \frac{\sigma_n(a, b)}{\widehat{\sigma}_n(a, b)} - 1 \right| & = \frac{\sigma_n(a, b) - \widehat{\sigma}_n(a, b)}{\widehat{\sigma}_n(a, b)} \\ & \leq \frac{|\widehat{\sigma}_n(a, b) - \sigma_n(a, b)|}{\sigma_n(a, b) - |\widehat{\sigma}_n(a, b) - \sigma_n(a, b)|} \\ & \leq \frac{\varepsilon_n}{2\sqrt{1 - \varepsilon_n} - \varepsilon_n}. \end{aligned}$$

Since $\lim_{n \rightarrow \infty} \frac{\varepsilon_n}{2\sqrt{1-\varepsilon_n-\varepsilon_n}} = 0$, for any $\delta > 0$, there exists n_0 such that if $n > n_0$, $\frac{\varepsilon_n}{2\sqrt{1-\varepsilon_n-\varepsilon_n}} \leq \delta$,

and thus

$$\begin{aligned} & \lim_{n \rightarrow \infty} \mathbb{P} \left(\left| \frac{\sigma_n(a, b)}{\widehat{\sigma}_n(a, b)} - 1 \right| > \delta \right) \\ & \leq \lim_{n \rightarrow \infty} \mathbb{P} \left(\frac{|\widehat{\sigma}_n^2(a, b) - \sigma_n^2(a, b)|}{\sigma_n^2(a, b)} > \frac{\varepsilon_n}{2\sqrt{1-\varepsilon_n-\varepsilon_n}} \right) \\ & \leq \lim_{n \rightarrow \infty} Cp_n^{-c} = 0. \end{aligned}$$

Here we write $p = p(n)$ to reflect the fact that p also tends to ∞ as n tends to ∞ . Therefore,

$$\frac{\sigma_n(a, b)}{\widehat{\sigma}_n(a, b)} \xrightarrow{p} 1.$$

Proof of Theorem 3. Combine the results in Theorem 2 and Proposition 3, and apply Slutsky's theorem, the proof is then complete. \square

G.4 Proof of Theorem 4

Under the null hypothesis $\mathcal{H}_0 : \Theta_{a,b}^* = 0$, Theorem 3 suggests that $\widehat{z}(a, b) \xrightarrow{d} \mathcal{N}(0, 1)$, and hence $\lim_{n, p \rightarrow \infty} \mathbb{P}(|\widehat{z}(a, b)| \geq z_{\alpha/2}) = 2F_Z(-z_{\alpha/2}) = \alpha$.

While under the alternative hypothesis $\mathcal{H}_A : \frac{\Theta_{a,b}^*}{\Theta_{a,a}^*} = \delta_n$, we have

$$\widehat{z}(a, b) = \frac{\delta_n}{\sigma_n(a, b)} \frac{\sigma_n(a, b)}{\widehat{\sigma}_n(a, b)} + \widehat{\sigma}_n^{-1}(a, b) (\widetilde{\theta}_b^{(a)} - \theta_b^{(a)*}).$$

If $\lim_{n, p \rightarrow \infty} \frac{\delta_n}{\sigma_n(a, b)} = \delta$ for some $\delta \in \mathbb{R}$, then Proposition 3 suggests that $\frac{\delta_n}{\sigma_n(a, b)} \frac{\sigma_n(a, b)}{\widehat{\sigma}_n(a, b)} \xrightarrow{p} \delta$.

By Slutsky's theorem and Theorem 3, $\widehat{z}(a, b) \xrightarrow{d} \mathcal{N}(\delta, 1)$, and hence

$$\lim_{n, p \rightarrow \infty} \mathbb{P}(|\widehat{z}(a, b)| \geq z_{\alpha/2}) = F_Z(-z_{\alpha/2} + \delta) + F_Z(-z_{\alpha/2} - \delta) \geq F_Z(|\delta| - z_{\alpha/2}).$$

In particular, when $\delta = 0$, $F_Z(-z_{\alpha/2} + \delta) + F_Z(-z_{\alpha/2} - \delta) = \alpha$, and $\lim_{n, p \rightarrow \infty} \mathbb{P}(|\widehat{z}(a, b)| \geq z_{\alpha/2}) = \alpha$.

Now we consider the last case: $\lim_{n, p \rightarrow \infty} \frac{|\delta_n|}{\sigma_n(a, b)} = +\infty$. Since

$$|\widehat{z}(a, b)| \geq \left| \frac{\delta_n}{\widehat{\sigma}_n(a, b)} \right| - \left| \widehat{\sigma}_n^{-1}(a, b) (\widetilde{\theta}_b^{(a)} - \theta_b^{(a)*}) \right|,$$

we have that for any $\delta > 0$

$$\begin{aligned} \mathbb{P}(|\widehat{z}(a, b)| < z_{\alpha/2}) &\leq \mathbb{P}\left(|\widehat{\sigma}_n^{-1}(a, b)(\widetilde{\theta}_b^{(a)} - \theta_b^{(a)*})| > \left|\frac{\delta_n}{\widehat{\sigma}_n(a, b)}\right| - z_{\alpha/2}\right) \\ &\leq \mathbb{P}\left(|\widehat{\sigma}_n^{-1}(a, b)(\widetilde{\theta}_b^{(a)} - \theta_b^{(a)*})| > \left|\frac{\delta_n}{\sigma_n(a, b)}\right|(1 - \delta) - z_{\alpha/2}\right) \\ &\quad + \mathbb{P}\left(\left|\frac{\sigma_n(a, b)}{\widehat{\sigma}_n(a, b)} - 1\right| > \delta\right). \end{aligned}$$

Recall the error term ε_n defined in (39). Let $\delta = \frac{\varepsilon_n}{2\sqrt{1-\varepsilon_n-\varepsilon_n}}$, and recall that in the proof of Proposition 3, we have shown that $\mathbb{P}\left(\left|\frac{\sigma_n(a, b)}{\widehat{\sigma}_n(a, b)} - 1\right| > \delta\right) \leq Cp^{-c}$. Since $\lim_{n, p \rightarrow \infty} \delta = 0$, $\lim_{n, p \rightarrow \infty} \frac{|\delta_n|}{\sigma_n(a, b)} = +\infty$, one has

$$C_n := \lim_{n, p \rightarrow \infty} \left|\frac{\delta_n}{\sigma_n(a, b)}\right|(1 - \delta) - z_{\alpha/2} = +\infty.$$

Hence for any $\epsilon > 0$, there exists N_1 such that if $n > N_1$ $C_n > z_{\epsilon/4}$; there also exists N_2 such that if $n > N_2$, $|\mathbb{P}(|\widehat{\sigma}_n^{-1}(a, b)(\widetilde{\theta}_b^{(a)} - \theta_b^{(a)*})| > z_{\epsilon/4}) - \mathbb{P}(|Z| > z_{\epsilon/4})| < \epsilon/2$, where Z follows standard Gaussian distribution. Therefore, for $n \geq N_1 \vee N_2$,

$$\begin{aligned} \mathbb{P}(|\widehat{\sigma}_n^{-1}(a, b)(\widetilde{\theta}_b^{(a)} - \theta_b^{(a)*})| > C_n) &\leq \mathbb{P}(|\widehat{\sigma}_n^{-1}(a, b)(\widetilde{\theta}_b^{(a)} - \theta_b^{(a)*})| > z_{\epsilon/4}) \\ &\leq \mathbb{P}(|Z| > z_{\epsilon/4}) + \epsilon/2 \\ &\leq \epsilon, \end{aligned}$$

which implies that $\lim_{n, p \rightarrow \infty} \mathbb{P}(|\widehat{\sigma}_n^{-1}(a, b)(\widetilde{\theta}_b^{(a)} - \theta_b^{(a)*})| > C_n) = 0$ and hence

$$\lim_{n, p \rightarrow \infty} \mathbb{P}(|\widehat{z}(a, b)| \geq z_{\alpha/2}) = 1.$$

G.5 Proof of Theorem 6

Here, we provide the detailed proofs of Theorem 6 with Assumptions 6 and 7. Let $m = p(p-1)/2$ be the number of edge-wise tests, $m_0 = \{(j, k) \in [p] : \Theta_{j, k}^* = 0\}$ be the number of node pairs for which the null hypothesis holds true, and the Gaussian tail probability function $G(t) = 2(1 - \Phi(t))$ for $t \geq 0$. Recall that $t_p = \sqrt{2 \log m - 2 \log \log m}$,

$$\text{FDP} = \frac{\sum_{(a, b) \in \mathcal{H}_0} \mathbb{1}_{\{p_{(a, b)} \leq \rho_0\}}}{R(\rho_0) \vee 1} = \frac{\sum_{(a, b) \in \mathcal{H}_0} \mathbb{1}_{\{|\widehat{z}(a, b)| \geq t_0\}}}{R(\rho_0) \vee 1},$$

where $t_0 = G^{-1}(\rho_0)$, $\rho_0 = \sup \left\{ G(t_p) \leq \rho \leq 1 : \frac{m\rho}{R(\rho)\sqrt{1}} \leq \alpha \right\}$, if there exists $G(t_p) \leq \rho \leq 1$ such that $\frac{m\rho}{R(\rho)\sqrt{1}} \leq \alpha$; otherwise, $\rho_0 = G(\sqrt{2 \log m})$.

Case I: $\rho_0 = G(\sqrt{2 \log m})$ We first show that when $\rho_0 = G(\sqrt{2 \log m})$ and $t_0 = \sqrt{2 \log m}$, $\text{FDP} \xrightarrow{p} 0$. Applying the decomposition in Theorem 2 to edge (a, b) , we have $\widehat{z}(a, b) = \frac{B(a, b) + E(a, b)}{\widehat{\sigma}_n(a, b)}$ if $(a, b) \in \mathcal{H}_0$, where

$$\frac{B(a, b)}{\sigma_n(a, b)} \leq C(\Theta^*; a, b) (\kappa_{\Theta^*}^2 + \sqrt{\gamma_a} + \sqrt{\gamma_b^{(a)}}) \frac{(d_a + d_b + 1) \log p}{\sqrt{n_1^{(a, b)}}} \sqrt{\frac{n_2^{(a, b)}}{n_1^{(a, b)}}} := \varepsilon_{a, b}^{(1)}$$

with probability at least $1 - Cp^{-c}$, and the proof of Proposition 3 implies that with the same probability,

$$\left| \frac{\sigma_n(a, b)}{\widehat{\sigma}_n(a, b)} - 1 \right| \leq \frac{C^2(\Theta^*; a, b) (d_a + d_b + 1) n_2^{(a, b)} \sqrt{\log p}}{\kappa_{\Theta^*}^2 (n_1^{(a, b)})^{3/2}} := \varepsilon_{a, b}^{(2)}.$$

Hence some calculations show that

$$\begin{aligned} \mathbb{P}(\text{FDP} > 0) &\leq \sum_{(a, b) \in \mathcal{H}_0} \mathbb{P} \left(|\widehat{z}(a, b)| \geq \sqrt{2 \log m} \right) \\ &\leq \sum_{(a, b) \in \mathcal{H}_0} \mathbb{P} \left(\left| \frac{B(a, b)}{\widehat{\sigma}_n(a, b)} + \frac{E(a, b)}{\widehat{\sigma}_n(a, b)} \right| \geq \sqrt{2 \log m} \right) \\ &\leq \sum_{(a, b) \in \mathcal{H}_0} \mathbb{P} \left(\left| \frac{B(a, b)}{\sigma_n(a, b)} \right| > \varepsilon_{a, b}^{(1)} \right) + \mathbb{P} \left(\left| \frac{\sigma_n(a, b)}{\widehat{\sigma}_n(a, b)} - 1 \right| > \varepsilon_{a, b}^{(2)} \right) + \\ &\quad \mathbb{P} \left(\left| \frac{E(a, b)}{\sigma_n(a, b)} \right| \geq \frac{t_0}{1 + \varepsilon_{a, b}^{(2)}} - \varepsilon_{a, b}^{(1)} \right) \\ &\leq Cp^{-c} + \sum_{(a, b) \in \mathcal{H}_0} \mathbb{P} \left(\left| \frac{E(a, b)}{\sigma_n(a, b)} \right| \geq \frac{t_0}{1 + \varepsilon_{a, b}^{(2)}} - \varepsilon_{a, b}^{(1)} \right). \end{aligned}$$

The following lemma concentrates the tail bound of $\frac{E(a, b)}{\sigma_n(a, b)}$ around the Gaussian tail.

Lemma 6. *For any node pair (a, b) , $t \geq 0$, $\varepsilon > 0$*

$$\begin{aligned} &\max \left\{ \mathbb{P} \left(\left| \frac{E(a, b)}{\sigma_n(a, b)} \right| > t \right) - G(t - \varepsilon), G(t + \varepsilon) - \mathbb{P} \left(\left| \frac{E(a, b)}{\sigma_n(a, b)} \right| > t \right) \right\} \\ &\leq C \exp \left\{ - \frac{c\varepsilon \lambda_{\min}^3(\Sigma^*) \sqrt{n_2^{(a, b)}}}{C \|\Sigma^*\|_{\infty}^3 (d_a + d_b + 1)^3} \right\}. \end{aligned}$$

Applying Lemma 6 with $\varepsilon = (\log p)^{-2}$ gives us

$$\begin{aligned} \mathbb{P}(\text{FDP} > 0) &\leq Cp^{-c} + \sum_{(a,b) \in \mathcal{H}_0} G\left(\frac{t_0}{1 + \varepsilon_{a,b}^{(2)}} - \varepsilon_{a,b}^{(1)} - (\log p)^{-2}\right) \\ &\quad + Cp^2 \exp\left\{-\frac{c\lambda_{\min}^3(\Sigma^*)\sqrt{n_2^{(a,b)}}}{C\|\Sigma^*\|_\infty^3(d_a + d_b + 1)^3(\log p)^2}\right\} \\ &\leq Cp^{-c} + \sum_{(a,b) \in \mathcal{H}_0} G\left(\frac{t_0}{1 + \varepsilon_{a,b}^{(2)}} - \varepsilon_{a,b}^{(1)} - (\log p)^{-2}\right), \end{aligned}$$

where the last line is due to Assumption 6. While for the last term, let $x = t_0 - \left(\frac{t_0}{1 + \varepsilon_{a,b}^{(2)}} - \varepsilon_{a,b}^{(1)} - (\log p)^{-2}\right)$, and we will also need the following lemma on Gaussian tail bound:

Lemma 7. *For any $t > 0$,*

$$\frac{2}{\sqrt{2\pi}(t + 1/t)}e^{-\frac{t^2}{2}} \leq G(t) \leq \frac{2}{\sqrt{2\pi}t}e^{-\frac{t^2}{2}}.$$

Lemma 7 is a standard Gaussian tail bound, which also appears in [26]. Hence we have

$$\begin{aligned} G(t_0 - x) &\leq \frac{2}{\sqrt{2\pi}(t_0 - x)}e^{-\frac{(t_0 - x)^2}{2}} \\ &\leq \frac{2}{\sqrt{2\pi}(t_0 - x)}e^{-\frac{t_0^2 - 2t_0x}{2}} \\ &\leq \frac{1}{\sqrt{2\pi}(t_0 - x)p^2}e^{\sqrt{\log p}x}. \end{aligned}$$

Further note that

$$\begin{aligned} x &= t_0 - \left(\frac{t_0}{1 + \varepsilon_{a,b}^{(2)}} - \varepsilon_{a,b}^{(1)} - (\log p)^{-2}\right) \\ &\leq \sqrt{2 \log m} \varepsilon_{a,b}^{(2)} + \varepsilon_{a,b}^{(1)} + (\log p)^{-2} \\ &\leq C_1 \frac{(d_a + d_b + 1)n_2^{(a,b)} \log p}{(n_1^{(a,b)})^{3/2}} + C_2 \frac{(d_a + d_b + 1) \log p \sqrt{n_2^{(a,b)}}}{n_1^{(a,b)}} + (\log p)^{-2}, \end{aligned}$$

and applying Assumption 6 leads to $\sqrt{\log p}x \leq \frac{C}{\log p}$, which implies

$$G(t_0 - x) \leq \frac{C}{p^2 \sqrt{\log p}}.$$

Therefore, when $t_0 = \sqrt{2 \log m}$,

$$\mathbb{E}(\text{FDP}) \leq \mathbb{P}(\text{FDP} > 0) \leq \frac{C}{\sqrt{\log p}},$$

where we have applied the boundedness of FDP in the inequality above.

Case II: $\rho_0 = \sup \left\{ G(t_p) \leq \rho \leq 1 : \frac{m\rho}{R(\rho)\vee 1} \leq \alpha \right\}$ Now suppose that

$\rho_0 = \sup \left\{ G(t_p) \leq \rho \leq 1 : \frac{m\rho}{R(\rho)\vee 1} \leq \alpha \right\}$, and $t_0 = G^{-1}(\rho_0)$, then

$$\begin{aligned} \text{FDP} &= \frac{\sum_{(a,b) \in \mathcal{H}_0} \mathbb{1}_{\{|\hat{z}(a,b)| \geq t_0\}}}{R(\rho_0) \vee 1} \\ &\leq \frac{\left| \sum_{(a,b) \in \mathcal{H}_0} (\mathbb{1}_{\{|\hat{z}(a,b)| \geq t_0\}} - \rho_0) \right| + \rho_0 m}{R(\rho_0) \vee 1} \\ &\leq \alpha \left(1 + \frac{\left| \sum_{(a,b) \in \mathcal{H}_0} (\mathbb{1}_{\{|\hat{z}(a,b)| \geq t_0\}} - G(t_0)) \right|}{mG(t_0)} \right) \\ &\leq \alpha \left(1 + \sup_{0 \leq t \leq t_p} \frac{\left| \sum_{(a,b) \in \mathcal{H}_0} (\mathbb{1}_{\{|\hat{z}(a,b)| \geq t\}} - G(t)) \right|}{mG(t)} \right). \end{aligned}$$

In fact, it suffices to show that

$$\sup_{0 \leq t \leq t_p} \left| \frac{\sum_{(a,b) \in \mathcal{H}_0} \mathbb{1}_{\{|\hat{z}(a,b)| \geq t\}}}{m_0 G(t)} - 1 \right| \rightarrow 0 \quad (40)$$

in probability, which immediately implies that $\lim_{n,p \rightarrow \infty} \mathbb{P}(\text{FDP} > \alpha + \epsilon) = 0$; In addition, by the boundedness of the quantity above, convergence in probability also implies convergence in expectation and hence we would have $\limsup_{n,p \rightarrow \infty} \text{FDR} \leq \alpha$.

We now discretize the interval $[0, t_p]$ into $0 = x_1 < x_2 < \dots < x_K = t_p$, where $x_k - x_{k-1} = \frac{1}{\sqrt{\log m \log \log m}}$. In the following, we show that (40) can be implied by

$$\max_{1 \leq k \leq K} \left| \frac{\sum_{(a,b) \in \mathcal{H}_0} \mathbb{1}_{\{|\hat{z}(a,b)| \geq x_k\}}}{m_0 G(x_k)} - 1 \right| \rightarrow 0 \quad (41)$$

in probability. Suppose for now that (41) holds, then for any $t \in [0, t_p]$, there exists $1 \leq l \leq K$ such that $x_l \leq t \leq x_{l+1}$, and hence

$$\begin{aligned} \frac{\sum_{(a,b) \in \mathcal{H}_0} \mathbb{1}_{\{|\hat{z}(a,b)| \geq x_{l+1}\}}}{m_0 G(x_l)} - 1 &\leq \frac{\sum_{(a,b) \in \mathcal{H}_0} \mathbb{1}_{\{|\hat{z}(a,b)| \geq t\}}}{m_0 G(t)} - 1 \leq \frac{\sum_{(a,b) \in \mathcal{H}_0} \mathbb{1}_{\{|\hat{z}(a,b)| \geq x_l\}}}{m_0 G(x_{l+1})} - 1 \\ \left| \frac{\sum_{(a,b) \in \mathcal{H}_0} \mathbb{1}_{\{|\hat{z}(a,b)| \geq t\}}}{m_0 G(t)} - 1 \right| &\leq \max_{1 \leq k \leq K} \left| \frac{\sum_{(a,b) \in \mathcal{H}_0} \mathbb{1}_{\{|\hat{z}(a,b)| \geq x_k\}}}{m_0 G(x_k)} - 1 \right| \frac{G(x_l)}{G(x_{l+1})} + \left| \frac{G(x_l)}{G(x_{l+1})} - 1 \right|. \end{aligned}$$

Let $\phi(\cdot)$ be the density function of standard Gaussian distribution. Now note that $\frac{G(x_{l+1})}{G(x_l)} \geq 1 - \frac{2(x_{l+1}-x_l)\phi(x_l)}{G(x_l)}$, and Lemma 7 suggests

$$\frac{\phi(x_l)}{G(x_l)} \leq \begin{cases} \frac{x_l+1}{2} \leq t_p, & x_l \geq 1, \\ \frac{\phi(0)}{G(1)}, & 0 \leq x_l \leq 1. \end{cases}$$

Hence $|\frac{G(x_{l+1})}{G(x_l)} - 1| \leq c\sqrt{\log \log m} \rightarrow 0$, and (41) implies (40).

The rest of the proof is devoted to showing (40). For any $\epsilon > 0$, some calculations show that

$$\begin{aligned}
& \mathbb{P} \left(\max_{1 \leq k \leq K} \left| \frac{\sum_{(a,b) \in \mathcal{H}_0} \mathbb{1}_{\{|\widehat{z}(a,b)| \geq x_k\}}}{m_0 G(x_k)} - 1 \right| > \epsilon \right) \\
& \leq \sum_{k=1}^K \mathbb{P} \left(\left| \frac{\sum_{(a,b) \in \mathcal{H}_0} \mathbb{1}_{\{|\widehat{z}(a,b)| \geq x_k\}}}{m_0 G(x_k)} - 1 \right| > \epsilon \right) \\
& \leq \frac{1}{\epsilon^2} \sum_{k=1}^K \mathbb{E} \left(\left| \frac{\sum_{(a,b) \in \mathcal{H}_0} \mathbb{1}_{\{|\widehat{z}(a,b)| \geq x_k\}}}{m_0 G(x_k)} - 1 \right|^2 \right) \\
& = \frac{1}{\epsilon^2} \frac{1}{m_0^2} \sum_{(a,b) \in \mathcal{H}_0, (a',b') \in \mathcal{H}_0} \sum_{k=1}^K \left(\frac{\mathbb{P}(|\widehat{z}(a,b)| \geq x_k, |\widehat{z}(a',b')| \geq x_k)}{G^2(x_k)} - 1 \right) \\
& \quad - \frac{1}{\epsilon^2} \frac{2}{m_0} \sum_{(a,b) \in \mathcal{H}_0} \sum_{k=1}^K \left(\frac{\mathbb{P}(|\widehat{z}(a,b)| \geq x_k)}{G(x_k)} - 1 \right),
\end{aligned} \tag{42}$$

and we will lower bound $\text{I}(a,b) = \sum_{k=1}^K \left(\frac{\mathbb{P}(|\widehat{z}(a,b)| \geq x_k)}{G(x_k)} - 1 \right)$, and upper bound $\text{II}(a,b,a',b') = \sum_{k=1}^K \left(\frac{\mathbb{P}(|\widehat{z}(a,b)| \geq x_k, |\widehat{z}(a',b')| \geq x_k)}{G^2(x_k)} - 1 \right)$, respectively.

Bounding $\text{I}(a,b)$: We first follow similar arguments to case I. Recall the decompositions and error bounds in the proof of Theorem 2 and Proposition 3, we have

$$\begin{aligned}
\mathbb{P}(|\widehat{z}(a,b)| \geq x_k) &= \mathbb{P} \left(\left| \frac{B(a,b)}{\widehat{\sigma}_n(a,b)} + \frac{E(a,b)}{\widehat{\sigma}_n(a,b)} \right| \geq x_k \right) \\
&\geq \mathbb{P} \left(\left| \frac{E(a,b)}{\sigma_n(a,b)} \right| \geq x_k(1 + \varepsilon_{a,b}^{(2)}) + \varepsilon_{a,b}^{(1)} \right) - Cp^{-c} \\
&\geq G(x_k(1 + \varepsilon_{a,b}^{(2)}) + \varepsilon_{a,b}^{(1)} + (\log p)^{-2}) - Cp^{-c} \\
&\quad - C \exp \left\{ - \frac{c\lambda_{\min}^3(\Sigma^*)\sqrt{n_2^{(a,b)}}}{C\|\Sigma^*\|_{\infty}^3(d_a + d_b + 1)^3(\log p)^2} \right\},
\end{aligned}$$

where we applied Lemma 6 with $\varepsilon = (\log p)^{-2}$ on the last line. Since $G(x_k) \geq G(t_p) \geq \frac{c}{t_p} e^{-\frac{t_p^2}{2}} \geq \frac{c}{p^2\sqrt{\log p}}$, $K = t_p\sqrt{\log m \log \log m} + 1 \leq C \log p\sqrt{\log \log p}$, one can show that

$$\begin{aligned}
\text{I}(a,b) &\geq \sum_{k=1}^K \frac{G(x_k(1 + \varepsilon_{a,b}^{(2)}) + \varepsilon_{a,b}^{(1)} + (\log p)^{-2}) - G(x_k)}{G(x_k)} \\
&\quad - C \exp \left\{ 3 \log p - \frac{c\lambda_{\min}^3(\Sigma^*)\sqrt{n_2^{(a,b)}}}{C\|\Sigma^*\|_{\infty}^3(d_a + d_b + 1)^3(\log p)^2} \right\} - Cp^{-c}.
\end{aligned}$$

Assumption 6 implies that the last two terms both converge to zero, thus it suffices to show

that $\sum_{k=1}^K \frac{G(x_k(1+\varepsilon_{a,b}^{(2)})+\varepsilon_{a,b}^{(1)}+(\log p)^{-2})-G(x_k)}{G(x_k)} \rightarrow 0$. In fact,

$$\begin{aligned}
0 &\leq \sum_{k=1}^K \frac{G(x_k) - G(x_k(1 + \varepsilon_{a,b}^{(2)}) + \varepsilon_{a,b}^{(1)} + (\log p)^{-2})}{G(x_k)} \\
&\leq \sum_{k=1}^K \frac{(x_k \varepsilon_{a,b}^{(2)} + \varepsilon_{a,b}^{(1)} + (\log p)^{-2}) \phi(x_k)}{G(x_k)} \\
&\leq C t_p \sum_{k=1}^K (t_p \varepsilon_{a,b}^{(2)} + \varepsilon_{a,b}^{(1)} + (\log p)^{-2}) \\
&\leq C_1 \frac{(d_a + d_b + 1)(\log p)^{\frac{5}{2}} \sqrt{\log \log p} n_2^{(a,b)}}{(n_1^{(a,b)})^{3/2}} + C_2 \frac{(d_a + d_b + 1)(\log p)^{\frac{5}{2}} \sqrt{\log \log p} \sqrt{n_2^{(a,b)}}}{n_1^{(a,b)}} + \sqrt{\frac{\log \log p}{\log p}},
\end{aligned}$$

and Assumption 6 suggests the right hand side of the inequality above would converge to zero.

Bounding $\text{II}(a, b, a', b')$: For any node pairs (a, b) and (a', b') , we can utilize the same decomposition for the test statistics $\widehat{z}(a, b)$ and $\widehat{z}(a', b')$. Following similar arguments to bounding $\text{I}(a, b)$, one can show that

$$\begin{aligned}
&\mathbb{P}(\widehat{z}(a, b) \geq x_k, \widehat{z}(a', b') \geq x_k) \\
&\leq C p^{-c} + \mathbb{P}\left(\left|\frac{E(a, b)}{\sigma(a, b)}\right| \geq \frac{x_k}{1 + \varepsilon_{a,b}^{(2)}} - \varepsilon_{a,b}^{(1)}, \left|\frac{E(a', b')}{\sigma(a', b')}\right| \geq \frac{x_k}{1 + \varepsilon_{a',b'}^{(2)}} - \varepsilon_{a',b'}^{(1)}\right).
\end{aligned}$$

The following lemma suggests that the tail bound for $(\frac{E(a,b)}{\sigma(a,b)}, \frac{E(a',b')}{\sigma(a',b')})$ can be well approximated by the tail bound for a bivariate normal distribution with the same covariance matrix.

Lemma 8. *For any node pairs (a, b) and (a', b') , $t_1, t_2 \geq 0$, $\varepsilon > 0$,*

$$\begin{aligned}
&\mathbb{P}\left(\left|\frac{E(a, b)}{\sigma_n(a, b)}\right| > t_1, \left|\frac{E(a', b')}{\sigma_n(a', b')}\right| > t_2\right) \\
&\leq \mathbb{P}(|z_1| > t_1 - \varepsilon, |z_2| > t_2 - \varepsilon) + C \exp\left\{-\frac{c\varepsilon \lambda_{\min}(\Sigma^*) \sqrt{n_2^{(a,b)} \vee n_2^{(a',b')}}}{C \|\Sigma^*\|_{\infty} (d+1) \alpha(\Theta^*, \{V_i\}_{i=1}^n)}\right\},
\end{aligned}$$

where (z_1, z_2) follows bivariate normal distribution with the same mean and covariance matrix

as $(\frac{E(a,b)}{\sigma_n(a,b)}, \frac{E(a',b')}{\sigma_n(a',b')})$.

We can apply Lemma 8 with $\varepsilon = (\log p)^{-2}$, and obtain the following:

$$\begin{aligned} \Pi(a, b, a', b') &= \sum_{k=1}^K \left(\frac{\mathbb{P}(|\widehat{z}(a, b)| \geq x_k, |\widehat{z}(a', b')| \geq x_k)}{G^2(x_k)} - 1 \right) \\ &\leq Cp^{-c} + C \exp \left\{ C \log p - \frac{c\lambda_{\min}(\Sigma^*) \sqrt{n_2^{(a,b)} \vee n_2^{(a',b')}}}{C\|\Sigma^*\|_{\infty}(d+1)\alpha(\Theta^*, \{V_i\}_{i=1}^n)} (\log p)^2 \right\} \\ &\quad + \sum_{k=1}^K \left(\frac{\mathbb{P}(|z_1| \geq x'_k, |z_2| \geq x'_k)}{G^2(x_k)} - 1 \right), \end{aligned}$$

where $x'_k = \frac{x_k}{1 + \max\{\varepsilon_{a,b}^{(2)}, \varepsilon_{a',b'}^{(2)}\}} - \max\{\varepsilon_{a,b}^{(1)}, \varepsilon_{a',b'}^{(1)}\} - (\log p)^{-2}$. Assumption 6 implies that the first two terms both converge to zero, hence we will focus on the last term in the following analysis. We will discuss three different cases separately: (i) $(a, b, a', b') \in \mathcal{A}_1(\rho_0)$; (ii) $(a, b, a', b') \in \mathcal{A}_2(\rho_0, \gamma)$; (iii) $(a, b, a', b') \in (\mathcal{H}_0 \times \mathcal{H}_0) \setminus (\mathcal{A}_1(\rho_0) \cup \mathcal{A}_2(\rho_0, \gamma))$.

For the case (i), one can show that

$$\begin{aligned} &\sum_{k=1}^K \left(\frac{\mathbb{P}(|z_1| \geq x'_k, |z_2| \geq x'_k)}{G^2(x_k)} - 1 \right) \\ &\leq \sum_{k=1}^K \frac{1}{G^2(x_k)} \\ &\leq \int_0^{t_p} G^{-1}(x) dx \sqrt{\log m \log \log m} \\ &\leq \left[\sqrt{\frac{\pi}{2}} \int_1^{t_p} \left(x + \frac{1}{x}\right) e^{-\frac{x^2}{2}} dx + \frac{1}{G(1)} \right] \sqrt{\log m \log \log m} \\ &\leq \left[\sqrt{2\pi} \int_1^{t_p} x e^{-\frac{x^2}{2}} dx + \sqrt{2\pi} e \right] \sqrt{\log m \log \log m} \\ &\leq \frac{\sqrt{2\pi} m \sqrt{\log \log m}}{\sqrt{\log m}}. \end{aligned}$$

Since $|\mathcal{A}_1(\rho_0)| \leq Cp^2$,

$$\sum_{(a,b,a',b') \in \mathcal{A}_1(\rho_0)} \Pi(a, b, a', b') \leq C \frac{\sqrt{\log \log p}}{\sqrt{\log p}} + Cp^{-c} \rightarrow 0.$$

Now we present a lemma on the tail bound of bivariate Gaussian distribution, which will be useful for the other two cases.

Lemma 9. *Suppose that $(z_1, z_2)^\top \sim \mathcal{N}(0, \begin{pmatrix} 1 & \rho \\ \rho & 1 \end{pmatrix})$.*

- If $|\rho| \leq C(\log p)^{-2-\gamma}$ for some $\gamma > 0$, then

$$\sup_{0 \leq x \leq \sqrt{C \log p}} \left| \frac{\mathbb{P}(|z_1| \geq x, |z_2| \geq x)}{G^2(x)} - 1 \right| \leq C(\log p)^{-1-\min\{\gamma, \frac{1}{2}\}}. \quad (43)$$

- If $|\rho| \leq \rho_0 < 1$ for some $\rho_0 > 0$, then

$$\mathbb{P}(|z_1| \geq t, |z_2| \geq t) \leq C(t+1)^{-2} \exp\{-t^2/(1+\rho_0)\} \quad (44)$$

holds uniformly over $0 \leq t \leq \sqrt{C \log p}$.

Lemma 9 is a direct implication of Lemma 6.1 and Lemma 6.2 in [34]. For the case (ii), we apply (44) to show that

$$\begin{aligned} & \sum_{k=1}^K \left(\frac{\mathbb{P}(|z_1| \geq x'_k, |z_2| \geq x'_k)}{G^2(x_k)} - 1 \right) \\ & \leq \sum_{k=1}^K \frac{(x_k+1)^2}{(x'_k+1)^2} \exp \left\{ \frac{\rho_0}{1+\rho_0} x_k^2 + \frac{x_k^2 - x_k'^2}{1+\rho_0} \right\}, \end{aligned}$$

where the second line is due to that $G(x_k) \geq \frac{C}{(x_k+1)} e^{-\frac{x_k^2}{2}}$. Further note that

$$x_k^2 - x_k'^2 \leq 2(x_k - x'_k)x_k \leq 2t_p^2 \max\{\varepsilon_{a,b}^{(2)}, \varepsilon_{a',b'}^{(2)}\} + 2t_p \max\{\varepsilon_{a,b}^{(1)}, \varepsilon_{a',b'}^{(1)}\} + 2t_p(\log p)^{-2} \rightarrow 0,$$

which then implies

$$\begin{aligned} & \sum_{k=1}^K \left(\frac{\mathbb{P}(|z_1| \geq x'_k, |z_2| \geq x'_k)}{G^2(x_k)} - 1 \right) \\ & \leq C \sum_{k=1}^K \exp \left\{ \frac{\rho_0}{1+\rho_0} x_k^2 \right\} \\ & \leq C \sqrt{\log m \log \log m} \int_0^{t_p} \exp \left\{ \frac{\rho_0}{1+\rho_0} x^2 \right\} dx \\ & \leq C m^{\frac{2\rho_0}{1+\rho_0}} (\log m)^{\frac{1}{2} - \frac{2\rho_0}{1+\rho_0}} \sqrt{\log \log m}. \end{aligned}$$

Therefore, Assumption 7 suggests

$$\sum_{(a,b,a',b') \in \mathcal{A}_2(\rho_0, \gamma)} \Pi(a, b, a', b') = o(m^2).$$

While for the case (iii), we have

$$\begin{aligned}
& \sum_{k=1}^K \left(\frac{\mathbb{P}(|z_1| \geq x'_k, |z_2| \geq x'_k)}{G^2(x_k)} - 1 \right) \\
& \leq \sum_{k=1}^K \left| \frac{\mathbb{P}(|z_1| \geq x'_k, |z_2| \geq x'_k)}{G^2(x'_k)} - 1 \right| \left| \frac{G^2(x'_k)}{G^2(x_k)} - 1 \right| + \left| \frac{\mathbb{P}(|z_1| \geq x'_k, |z_2| \geq x'_k)}{G^2(x'_k)} - 1 \right| + \left| \frac{G^2(x'_k)}{G^2(x_k)} - 1 \right| \\
& \leq C(\log p)^{-1-\min\{\gamma, \frac{1}{2}\}} + C \frac{\phi(x'_k)(x_k - x'_k)}{G(x_k)} \\
& \leq C\sqrt{\log \log p}(\log p)^{-\min\{\gamma, \frac{1}{2}\}} + C \log p \sqrt{\log \log p} (t_p \max\{\varepsilon_{a,b}^{(2)}, \varepsilon_{a',b'}^{(2)}\} + \max\{\varepsilon_{a,b}^{(1)}, \varepsilon_{a',b'}^{(1)}\} + (\log p)^{-2}),
\end{aligned}$$

which converges to zero by Assumption 6. Therefore,

$$\sum_{(a,b,a',b') \notin \mathcal{A}_1(\rho_0) \cup \mathcal{A}_2(\rho_0, \gamma)} \Pi(a, b, a', b') = o(m^2).$$

Now we have shown that (42) converges to zero for any $\epsilon > 0$, and hence (40) holds. The proof of Theorem 6 is complete.

G.6 Proof of Supporting Lemmas and Auxiliary Propositions

Before presenting the proofs of the supporting lemmas, here we first introduce the notions of sub-Gaussian and sub-exponential random variables, ψ_α norm, which was introduced in [1] as a generalization of the sub-Gaussian and sub-exponential norms when $\alpha = 2$ or $\alpha = 1$.

Definition 1 (ψ_α -norm [1, 54]). *The ψ_α -norm of any random variable X and $\alpha > 0$ is defined as $\|X\|_{\psi_\alpha} := \inf\{C \in (0, \infty) : \mathbb{E}[\exp\{(|X|/C)^\alpha\}] \leq 2\}$*

The following two lemmas from [22] provide useful properties for product of random variables with bounded ψ_α norm.

Lemma 10 (ψ_α norm of product of r.v.s [22]). *Suppose X_1, \dots, X_m are m random variables (not necessarily independent) with ψ_α -norm bounded by $\|X_j\|_{\psi_\alpha} \leq K_j$. Then the $\psi_{\alpha/m}$ -norm of $\prod_{j=1}^m X_j$ is bounded as $\|\prod_{j=1}^m X_j\|_{\psi_{\alpha/m}} \leq \prod_{j=1}^m K_j$.*

Lemma 11 (Concentration of sum of r.v.s with bounded ψ_α -norm [22, 46]). *Suppose $0 < \alpha \leq 1$, X_1, \dots, X_n are independent random variables satisfying $\|X_i\|_{\psi_\alpha} \leq b$. Then there*

exists absolute constant $C(\alpha)$ only depending on α such that for any $a = (a_1, \dots, a_n) \in \mathbb{R}^n$

and $0 < \delta < 1/e^2$,

$$\left| \sum_{i=1}^n a_i X_i - \mathbb{E} \left(\sum_{i=1}^n a_i X_i \right) \right| \leq C(\alpha) b \|a\|_2 (\log \delta^{-1})^{1/2} + C(\alpha) b \|a\|_\infty (\log \delta^{-1})^{1/\alpha}$$

with probability at least $1 - \delta$.

Lemma 11 is a direct combination of Lemma 6 in [22] and Proposition 5.16 in [46].

Proof of Lemma 2. We first provide an entry-wise error bound for

$$\left| \widehat{\Sigma}_{j,k} - \Sigma_{j,k}^* \right| = \left| \frac{1}{n_{j,k}} \sum_{i:j,k \in V_i} (x_{i,j} x_{i,k} - \Sigma_{j,k}^*) \right|,$$

over $1 \leq j, k \leq p$.

Since $\frac{x_{i,j}}{\sqrt{\Sigma_{j,j}^*}} \sim \mathcal{N}(0, 1)$, we have $\|x_{i,j}\|_{\psi_2} \leq C_1 \sqrt{\Sigma_{j,j}^*}$ for some universal constant C_1 [see e.g., Lemma 5.14 in 46]. By Lemma 10, for each (j, k) , $\|x_{i,j} x_{i,k}\|_{\psi_1} \leq C_1^2 \|\Sigma^*\|_\infty$. Therefore, by Lemma 11, we have

$$|\widehat{\Sigma}_{j,k} - \Sigma_{j,k}^*| \leq C \|\Sigma^*\|_\infty \sqrt{\frac{\log p}{n_{j,k}}},$$

with probability at least $1 - \exp\{-c \log p\}$.

By the definition of $\widetilde{\Sigma}$ in (1), we know that

$$\begin{aligned} \sqrt{n_{j,k}} |\widetilde{\Sigma}_{j,k} - \widehat{\Sigma}_{j,k}| &\leq \max_{j',k'} \sqrt{n_{j',k'}} |\widetilde{\Sigma}_{j',k'} - \widehat{\Sigma}_{j',k'}| \\ &\leq \max_{j',k'} \sqrt{n_{j',k'}} |\Sigma_{j',k'}^* - \widehat{\Sigma}_{j',k'}|, \end{aligned}$$

hence we can bound $|\widetilde{\Sigma}_{j,k} - \Sigma_{j,k}^*|$ as follows:

$$\begin{aligned} |\widetilde{\Sigma}_{j,k} - \Sigma_{j,k}^*| &\leq |\widehat{\Sigma}_{j,k} - \Sigma_{j,k}^*| + |\widetilde{\Sigma}_{j,k} - \widehat{\Sigma}_{j,k}| \\ &\leq \frac{2}{\sqrt{n_{j,k}}} \max_{j',k'} \sqrt{n_{j',k'}} |\widehat{\Sigma}_{j',k'} - \Sigma_{j',k'}^*| \\ &\leq C \|\Sigma^*\|_\infty \sqrt{\frac{\log p}{n_{j,k}}}. \end{aligned}$$

□

Proof of Lemma 4. By the definition of \mathcal{E}_1 ,

$$\begin{aligned} (\mathcal{E}_1)_{j,k,j',k'} &= \widehat{\Sigma}_{j,j'} \widehat{\Sigma}_{k,k'} - \Sigma_{j,j'}^* \Sigma_{k,k'}^* \\ &= (\widehat{\Sigma}_{j,j'} - \Sigma_{j,j'}^*) \Sigma_{k,k'}^* + \Sigma_{j,j'}^* (\widehat{\Sigma}_{k,k'} - \Sigma_{k,k'}^*) + (\widehat{\Sigma}_{j,j'} - \Sigma_{j,j'}^*) (\widehat{\Sigma}_{k,k'} - \Sigma_{k,k'}^*). \end{aligned}$$

By Lemma 2, with probability at least $1 - Cp^{-c}$,

$$|(\mathcal{E}_1)_{j,k,j',k'}| \leq C \|\Sigma^*\|_\infty^2 \left(\sqrt{\frac{\log p}{n_{j,j'}}} + \sqrt{\frac{\log p}{n_{k,k'}}} + \frac{\log p}{\sqrt{n_{j,j'} n_{k,k'}}} \right)$$

holds for all $j, k, j', k' \in [p]$. □

Proof of Lemma 5. First we can decompose the error tensor as follows:

$$\begin{aligned} & [(u^{(1)} + \epsilon^{(1)}) \otimes (u^{(2)} + \epsilon^{(2)}) \otimes (u^{(3)} + \epsilon^{(3)}) \otimes (u^{(4)} + \epsilon^{(4)}) \\ & - u^{(1)} \otimes u^{(2)} \otimes u^{(3)} \otimes u^{(4)}] \circ \mathcal{N} \\ & = \mathcal{D}_1 + \mathcal{D}_2 + \mathcal{D}_3 + \mathcal{D}_4, \end{aligned}$$

where \mathcal{D}_i is the sum of error terms of the i th order (including product of i error terms). In particular,

$$\begin{aligned} \mathcal{D}_1 &= (\epsilon^{(1)} \otimes u^{(2)} \otimes u^{(3)} \otimes u^{(4)}) \circ \mathcal{N} \\ &+ (u^{(1)} \otimes \epsilon^{(2)} \otimes u^{(3)} \otimes u^{(4)}) \circ \mathcal{N} \\ &+ (u^{(1)} \otimes u^{(2)} \otimes \epsilon^{(3)} \otimes u^{(4)}) \circ \mathcal{N} \\ &+ (u^{(1)} \otimes u^{(2)} \otimes u^{(3)} \otimes \epsilon^{(4)}) \circ \mathcal{N}. \end{aligned} \tag{45}$$

We will prove an upper bound for $\|\mathcal{D}_1\|_1$ and show that all higher-order terms can be controlled by $C\|\mathcal{D}_1\|_1$ for some universal constant C .

Now we bound each term in (45). For the first term,

$$\begin{aligned}
& \|(\epsilon^{(1)} \otimes u^{(2)} \otimes u^{(3)} \otimes u^{(4)}) \circ \mathcal{N}\|_1 \\
&= \sum_{j,k,j',k'} \frac{n_{j,k,j',k'}}{n_{j,k}n_{j',k'}} |\epsilon_j^{(1)}| |u_k^{(2)}| |u_{j'}^{(3)}| |u_{k'}^{(4)}| \\
&\leq \sum_{j,k,j',k'} \frac{1}{n_{j,k}} |\epsilon_j^{(1)}| |u_k^{(2)}| |u_{j'}^{(3)}| |u_{k'}^{(4)}| \\
&\leq \sum_j \frac{|\epsilon_j^{(1)}|}{\sqrt{\max_k n_{j,k}}} \sum_k \frac{|u_k^{(2)}|}{\sqrt{\max_j n_{j,k}}} \|u^{(3)}\|_1 \|u^{(4)}\|_1 \\
&\leq \sum_j \frac{|\epsilon_j^{(1)}|}{\sqrt{\max_k n_{j,k}}} \frac{\|u^{(2)}\|_1}{\sqrt{\min_{k \in \text{supp}(u^{(2)})} \min_k n_{j,k}}} \|u^{(3)}\|_1 \|u^{(4)}\|_1
\end{aligned}$$

where the third line is due to that $n_{j,k,j',k'} \leq n_{j,k} n_{j',k'}$. Following similar arguments to the above, we have

$$\begin{aligned}
& \|(u^{(1)} \otimes \epsilon^{(2)} \otimes u^{(3)} \otimes u^{(4)}) \circ \mathcal{N}\|_1 \\
&\leq \frac{\|u^{(1)}\|_1}{\sqrt{\min_{k \in \text{supp}(u^{(1)})} \min_k n_{j,k}}} \sum_k \frac{|\epsilon_k^{(2)}|}{\sqrt{\max_j n_{j,k}}} \|u^{(3)}\|_1 \|u^{(4)}\|_1, \\
& \|(u^{(1)} \otimes u^{(2)} \otimes \epsilon^{(3)} \otimes u^{(4)}) \circ \mathcal{N}\|_1 \\
&\leq \|u^{(1)}\|_1 \|u^{(2)}\|_1 \sum_{j'} \frac{|\epsilon_{j'}^{(3)}|}{\sqrt{\max_{k'} n_{j',k'}}} \sum_{k'} \frac{\|u^{(4)}\|_1}{\sqrt{\min_{k \in \text{supp}(u^{(4)})} \min_k n_{j,k}}},
\end{aligned}$$

and

$$\begin{aligned}
& \|(u^{(1)} \otimes u^{(2)} \otimes u^{(3)} \otimes \epsilon^{(4)}) \circ \mathcal{N}\|_1 \\
&\leq \|u^{(1)}\|_1 \|u^{(2)}\|_1 \frac{\|u^{(3)}\|_1}{\sqrt{\min_{k \in \text{supp}(u^{(3)})} \min_k n_{j,k}}} \sum_{k'} \frac{|\epsilon_{k'}^{(4)}|}{\sqrt{\max_{j'} n_{j',k'}}}.
\end{aligned}$$

Combining the bounds above, we have

$$|\mathcal{D}_1| \leq \sum_{l=1}^4 \left[\sum_{j=1}^p \frac{|\epsilon_j^{(l)}|}{\sqrt{\min_{k \in [p]} n_{j,k}}} \frac{\|u^{(i_l)}\|_1}{\sqrt{\min_{k \in \text{supp}(u^{(i_l)})} \min_k n_{j,k}}} \prod_{m \neq l, i_l} \|u^{(m)}\|_1 \right].$$

While for the higher order terms, we can still apply the same argument. For instance,

$(\epsilon^{(1)} \otimes \epsilon^{(2)} \otimes u^{(3)} \otimes u^{(4)}) \circ \mathcal{N}$ is one term in \mathcal{D}_2 , and it satisfies

$$\begin{aligned} & \|(\epsilon^{(1)} \otimes \epsilon^{(2)} \otimes u^{(3)} \otimes u^{(4)}) \circ \mathcal{N}\|_1 \\ & \leq \sum_j \frac{|\epsilon_j^{(1)}|}{\sqrt{\max_k n_{j,k}}} \sum_k \frac{\epsilon_k^{(2)}}{\sqrt{\max_j n_{j,k}}} \|u^{(3)}\|_1 \|u^{(4)}\|_1 \\ & \leq C_1 \sum_j \frac{|\epsilon_j^{(1)}|}{\sqrt{\max_k n_{j,k}}} \frac{\|u^{(2)}\|_1}{\sqrt{\min_{k \in \text{supp}(u^{(2)})} \min_k n_{j,k}}} \|u^{(3)}\|_1 \|u^{(4)}\|_1, \end{aligned}$$

where in the last line we have utilized the condition that

$$\sum_{j=1}^p \left| \frac{\epsilon_j^{(l)}}{\sqrt{\min_{k \in [p]} n_{j,k}}} \right| \leq C_1 \frac{\|u^{(l)}\|_1}{\sqrt{\min_{k \in \text{supp}(u^{(l)})} \min_k n_{j,k}}}.$$

While for $(\epsilon^{(1)} \otimes u^{(2)} \otimes \epsilon^{(3)} \otimes u^{(4)}) \circ \mathcal{N}$,

$$\begin{aligned} & \|(\epsilon^{(1)} \otimes u^{(2)} \otimes \epsilon^{(3)} \otimes u^{(4)}) \circ \mathcal{N}\|_1 \\ & \leq \sum_j \frac{|\epsilon_j^{(1)}|}{\sqrt{\max_k n_{j,k}}} \sum_k \frac{u_k^{(2)}}{\sqrt{\max_j n_{j,k}}} \|\epsilon^{(3)}\|_1 \|u^{(4)}\|_1 \\ & \leq C_1 \sum_j \frac{|\epsilon_j^{(1)}|}{\sqrt{\max_k n_{j,k}}} \sum_k \frac{u_k^{(2)}}{\sqrt{\max_j n_{j,k}}} \|u^{(3)}\|_1 \|u^{(4)}\|_1, \end{aligned}$$

where the last line is due to that $\|\epsilon^{(l)}\|_1 \leq C_1 \|u^{(l)}\|_1$. By applying similar arguments to all terms in \mathcal{D}_2 , \mathcal{D}_3 and \mathcal{D}_4 , our proof is complete. \square

Lemma 12. *Assume that all conditions in Lemma 5 hold, and let $j_l \in \{1, \dots, 4\}$ satisfy $j_l \equiv l + 2 \pmod{4}$, then we have*

$$\begin{aligned} & \|[(u^{(1)} + \epsilon^{(1)}) \otimes (u^{(2)} + \epsilon^{(2)}) \otimes (u^{(3)} + \epsilon^{(3)}) \otimes (u^{(4)} + \epsilon^{(4)}) \\ & \quad - u^{(1)} \otimes u^{(2)} \otimes u^{(3)} \otimes u^{(4)}] \circ \tilde{\mathcal{N}}^{(1)}\|_1 \\ & \leq C_2 \sum_{l=1}^4 \left[\sum_{j=1}^p \frac{|\epsilon_j^{(l)}|}{\sqrt{\min_k n_{j,k}}} \frac{\|u^{(i_l)}\|_1 \|u^{(j_l)}\|_1}{\min_{j \in \text{supp}(u^{(i_l)}) \cup \text{supp}(u^{(j_l)})} \min_k n_{j,k}} \prod_{m \neq l, i_l, j_l} \|u^{(m)}\|_1 \right], \\ & \|[(u^{(1)} + \epsilon^{(1)}) \otimes (u^{(2)} + \epsilon^{(2)}) \otimes (u^{(3)} + \epsilon^{(3)}) \otimes (u^{(4)} + \epsilon^{(4)}) \\ & \quad - u^{(1)} \otimes u^{(2)} \otimes u^{(3)} \otimes u^{(4)}] \circ \tilde{\mathcal{N}}^{(2)}\|_1 \\ & \leq C_2 \sum_{l=1}^4 \left[\sum_{j=1}^p \frac{|\epsilon_j^{(l)}|}{\sqrt{\min_k n_{j,k}}} \prod_{m \neq l} \frac{\|u^{(m)}\|_1}{\min_{j \in \text{supp}(u^{(m)})} \min_k n_{j,k}} \right], \end{aligned}$$

where C_2 is also a universal constant.

Proof of Lemma 12. The proof is very similar to the proof of Lemma 5. In the following, we only show the detailed upper bounds for the first-order error terms (4 terms for each of the two cases, with $\mathcal{N}^{(1)}$ and $\mathcal{N}^{(2)}$ respectively), while the higher-order error terms can be bounded as a constant factor multiplying the first-order error bounds using the same arguments as in the the proof of Lemma 5.

In particular, one can show that one of the first-order error term satisfies

$$\begin{aligned}
& \|(\epsilon^{(1)} \otimes u^{(2)} \otimes u^{(3)} \otimes u^{(4)}) \circ \mathcal{N}^{(1)}\|_1 \\
&= \sum_{j,k,j',k'} \frac{\sqrt{n_{j,k,j',k'}}}{n_{j,k}n_{j',k'}} |\epsilon_j^{(1)}| \|u_k^{(2)}\| \|u_{j'}^{(3)}\| \|u_{k'}^{(4)}\| \\
&\leq \sum_{j,k,j',k'} \frac{1}{n_{j,k}\sqrt{n_{j',k'}}} |\epsilon_j^{(1)}| \|u_k^{(2)}\| \|u_{j'}^{(3)}\| \|u_{k'}^{(4)}\| \\
&\leq \sum_j \frac{|\epsilon_j^{(1)}|}{\sqrt{\max_k n_{j,k}}} \sum_k \frac{|u_k^{(2)}|}{\sqrt{\max_j n_{j,k}}} \sum_{j'} \frac{|u_{j'}^{(3)}|}{\sqrt{\max_{k'} n_{j',k'}}} \|u^{(4)}\|_1 \\
&\leq \sum_j \frac{|\epsilon_j^{(1)}|}{\sqrt{\max_k n_{j,k}}} \frac{\|u^{(2)}\|_1 \|u^{(3)}\|_1}{\min_{k \in \text{supp}(u^{(2)}) \cup \text{supp}(u^{(3)})} \min_k n_{j,k}} \|u^{(4)}\|_1,
\end{aligned}$$

where we applied $n_{j,k,j',k'} \leq n_{j',k'}$ on the third line, and

$$\begin{aligned}
& \|(\epsilon^{(1)} \otimes u^{(2)} \otimes u^{(3)} \otimes u^{(4)}) \circ \mathcal{N}^{(2)}\|_1 \\
&= \sum_{j,k,j',k'} \frac{1}{n_{j,k}n_{j',k'}} |\epsilon_j^{(1)}| \|u_k^{(2)}\| \|u_{j'}^{(3)}\| \|u_{k'}^{(4)}\| \\
&\leq \sum_j \frac{|\epsilon_j^{(1)}|}{\sqrt{\max_k n_{j,k}}} \sum_k \frac{|u_k^{(2)}|}{\sqrt{\max_j n_{j,k}}} \sum_{j'} \frac{|u_{j'}^{(3)}|}{\sqrt{\max_{k'} n_{j',k'}}} \sum_{k'} \frac{|u_{k'}^{(4)}|}{\sqrt{\max_{j'} n_{j',k'}}} \\
&\leq \sum_j \frac{|\epsilon_j^{(1)}|}{\sqrt{\max_k n_{j,k}}} \prod_{m \neq 1} \frac{\|u^{(m)}\|_1}{\min_{k \in \text{supp}(u^{(m)})} \min_k n_{j,k}}.
\end{aligned}$$

Similarly, one can show that

$$\begin{aligned}
& \|(u^{(1)} \otimes \epsilon^{(2)} \otimes u^{(3)} \otimes u^{(4)}) \circ \mathcal{N}^{(1)}\|_1 \\
&\leq \frac{\|u^{(1)}\|_1 \|u\|_3}{\sqrt{\min_{k \in \text{supp}(u^{(1)}) \cup \text{supp}(u^{(3)})} \min_k n_{j,k}}} \sum_k \frac{|\epsilon_k^{(2)}|}{\sqrt{\max_j n_{j,k}}} \|u^{(4)}\|_1,
\end{aligned}$$

$$\begin{aligned}
& \| (u^{(1)} \otimes u^{(2)} \otimes \epsilon^{(3)} \otimes u^{(4)}) \circ \mathcal{N} \|_1 \\
& \leq \|u^{(2)}\|_1 \sum_{j'} \frac{|\epsilon_{j'}^{(3)}|}{\sqrt{\max_{k'} n_{j',k'}}} \sum_{k'} \frac{\|u^{(4)}\|_1 \|u^{(1)}\|_1}{\sqrt{\min_{k \in \text{supp}(u^{(4)}) \cup \text{supp}(u^{(2)})} \min_k n_{j,k}}},
\end{aligned}$$

and

$$\begin{aligned}
& \| (u^{(1)} \otimes u^{(2)} \otimes u^{(3)} \otimes \epsilon^{(4)}) \circ \mathcal{N} \|_1 \\
& \leq \|u^{(1)}\|_1 \frac{\|u^{(3)}\|_1 \|u^{(2)}\|_1}{\sqrt{\min_{k \in \text{supp}(u^{(3)})} \cup \text{supp}(u^{(2)}) \min_k n_{j,k}}} \sum_{k'} \frac{|\epsilon_{k'}^{(4)}|}{\sqrt{\max_{j'} n_{j',k'}}};
\end{aligned}$$

$$\begin{aligned}
& \| (u^{(1)} \otimes \epsilon^{(2)} \otimes u^{(3)} \otimes u^{(4)}) \circ \mathcal{N}^{(2)} \|_1 \\
& \leq \sum_k \frac{|\epsilon_k^{(2)}|}{\sqrt{\max_j n_{j,k}}} \prod_{m \neq 2} \frac{\|u^{(m)}\|_1}{\min_{k \in \text{supp}(u^{(m)})} \min_k n_{j,k}},
\end{aligned}$$

$$\begin{aligned}
& \| (u^{(1)} \otimes u^{(2)} \otimes \epsilon^{(3)} \otimes u^{(4)}) \circ \mathcal{N}^{(2)} \|_1 \\
& \leq \sum_k \frac{|\epsilon_k^{(3)}|}{\sqrt{\max_j n_{j,k}}} \prod_{m \neq 3} \frac{\|u^{(m)}\|_1}{\min_{k \in \text{supp}(u^{(m)})} \min_k n_{j,k}},
\end{aligned}$$

$$\begin{aligned}
& \| (u^{(1)} \otimes u^{(2)} \otimes u^{(3)} \otimes \epsilon^{(4)}) \circ \mathcal{N}^{(2)} \|_1 \\
& \leq \sum_k \frac{|\epsilon_k^{(4)}|}{\sqrt{\max_j n_{j,k}}} \prod_{m \neq 4} \frac{\|u^{(m)}\|_1}{\min_{k \in \text{supp}(u^{(m)})} \min_k n_{j,k}}.
\end{aligned}$$

Hence the first-order error terms for both cases ($\mathcal{N}^{(1)}$ and $\mathcal{N}^{(2)}$) are bounded accordingly. \square

Proof of Proposition 1. Recall the definition of $S_2(a, b)$ in Section 3.1. Note that if $(j, k) \notin \overline{\mathcal{N}}_a \times \overline{\mathcal{N}}_b^{(a)}$ and $(j, k) \notin \overline{\mathcal{N}}_b^{(a)} \times \overline{\mathcal{N}}_a$, one has $\Theta_{j,b}^{(a)*} \Theta_{k,a}^* + \Theta_{k,b}^{(a)*} \Theta_{j,a}^* = 0$ and hence $(j, k) \notin S_2(a, b)$. This implies that $S_2(a, b) \subseteq (\overline{\mathcal{N}}_a \times \overline{\mathcal{N}}_b^{(a)}) \times (\overline{\mathcal{N}}_b^{(a)} \times \overline{\mathcal{N}}_a)$. If $S_2(a, b) \neq (\overline{\mathcal{N}}_a \times \overline{\mathcal{N}}_b^{(a)}) \times (\overline{\mathcal{N}}_b^{(a)} \times \overline{\mathcal{N}}_a)$, then there exists $(j, k) \in (\overline{\mathcal{N}}_a \times \overline{\mathcal{N}}_b^{(a)})$ such that $\Theta_{j,b}^{(a)*} \Theta_{k,a}^* = -\Theta_{k,b}^{(a)*} \Theta_{j,a}^* \neq 0$, which defines a set of measure zero.

While for $\overline{\mathcal{N}}_a^{(b)}$, by definition, $j \in \overline{\mathcal{N}}_a^{(b)}$ if and only if $\Theta_{b,j}^* \Theta_{a,a}^* - \Theta_{a,j}^* \Theta_{a,b}^* \neq 0$. If $b \notin \mathcal{N}_a$, $\Theta_{a,b}^* = 0$, and this condition is equivalent to $\Theta_{b,j}^* \neq 0$ and hence $\overline{\mathcal{N}}_a^{(b)} = \overline{\mathcal{N}}_b$.

Otherwise, if $j \notin \overline{\mathcal{N}}_b \cup \overline{\mathcal{N}}_a$, one has $\Theta_{b,j}^* \Theta_{a,a}^* - \Theta_{a,j}^* \Theta_{a,b}^* \neq 0$ which implies $j \notin \overline{\mathcal{N}}_a^{(b)}$. Thus $\overline{\mathcal{N}}_a^{(b)} \subseteq \overline{\mathcal{N}}_b \cup \overline{\mathcal{N}}_a$. In this case, $\overline{\mathcal{N}}_a^{(b)} \neq \overline{\mathcal{N}}_b \cup \overline{\mathcal{N}}_a$ only happens when there exists $j \in \overline{\mathcal{N}}_b \cup \overline{\mathcal{N}}_a$ such that $\Theta_{b,j}^* \Theta_{a,a}^* = \Theta_{a,j}^* \Theta_{a,b}^*$, which also defines a set of measure zero. \square

Proof of Lemma 6. First note that we can write $\frac{E(a,b)}{\sigma_n(a,b)} = \sum_{i=1}^n \frac{\epsilon_i(a,b)}{\sigma_n(a,b)}$, where

$$\epsilon_i(a,b) = \sum_{j,k} (x_{i,j} x_{i,k} - \Sigma_{j,k}^*) \frac{\delta_{j,k}^{(i)}}{n_{j,k}} \frac{\Theta_{j,b}^{(a)*} \Theta_{k,a}^* + \Theta_{k,b}^{(a)*} \Theta_{j,a}^*}{2\Theta_{a,a}^*},$$

and hence $\{\frac{\epsilon_i(a,b)}{\sigma_n(a,b)}\}_{i=1}^n$ are independent mean zero random variables. The following Gaussian approximation result for sum of independent r.v.s is useful for our proof:

Lemma 13 (Theorem 1.1 in [60]). *Let $\tau > 0$ and $\xi_1, \dots, \xi_n \in \mathbb{R}^k$ be independent mean zero random vectors such that*

$$|\mathbb{E}(\langle \xi_i, t \rangle^2 \langle \xi_i, u \rangle^{m-2})| \leq \frac{1}{2} m! \tau^{m-2} \|u\|^{m-2} \mathbb{E}(\langle \xi_i, t \rangle^2) \quad (46)$$

holds for $m \geq 3$, $t, u \in \mathbb{R}^k$, and $i = 1, \dots, n$. Let $S = \sum_{i=1}^n \xi_i$. Denote by $Z \in \mathbb{R}^k$ a multivariate Gaussian random variable with the zero mean and the same covariance as that of S . Then for all $\varepsilon > 0$,

$$\sup_{B \subset \mathbb{R}^k} \max\{\mathbb{P}(S \in B) - \mathbb{P}(Z \in B^\varepsilon), \mathbb{P}(Z \in B) - \mathbb{P}(S \in B^\varepsilon)\} \leq C_1(k) \exp\left\{-\frac{\varepsilon}{C_2(k)\tau}\right\},$$

where $B^\varepsilon = \{x \in \mathbb{R}^k : \inf_{y \in B} \|x - y\|_2 \leq \varepsilon\}$ for any set $B \subset \mathbb{R}^k$.

In the following, we will let $\xi_i(a,b) = \frac{\epsilon_i(a,b)}{\sigma_n(a,b)}$ and show that $\xi_i(a,b)$ satisfies (46). Recall the $\|\cdot\|_{\psi_\alpha}$ norm in Definition 1, and by the equivalence between some properties of sub-exponential random variables [see 46, Definition 5.13], we have

$$\begin{aligned} |\mathbb{E}(\langle \xi_i(a,b), t \rangle^2 \langle \xi_i(a,b), u \rangle^{m-2})| &\leq t^2 |u|^{m-2} \mathbb{E}|\xi_i(a,b)|^m \\ &\leq t^2 |u|^{m-2} m^m \|\xi_i(a,b)\|_{\psi_1}^m \\ &\leq |u|^{m-2} t^2 \frac{1}{2} m! \tau_i^{m-2} \mathbb{E}(\xi_i^2(a,b)), \end{aligned}$$

where $\tau_i = 12 \|\xi_i(a,b)\|_{\psi_1} \left(\frac{\|\xi_i(a,b)\|_{\psi_1}^2}{\mathbb{E}(\xi_i^2(a,b))} \vee 1 \right)$. The last line is due to that

$$\frac{2m^m}{m!} \leq \frac{2e^m}{\sqrt{2\pi m}} \leq \frac{e^m}{\sqrt{m}} \leq \left(\frac{e^3}{\sqrt{3}}\right)^{m-2} \leq 12^{m-2},$$

where the first inequality is due to Stirling's formula: $m! \geq \sqrt{2\pi m} \left(\frac{m}{e}\right)^m$, and

$$\begin{aligned} m^m \|\xi_i(a, b)\|_{\psi_1}^m &\leq \frac{1}{2} m! 12^{m-2} \|\xi_i(a, b)\|_{\psi_1}^{m-2} \frac{\|\xi_i(a, b)\|_{\psi_1}^2}{\mathbb{E}(\xi_i^2(a, b))} \mathbb{E}(\xi_i^2(a, b)) \\ &\leq \frac{1}{2} m! \left(12 \|\xi_i(a, b)\|_{\psi_1} \left(\frac{\|\xi_i(a, b)\|_{\psi_1}^2}{\mathbb{E}(\xi_i^2(a, b))} \vee 1 \right) \right)^{m-2} \mathbb{E}(\xi_i^2(a, b)). \end{aligned}$$

Now it suffices to show that each $\tau_i \leq \frac{C\|\Sigma^*\|_\infty^3 (d_a + d_b + 1)^3}{\lambda_{\min}^3(\Sigma^*) \sqrt{n_2^{(a,b)}}}$. Recall that we have defined $U_{j,k}^{(\delta,i)} = \frac{U_{j,k} \delta_{j,k}^{(i)}}{n_{j,k}}$, where $U_{j,k} = \frac{\Theta_{j,b}^{(a)*} \Theta_{k,a}^{(a)*} + \Theta_{k,b}^{(a)*} \Theta_{j,a}^{(a)*}}{2\Theta_{a,a}^{(a)*}}$ in the proof of Theorem 2. Then we can also write $\xi_i(a, b) = \frac{1}{\sigma_n(a, b)} \sum_{j,k} (x_{i,j} x_{i,k} - \Sigma_{j,k}^*) U_{j,k}^{(\delta,i)}$. It has been shown in the proof of Theorem 2 that $\sigma_n(a, b) \geq \sqrt{2} \lambda_{\min}(\Sigma^*) \sqrt{\sum_{j,k} U_{j,k}^2 n_{j,k}^{-1}}$. Since $\|x_{i,j} x_{i,k} - \Sigma_{j,k}^*\|_{\psi_1} \leq C \|\Sigma^*\|_\infty$, as has been shown in the proof of Lemma 2, we have

$$\begin{aligned} \|\xi_i(a, b)\|_{\psi_1} &\leq \frac{C \|\Sigma^*\|_\infty \|U^{(\delta,i)}\|_1}{\lambda_{\min}(\Sigma^*) \sqrt{\sum_{j,k} U_{j,k}^2 n_{j,k}^{-1}}} \\ &\leq \frac{C \|\Sigma^*\|_\infty (d_a + d_b + 1) \|U^{(\delta,i)}\|_F}{\lambda_{\min}(\Sigma^*) \sqrt{\sum_{j,k} U_{j,k}^2 n_{j,k}^{-1}}} \\ &\leq \frac{C \|\Sigma^*\|_\infty (d_a + d_b + 1)}{\lambda_{\min}(\Sigma^*)} \sqrt{\frac{\sum_{j,k} U_{j,k}^2 n_{j,k}^{-2}}{\sum_{j,k} U_{j,k}^2 n_{j,k}^{-1}}} \\ &\leq \frac{C \|\Sigma^*\|_\infty (d_a + d_b + 1)}{\lambda_{\min}(\Sigma^*) \sqrt{n_2^{(a,b)}}}. \end{aligned}$$

Furthermore, we can upper bound $\frac{\|\xi_i\|_{\psi_1}^2}{\mathbb{E}(\xi_i^2)}$ as follows:

$$\begin{aligned} \frac{\|\xi_i(a, b)\|_{\psi_1}^2}{\mathbb{E}(\xi_i^2(a, b))} &= \frac{\|\epsilon_i(a, b)\|_{\psi_1}^2}{\mathbb{E}(\epsilon_i(a, b)^2)} \\ &\leq \frac{C \|\Sigma^*\|_\infty^2 (d_a + d_b + 1)^2 \|U^{(\delta,i)}\|_F^2}{\lambda_{\min}^2(\Sigma^*) \|U^{(\delta,i)}\|_F^2} \\ &= \frac{C \|\Sigma^*\|_\infty^2 (d_a + d_b + 1)^2}{\lambda_{\min}^2(\Sigma^*)}. \end{aligned}$$

Therefore, we have shown that $\tau_i = 12 \|\xi_i(a, b)\|_{\psi_1} \left(\frac{\|\xi_i(a, b)\|_{\psi_1}^2}{\mathbb{E}(\xi_i^2(a, b))} \vee 1 \right) \leq \frac{C \|\Sigma^*\|_\infty^3 (d_a + d_b + 1)^3}{\lambda_{\min}^3(\Sigma^*) \sqrt{n_2^{(a,b)}}}$, and the proof is now complete. \square

Proof of Lemma 8. Similar to the proof of Lemma 6, we will apply the Gaussian approximation bound in Lemma 13 by validating (46) for $(\xi_i(a, b), \xi_i(a', b'))^\top \in \mathbb{R}^2$.

For any two-dimensional random vector $X = (X_1, X_2)^\top$, and $t, u \in \mathbb{R}^2$, we can show that

$$\mathbb{E}(\langle X, t \rangle^2 \langle X, u \rangle^{m-2}) \leq \sqrt{\mathbb{E}\|X\|_2^4} \sqrt{\mathbb{E}\|X\|_2^{2m-4}} \|u\|_2^{m-2} \|t\|_2^2,$$

and for any integer k ,

$$\begin{aligned} \mathbb{E}\|X\|_2^{2k} &\leq \mathbb{E}(X_1^2 + X_2^2)^k \leq 2^{k-1}(\mathbb{E}|X_1|^{2k} + \mathbb{E}|X_2|^{2k}) \leq 2^{k-1}(2k)^{2k}(\|X_1\|_{\psi_1}^{2k} + \|X_2\|_{\psi_1}^{2k}) \\ &\leq (2\sqrt{2}k)^{2k}(\|X_1\|_{\psi_1} \vee \|X_2\|_{\psi_1})^{2k} \end{aligned}$$

where the second inequality is due to the Jensen's inequality, the third inequality is due to the property of $\|\cdot\|_{\psi_1}$ norm. Hence we have

$$\begin{aligned} \mathbb{E}(\langle X, t \rangle^2 \langle X, u \rangle^{m-2}) &\leq \sqrt{\mathbb{E}\|X\|_2^4} \sqrt{\mathbb{E}\|X\|_2^{2m-4}} \|u\|_2^{m-2} \|t\|_2^2 \\ &\leq 32(2\sqrt{2}m)^{m-2}(\|X_1\|_{\psi_1} \vee \|X_2\|_{\psi_1})^m \|u\|_2^{m-2} \|t\|_2^2 \\ &\leq \frac{32}{m^2} [2\sqrt{2}(\|X_1\|_{\psi_1} \vee \|X_2\|_{\psi_1})]^{m-2} \frac{\|X_1\|_{\psi_1}^2 \vee \|X_2\|_{\psi_1}^2}{\lambda_{\min}(\text{Cov}(X))} \lambda_{\min}(\text{Cov}(X)) m^m \|u\|_2^{m-2} \|t\|_2^2 \\ &\leq \frac{1}{2} m! \|u\|_2^{m-2} \tau^{m-2} \mathbb{E}(\langle X, t \rangle^2), \end{aligned}$$

where $\tau = \frac{120(\|X_1\|_{\psi_1} \vee \|X_2\|_{\psi_1})^3}{\lambda_{\min}(\text{Cov}(X))}$, and we have applied the fact that $\frac{2m^m}{m!} \leq (\frac{e^3}{\sqrt{3}})^{m-2}$ and $\mathbb{E}(\langle X, t \rangle^2) \geq \|t\|_2^2 \lambda_{\min}(\text{Cov}(X))$ on the last line.

Recall the proof of Lemma 6 and the definition of $\alpha(\Theta^*, \{V_i\}_{i=1}^n)$, we have

$$\|\xi_i(a, b)\|_{\psi_1}, \|\xi_i(a', b')\|_{\psi_1} \leq \frac{C\|\Sigma^*\|_\infty(d+1)}{\lambda_{\min}(\Sigma^*) \sqrt{n_2^{(a,b)} \vee n_2^{(a',b')}}},$$

and $(\xi_i(a, b), \xi_i(a', b'))^\top$ satisfies (46) with $\tau = \frac{C\|\Sigma^*\|_\infty(d+1)\alpha(\Theta^*, \{V_i\}_{i=1}^n)}{\lambda_{\min}(\Sigma^*) \sqrt{n_2^{(a,b)} \vee n_2^{(a',b')}}}$. The proof completes with the application of Lemma 13. \square

References

- [1] Radoslaw Adamczak, Alexander E Litvak, Alain Pajor, and Nicole Tomczak-Jaegermann. Restricted isometry property of matrices with independent columns and neighborly polytopes by random sampling. *Constructive Approximation*, 34(1):61–88, 2011.

- [2] Genevera I Allen and Zhandong Liu. A log-linear graphical model for inferring genetic networks from high-throughput sequencing data. In *2012 IEEE International Conference on Bioinformatics and Biomedicine*, pages 1–6. IEEE, 2012.
- [3] J Alexander Bae, Mahaly Baptiste, Agnes L Bodor, Derrick Brittain, JoAnn Buchanan, Daniel J Bumbarger, Manuel A Castro, Brendan Celii, Erick Cobos, Forrest Collman, et al. Functional connectomics spanning multiple areas of mouse visual cortex. *BioRxiv*, 2021.
- [4] Alexandre Belloni, Victor Chernozhukov, and Abhishek Kaul. Confidence bands for coefficients in high dimensional linear models with error-in-variables. *arXiv preprint arXiv:1703.00469*, 2017.
- [5] Stephen Boyd, Neal Parikh, and Eric Chu. *Distributed optimization and statistical learning via the alternating direction method of multipliers*. Now Publishers Inc, 2011.
- [6] Tianxi Cai, T Tony Cai, and Anru Zhang. Structured matrix completion with applications to genomic data integration. *Journal of the American Statistical Association*, 111(514):621–633, 2016.
- [7] Tony Cai, Weidong Liu, and Xi Luo. A constrained ℓ_1 minimization approach to sparse precision matrix estimation. *Journal of the American Statistical Association*, 106(494):594–607, 2011.
- [8] Andersen Chang and Genevera I Allen. Extreme graphical models with applications to functional neuronal connectivity. *arXiv preprint arXiv:2106.11554*, 2021.
- [9] Andersen Chang, Tianyi Yao, and Genevera I Allen. Graphical models and dynamic latent factors for modeling functional brain connectivity. In *2019 IEEE Data Science Workshop (DSW)*, pages 57–63. IEEE, 2019.

- [10] Shizhe Chen, Daniela M Witten, and Ali Shojaie. Selection and estimation for mixed graphical models. *Biometrika*, 102(1):47–64, 2015.
- [11] Li-Fang Chu, Ning Leng, Jue Zhang, Zhonggang Hou, Daniel Mamott, David T Vereide, Jeea Choi, Christina Kendziorski, Ron Stewart, and James A Thomson. Single-cell rna-seq reveals novel regulators of human embryonic stem cell differentiation to definitive endoderm. *Genome biology*, 17(1):1–20, 2016.
- [12] Spyros Darmanis, Steven A Sloan, Ye Zhang, Martin Enge, Christine Caneda, Lawrence M Shuer, Melanie G Hayden Gephart, Ben A Barres, and Stephen R Quake. A survey of human brain transcriptome diversity at the single cell level. *Proceedings of the National Academy of Sciences*, 112(23):7285–7290, 2015.
- [13] Gautam Dasarathy. Gaussian graphical model selection from size constrained measurements. In *2019 IEEE International Symposium on Information Theory (ISIT)*, pages 1302–1306. IEEE, 2019.
- [14] Gautam Dasarathy, Aarti Singh, Maria-Florina Balcan, and Jong H Park. Active learning algorithms for graphical model selection. In *Artificial Intelligence and Statistics*, pages 1356–1364. PMLR, 2016.
- [15] Abhirup Datta and Hui Zou. Cocolasso for high-dimensional error-in-variables regression. *The Annals of Statistics*, 45(6):2400–2426, 2017.
- [16] Adrian Dobra, Chris Hans, Beatrix Jones, Joseph R Nevins, Guang Yao, and Mike West. Sparse graphical models for exploring gene expression data. *Journal of Multivariate Analysis*, 90(1):196–212, 2004.
- [17] Adrian Dobra and Alex Lenkoski. Copula gaussian graphical models and their application to modeling functional disability data. *The Annals of Applied Statistics*, 5(2A):969–993, 2011.

- [18] Jerome Friedman, Trevor Hastie, and Robert Tibshirani. Sparse inverse covariance estimation with the graphical lasso. *Biostatistics*, 9(3):432–441, 2008.
- [19] Luqin Gan, Giuseppe Vinci, and Genevera I Allen. Correlation imputation in single cell rna-seq using auxiliary information and ensemble learning. In *Proceedings of the 11th ACM International Conference on Bioinformatics, Computational Biology and Health Informatics*, pages 1–6, 2020.
- [20] Wuming Gong, Il-Youp Kwak, Pruthvi Pota, Naoko Koyano-Nakagawa, and Daniel J Garry. Drimpute: imputing dropout events in single cell rna sequencing data. *BMC bioinformatics*, 19(1):1–10, 2018.
- [21] Quanquan Gu, Yuan Cao, Yang Ning, and Han Liu. Local and global inference for high dimensional gaussian copula graphical models. *arXiv preprint arXiv:1502.02347*, 2015.
- [22] Botao Hao, Anru R Zhang, and Guang Cheng. Sparse and low-rank tensor estimation via cubic sketchings. In *International Conference on Artificial Intelligence and Statistics*, pages 1319–1330. PMLR, 2020.
- [23] Mo Huang, Jingshu Wang, Eduardo Torre, Hannah Dueck, Sydney Shaffer, Roberto Bonasio, John I Murray, Arjun Raj, Mingyao Li, and Nancy R Zhang. Saver: gene expression recovery for single-cell rna sequencing. *Nature methods*, 15(7):539–542, 2018.
- [24] Jana Jankova and Sara Van De Geer. Confidence intervals for high-dimensional inverse covariance estimation. *Electronic Journal of Statistics*, 9(1):1205–1229, 2015.
- [25] Jana Janková and Sara van de Geer. Honest confidence regions and optimality in high-dimensional precision matrix estimation. *Test*, 26(1):143–162, 2017.
- [26] Adel Javanmard and Hamid Javadi. False discovery rate control via debiased lasso. *Electronic Journal of Statistics*, 13(1):1212–1253, 2019.

- [27] Hyundoo Jeong and Zhandong Liu. Prime: a probabilistic imputation method to reduce dropout effects in single-cell rna sequencing. *Bioinformatics*, 36(13):4021–4029, 2020.
- [28] Mladen Kolar and Eric P Xing. Estimating sparse precision matrices from data with missing values. 2012.
- [29] Daphne Koller and Nir Friedman. *Probabilistic graphical models: principles and techniques*. MIT press, 2009.
- [30] Ed S Lein, Michael J Hawrylycz, Nancy Ao, Mikael Ayres, Amy Bensinger, Amy Bernard, Andrew F Boe, Mark S Boguski, Kevin S Brockway, Emi J Byrnes, et al. Genome-wide atlas of gene expression in the adult mouse brain. *Nature*, 445(7124):168–176, 2007.
- [31] Han Liu, Fang Han, Ming Yuan, John Lafferty, and Larry Wasserman. High-dimensional semiparametric gaussian copula graphical models. *The Annals of Statistics*, 40(4):2293–2326, 2012.
- [32] Han Liu, John Lafferty, and Larry Wasserman. The nonparanormal: Semiparametric estimation of high dimensional undirected graphs. *Journal of Machine Learning Research*, 10(10), 2009.
- [33] Han Liu, Kathryn Roeder, and Larry Wasserman. Stability approach to regularization selection (stars) for high dimensional graphical models. *Advances in neural information processing systems*, 24(2):1432, 2010.
- [34] Weidong Liu. Gaussian graphical model estimation with false discovery rate control. *The Annals of Statistics*, 41(6):2948–2978, 2013.
- [35] Nicolai Meinshausen and Peter Bühlmann. High-dimensional graphs and variable selection with the lasso. *The annals of statistics*, 34(3):1436–1462, 2006.

- [36] Marius Pachitariu, Carsen Stringer, Mario Dipoppa, Sylvia Schröder, L Federico Rossi, Henry Dalglish, Matteo Carandini, and Kenneth D Harris. Suite2p: beyond 10,000 neurons with standard two-photon microscopy. *BioRxiv*, page 061507, 2017.
- [37] Seongoh Park, Xinlei Wang, and Johan Lim. Estimating high-dimensional covariance and precision matrices under general missing dependence. *Electronic Journal of Statistics*, 15(2):4868–4915, 2021.
- [38] Eftychios A Pnevmatikakis, Daniel Soudry, Yuanjun Gao, Timothy A Machado, Josh Merel, David Pfau, Thomas Reardon, Yu Mu, Clay Lacefield, Weijian Yang, et al. Simultaneous denoising, deconvolution, and demixing of calcium imaging data. *Neuron*, 89(2):285–299, 2016.
- [39] Pradeep Ravikumar, Martin J Wainwright, Garvesh Raskutti, and Bin Yu. High-dimensional covariance estimation by minimizing ℓ_1 -penalized log-determinant divergence. *Electronic Journal of Statistics*, 5:935–980, 2011.
- [40] Zhao Ren, Tingni Sun, Cun-Hui Zhang, and Harrison H Zhou. Asymptotic normality and optimalities in estimation of large gaussian graphical models. *The Annals of Statistics*, 43(3):991–1026, 2015.
- [41] Konstantinos Slavakis, Yannis Kopsinis, and Sergios Theodoridis. Adaptive algorithm for sparse system identification using projections onto weighted ℓ_1 balls. In *2010 IEEE International Conference on Acoustics, Speech and Signal Processing*, pages 3742–3745. IEEE, 2010.
- [42] Nicolas Städler and Peter Bühlmann. Missing values: sparse inverse covariance estimation and an extension to sparse regression. *Statistics and Computing*, 22(1):219–235, 2012.
- [43] Christoph Stosiek, Olga Garaschuk, Knut Holthoff, and Arthur Konnerth. In vivo two-

- photon calcium imaging of neuronal networks. *Proceedings of the National Academy of Sciences*, 100(12):7319–7324, 2003.
- [44] Carsen Stringer, Marius Pachitariu, Nicholas Steinmetz, Charu Bai Reddy, Matteo Carandini, and Kenneth D Harris. Spontaneous behaviors drive multidimensional, brainwide activity. *Science*, 364(6437):eaav7893, 2019.
- [45] Sara Van de Geer, Peter Bühlmann, Ya’acov Ritov, and Ruben Dezeure. On asymptotically optimal confidence regions and tests for high-dimensional models. *The Annals of Statistics*, 42(3):1166–1202, 2014.
- [46] Roman Vershynin. Introduction to the non-asymptotic analysis of random matrices. *arXiv preprint arXiv:1011.3027*, 2010.
- [47] Giuseppe Vinci, Gautam Dasarathy, and Genevera I Allen. Graph quilting: graphical model selection from partially observed covariances. *arXiv preprint arXiv:1912.05573*, 2019.
- [48] Giuseppe Vinci, Valérie Ventura, Matthew A Smith, and Robert E Kass. Adjusted regularization in latent graphical models: Application to multiple-neuron spike count data. *The annals of applied statistics*, 12(2):1068, 2018.
- [49] Martin J Wainwright. Sharp thresholds for high-dimensional and noisy sparsity recovery using ℓ_1 -constrained quadratic programming (lasso). *IEEE transactions on information theory*, 55(5):2183–2202, 2009.
- [50] Martin J Wainwright. *High-dimensional statistics: A non-asymptotic viewpoint*, volume 48. Cambridge University Press, 2019.
- [51] Huahua Wang, Farideh Fazayeli, Soumyadeep Chatterjee, and Arindam Banerjee. Gaussian copula precision estimation with missing values. In *Artificial Intelligence and Statistics*, pages 978–986. PMLR, 2014.

- [52] Minjie Wang and Genevera I Allen. Thresholded graphical lasso adjusts for latent variables: Application to functional neural connectivity. *arXiv preprint arXiv:2104.06389*, 2021.
- [53] Justin Williams, Hector Corrada Bravo, Jennifer Tom, and Joseph Nathaniel Paulson. microbiomedasim: Simulating longitudinal differential abundance for microbiome data. *F1000Research*, 8, 2019.
- [54] Dong Xia, Anru R Zhang, and Yuchen Zhou. Inference for low-rank tensors—no need to debias. *The Annals of Statistics*, 50(2):1220–1245, 2022.
- [55] Eunho Yang, Yulia Baker, Pradeep Ravikumar, Genevera Allen, and Zhandong Liu. Mixed graphical models via exponential families. In *Proceedings of the Seventeenth International Conference on Artificial Intelligence and Statistics*, pages 1042–1050, 2014.
- [56] Eunho Yang, Pradeep Ravikumar, Genevera I Allen, and Zhandong Liu. Graphical models via univariate exponential family distributions. *The Journal of Machine Learning Research*, 16(1):3813–3847, 2015.
- [57] Dimitri Yatsenko, Krešimir Josić, Alexander S Ecker, Emmanouil Froudarakis, R James Cotton, and Andreas S Tolias. Improved estimation and interpretation of correlations in neural circuits. *PLoS computational biology*, 11(3):e1004083, 2015.
- [58] Ming Yu, Varun Gupta, and Mladen Kolar. Simultaneous inference for pairwise graphical models with generalized score matching. *J. Mach. Learn. Res.*, 21(91):1–51, 2020.
- [59] Ming Yuan and Yi Lin. Model selection and estimation in the gaussian graphical model. *Biometrika*, 94(1):19–35, 2007.
- [60] A Yu Zaitsev. On the gaussian approximation of convolutions under multidimensional analogues of sn bernstein’s inequality conditions. *Probability theory and related fields*, 74(4):535–566, 1987.

- [61] Cun-Hui Zhang and Stephanie S Zhang. Confidence intervals for low dimensional parameters in high dimensional linear models. *Journal of the Royal Statistical Society: Series B (Statistical Methodology)*, 76(1):217–242, 2014.
- [62] Lili Zheng and Genevera I Allen. Learning gaussian graphical models with differing pairwise sample sizes. In *ICASSP 2022-2022 IEEE International Conference on Acoustics, Speech and Signal Processing (ICASSP)*, pages 5588–5592. IEEE, 2022.
- [63] Lili Zheng, Zachary T Rewolinski, and Genevera I Allen. A low-rank tensor completion approach for imputing functional neuronal data from multiple recordings. In *2022 IEEE Data Science and Learning Workshop (DSLW)*, pages 1–6. IEEE, 2022.